Characterization of RIS presynaptic circuits for sleep regulation in *Caenorhabditis elegans*

Dissertation

for the award of the degree

"Doctor rerum naturalium"

(Dr. rer. nat.)

of the Georg-August-Universität Göttingen

within the doctoral program Systems Neuroscience

of the Göttingen Graduate School for Neurosciences, Biophysics, and Molecular Biosciences (GGNB)

submitted by

Elisabeth Maluck

from Döbeln, Germany

Göttingen 2019

Thesis Committee Members

PD Dr. Henrik Bringmann	Max Planck Research Group "Sleep and Waking"
(1st Reviewer)	MPI for Biophysical Chemistry, Göttingen
Prof. Dr. Nils Brose	Department of Molecular Neurobiology
(2nd Reviewer)	MPI for Experimental Medicine, Göttingen
Ph.D. Camin Dean	Research Group "Trans-synaptic Signaling"
	European Neuroscience Institute, Göttingen

Examination Board Members

Prof. Dr. Andreas Stumpner	Department of Cellular Neurobiology
	Schwann-Schleiden Research Centre, Göttingen
Prof. Dr. Reinhard Schuh	Research Group "Molecular Organogenesis"
	MPI for Biophysical Chemistry, Göttingen
Prof. Dr. André Fiala	Department of Neurobiology and Behavior
	Georg-August University Göttingen, Göttingen

Date of oral examination: 24th May, 2019

Affidavit

I herewith declare that this thesis was produced entirely by myself and that I have only used sources and materials cited. The thesis has not been submitted to any other examination board for any other academic award.

Elisabeth Maluck

Summary

Within the field of sleep research, it is well established that all organisms, which possess a nervous system, need to sleep. This underlines the severity of sleep functions. In humans, sleep is essential for memory function, immune system function and energy conservation. However, none of these functions explain why sleep induces a change in consciousness.

To answer these and other remaining questions about sleep, *C. elegans* is the optimal model organism. It offers the opportunity to study sleep in a very simple environment. Adult hermaphrodites have only 302 neurons. The connectivity of all neurons is known. Furthermore, its complete genome is sequenced. Finally, its transparency and its easy genetic tractability allow for the application of almost all known imaging methods and tools to manipulate its behavior.

In my thesis, I focused on the quiescence behavior taking place throughout the development of *C. elegans*, which I will be referring to as sleep or lethargus. Lethargus takes places at the end of each of the four larval stages. Despite its simplicity, sleep in *C. elegans* displays an astonishing amount of similarities to mammalian systems. In mammals, wake-active and sleep-active brain regions mutually inhibit each other in a so-called flip-flop switch. In *C. elegans*, the single interneuron RIS was proven to be sleep-active. Similarly to mammalian systems, high RIS activity dampens the activity of the whole nervous system in the worm.

What is not known about RIS are the neuronal networks controlling it. To shed light on that question former colleagues and I screened through all RIS presynaptic neurons using the optogenetic tools ReaChR and ArchT. Their optogenetic depolarization and hyperpolarization revealed that RIS presynaptic neurons differ in their effect on RIS. Amongst all RIS presynaptic neurons, PVC neurons were identified as activators of RIS in lethargus and RIM as modulators of RIS activity in lethargus. Both PVC and RIM neurons belong to the class of command locomotion interneurons. The regulation of RIS by command locomotion interneurons allows a direct link of sleep to locomotion, arousal and homeostasis.

A side project of my thesis, aimed for the identification of potential suppressors of the *aptf-1* mutant phenotype. *Aptf-1* mutants fail to immobilize in lethargus. After EMS mutagenesis, two suppressor candidates were successfully isolated according to their ability to immobilize in lethargus. The identification of candidate genes is still under research.

Taken together, the presented work reveals a complex regulation of RIS in lethargus by its directly presynaptic neurons. The fact that even such a simple organism has a highly complex neuronal network for sleep regulation, strengthens the choice of *C. elegans* as the best model organism for sleep research. With the vast amount of available tools, not only it allows for the identification of RIS-regulating neurons, like PVC and RIM neurons, but it also opens the door for a closer understanding of regulatory pathways upstream of PVC and RIM neurons respectively as a future perspective. The introduced circuit model for sleep regulation, provides in-depth insights into RIS regulation and explains how lethargus in *C. elegans* is potentially adjusted to the needs of arousal and sleep homeostasis.

Table of contents

1 Introduction

1.1 Sleep in mammals

1.1.1 The sleep state

For the majority of organisms having a nervous system sleep is an essential behavior. It was detected in mammals and birds as well as in major animal models like the zebrafish *Danio rerio*, the fruit fly *Drosophila melanogaster* and the nematode *Caenorhabditis elegans* [1–8]. Already in 1937 Loomis, Harvey and Hobert discovered two phases of sleep in humans [9]. They identified the sleep phases using electroencephalography (EEG). EEG measures locally restricted field potentials in the brain cortex. One sleep phase was classified as rapid (or random) eye movement sleep, short REM sleep. In this phase the brain shows asynchronous activity patterns, which are comparable to those measured in the cerebrum during wakefulness. This is one of the reasons why it is referred to as "active" sleep. It is thought to be important for higher brain functions like learning or forgetting. Contrary to that, the second identified sleep phase is referred to as "quiet" sleep or non-rapid eye movement (NREM) sleep. It is characterized by strongly reduced muscle tones and brain activities. In EEG data it can be identified by slow oscillatory patterns (so called slow waves). These slow waves are also used as a measure for sleep depth. Even invertebrates show brain activities, which are typical for NREM sleep. In invertebrates NREM sleep is represented by an overall reduction of neuronal activity [10–12]. Because EEG data cannot be generated from all sleeping animals it was necessary to define additional behavior criteria to identify sleep [13–15].

1.1.2 Sleep regulation

In mammals the circadian clock controls the sleep-wake cycle. Thereby the master circadian pacemaker is located at the suprachiasmatic nuclei (SCN) [16]. For its function as pacemaker SCN requires the action of the transcription factor CLOCK (Circadian Locomotor Output Cycles Kaput) in this tissue. CLOCK regulates the transcription of *PERIOD* and PERIOD was shown to reset the circadian clock to light cues [17]. The SCN is connected to several wake- and sleep-active brain regions [18]. The activity of wake- and sleep-active brain regions is mutually exclusive. This is ensured by a so-called flip-flop switch [19]. Wake-active neurons are located in the locus coeruleus (LC), tuberomammillary nucleus (TMN) and the Raphe nuclei. These brain regions release monoaminergic neurotransmitters like noradrenaline, histamine, dopamine and serotonin to inhibit sleep-promoting brain regions and to keep the organism awake. Additionally, this active arousal system gets reinforced and stabilized by orexinergic neurons. In sleep however, sleep-promoting brain regions like the ventrolateral preoptic nucleus (VLPO) release γ-aminobutyric acid (GABA) and the neuropeptide galanin to inhibit wake-promoting brain regions [20,21]. Also orexinergic neurons are inhibited, what further diminishes the activity of wake-active brain regions [19] (**Figure 1**).

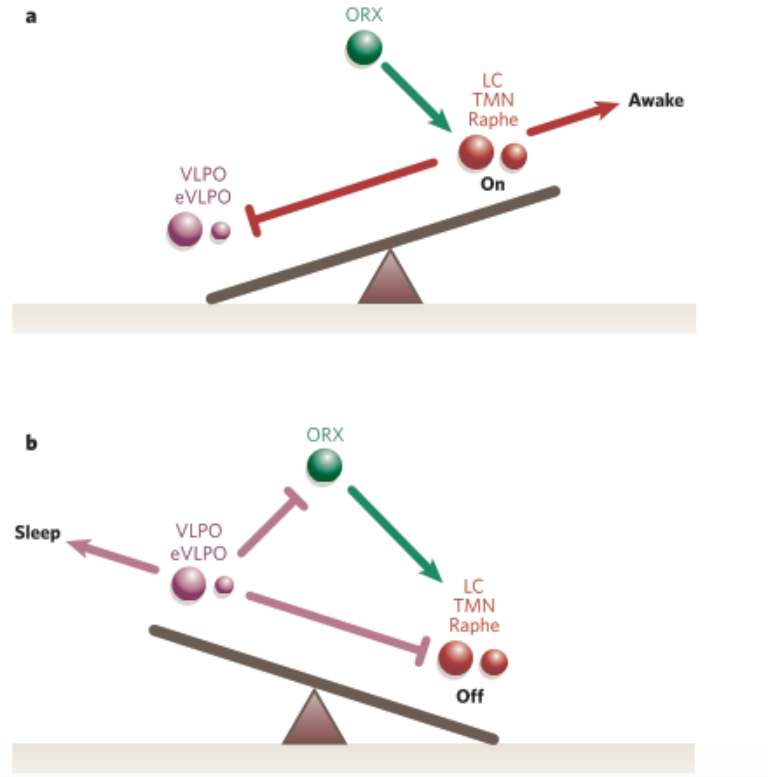

Figure 1. Sleep in mammals is regulated by a flip-flop switch.

Working principle of the mammalian flip-flop switch is depicted as a scheme. Activity of wake-active and sleep-active brain regions is mutually exclusive.

A) Working principle of the mammalian flip-flop switch in wakefulness. Wake-active neurons (depicted in red) are located in the locus coeruleus (LC), in the tuberomammillary nucleus (TMN) and in the Raphe nuclei. These neurons release monoaminergic neurotransmitters to inhibit sleep-active brain regions, which can be found at the ventrolateral preoptic nucleus (VLPO) and the extended ventrolateral preoptic nucleus (eVLPO) (depicted in violet). Orexinergic neurons (ORX, depicted in green) additionally stabilize and reinforce the active arousal system.

B) Working principle of the mammalian flip-flop switch in sleep. To establish the sleep-state, sleep-active neurons inhibit wake-active brain regions via GABA and the neuropeptide galanin. The sleep state is additionally stabilized by the inhibition of orexinergic neurons. The figure was taken from [18].

1.1.3 Sleep homeostasis

Despite the circadian clock, sleep is also under homeostatic control. Sleep homeostasis can be understood as a prolonged period of sleep following a prolonged period of wakefulness. The subsequent sleep period after a prolonged period of wakefulness is enriched with slow wave activity (SWA). SWA describes slow, synchronized and oscillatory activity in EEG data. In mammals, both REM and NREM sleep are under homeostatic control [22]. Borbély introduced in 1982 a two-process model for the regulation of sleep homeostasis [23]. In his model, Borbély

described an increase in the sleep propensity ("sleep pressure") with a prolonged time spend awake. The longer an organism is awake, the more sleep pressure is accumulated in the brain. Consequently, it takes longer until the sleep pressure is dissipated by a recovery sleep [23]. Experimental data could prove that in humans and animals neuronal activity is one of the driving forces for sleep homeostasis. Brain regions, which were more active during prolonged wakefulness, show more SWA during the subsequent sleep period [24–26]. In general, sleep homeostasis is believed to have a frontal dominance because the largest SWA is found in frontal brain regions [27,28]. It is possible that mechanisms regulating sleep homeostasis partly overlap with mechanisms regulating the spontaneous wake-sleep cycle. For example, cytokines are upregulated during prolonged wakefulness, but their inactivation causes a decrease in the sleep amount during the spontaneous wake-sleep cycle [29–31].

1.1.4 Sleep functions

Very early in sleep research it turned out that sleep deprivation is the best tool to study functions of sleep. As indicated by the various functions of sleep/ homeostatic factors sleep restriction can induce multiple changes, amongst others in behavior, energy metabolism, brain functions and in the immune system [32]. Regarding behavior, tiredness can cause loss in productivity, decrease in mood and sleep loss makes it more difficult to understand logical problems [33]. Regarding energy metabolism, sleep is hypothesized to serve as an energy saving function. During sleep the caloric use is reduced, which allows energy stores to be refilled [34]. Experimental proof for that was found in sleep deprived rats. Sleep deprived rats show increased food intake, increased metabolic rate, weight loss and finally, within weeks, lethality [35]. However, the energy saving function of sleep seems to be restricted to NREM sleep. Surprisingly, REM sleep was reported to have even higher energy consumptions than the wake state [34,36]. Regarding brain functions, sleep serves the removal of neurotoxic metabolites. It was shown that sleep is capable of preventing the accumulation and aggregation of extracellular amyloid-β, which is involved in Alzheimer's disease [37]. Furthermore, sleep is fundamental for memory formation and consolidation. For example, new experiences are temporally stored in the hippocampus and during the subsequent sleep period transferred to the neocortex [38]. As major process of memory

consolidation, synaptic plasticity is relying on sleep [39,40]. New synapses are formed during wakefulness, but particularly during NREM sleep synapses are downscaled. The maintenance of postsynaptic excitability by regulating the synaptic strength ensures functional neuronal plasticity and synaptic homeostasis [41]. Finally, sleep is also essential for immune functions. There was evidence found for that in sleep-deprived rats. Blood samples of sleep deprived rats show a reduced amount of lymphocytes [42]. Furthermore, in mice with a fragmented sleep pattern, it was shown that they have lowered capability to fight cancer [43]. Additionally, Besedovsky and co-workers showed in 2012 that during sleep T-cells are redistributed to the lymph nodes [44].

1.2 *C. elegans* as a model organism for sleep research

1.2.1 Sleep conservation

C. elegans can be used as a model organism for sleep research because as mentioned before, sleep is found in all organisms having a nervous system. It was even detected in basal metazoans, like cnidarians. Therefore, it is hypothesized that sleep evolved together with the nervous system [10,45,46] and that sleep regulating pathways are conserved [47–49]. In agreement to that, *C. elegans* possesses sleep-inducing pathways also found in other species like nucleotide-dependent kinases [4,48], epidermal growth factor (EGF) signaling [50], Notch signaling [51], sleep-regulating neurotransmitters like dopamine and serotonin, potassium channels and neuropeptidergic signaling [52–56]. A perfect example of sleep research in *C. elegans* transferring to other organisms and even humans, was made by the identification of the AP2 transcription factor as a sleep regulator in *C. elegans* [57]. A neuronal RNAi knockdown of the Drosophila homolog TfAP2 leads to nearly abolished night sleep in the fruit fly [58]. In humans, mutations in TFAP2β cause the Char syndrome which is, amongst others, connected to insomnia [59].

1.2.2 *C. elegans* life cycle

Another reason why *C. elegans* is a perfect model organism to use, is its short generation time. *C. elegans* belongs to the group of ecdysozoa (molting animals) and can be naturally found in rotting material [60]. It mainly feeds on bacteria. At a temperature of 22°C *C. elegans* develops from egg to adulthood in only 2.5 days. Its embryogenesis is split in a development *in utero* and *ex utero* until the worm hatches. Thereby, the cell lineage through the embryonic development is invariant [61,62]. Hatched worms go through four larval stages numbered from L1 to L4 stage. After each of these stages *C. elegans* enters the *lethargus*, which is a phase of behavioral quiescence. In the course of this work, lethargus and sleep have synonymous meanings. This phase is finished with the shedding off the old cuticle. After the fourth molt *C. elegans* reaches adulthood [63]. There are two sexes in *C. elegans*, self-fertilizing hermaphrodites (XX) and males (X0). Naturally, males occur to a percentage of 0.1% by spontaneous non-disjunction in the germline of the hermaphrodite. Through mating the percentage of males is increased up to 50 %. Mating can be used to easily move mutations between strains. The use of hermaphrodites however, allows easy maintenance of mutant strains. Through the hermaphrodites' self-fertilization genetically identical offspring is produced [64] (**Figure 2**).

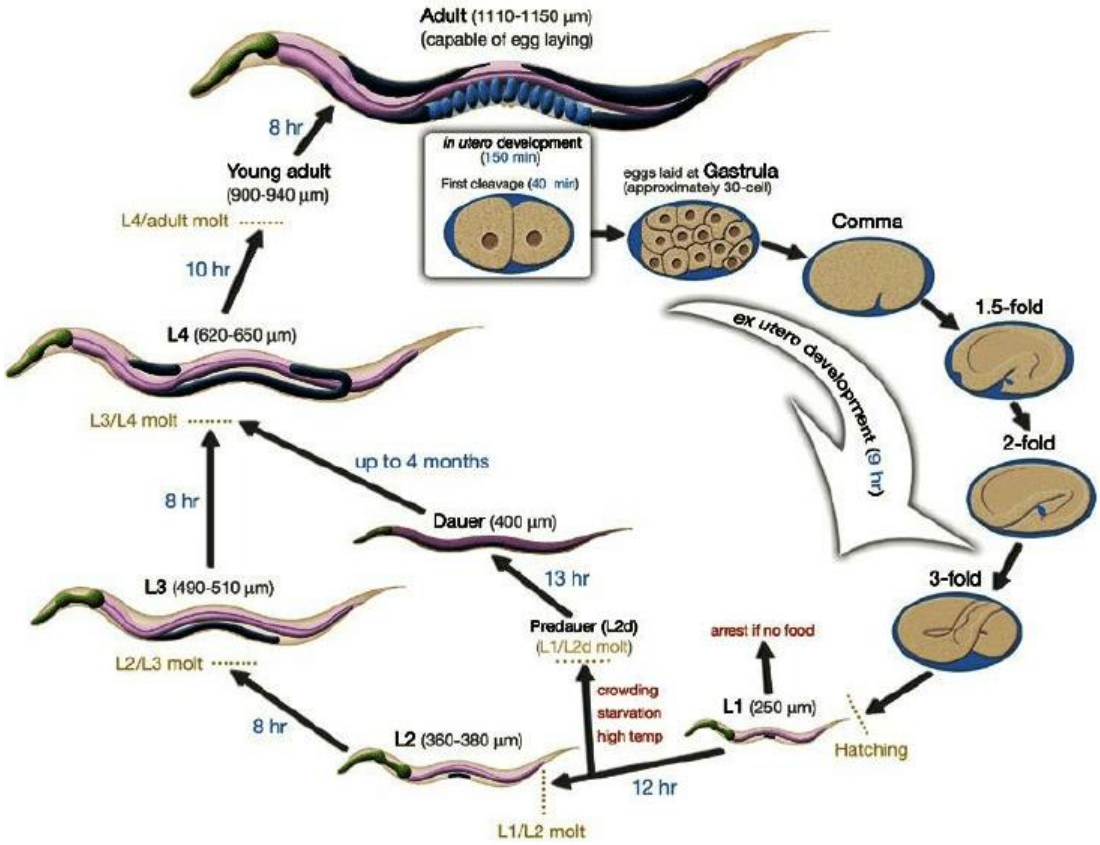

Figure 2. *C. elegans* reproducing life cycle.

At 22°C *C. elegans* develops from egg to mature adult hermaphrodite in around 2.5 days. Being laid, *C. elegans* eggs go through five stages of *ex utero* development before hatching. After hatching, worms go through four larval stages, which are numbered from L1 to L4. Larval stages are separated from another by a period of behavioral quiescence and a molting phase. Under environmentally unfavorable conditions, worms can enter a dauer stage. Blue numbers indicate the duration of each stage. Worm sizes at individual stages are indicated in brackets. This figure was adopted from [64].

The reproducing *C. elegans* can enter two "resting" stages to overcome environmentally unfavorable conditions. If the worm hatches and no food is available, it enters the L1 arrest stage. Arrest refers to the arrest of development. In L1 arrest worms can survive for weeks and it is reversible. As soon as food is available again, worms continue their development through all four larval stages [65]. The second "resting" state happens later in development. It can be viewed as an alternative L3 stage and is induced in L2 larvae by the absence of food. Starved L2 larvae directly molt into so called "dauer larva". In dauer larva development is also arrested. In case of a return to better living conditions, worms molt and continue their development as slightly different L4 larvae [66,67].

1.2.3 *C. elegans* nervous system

Comparable to the short and easy life cycle, *C. elegans* also possesses a simple nervous system. In 1986, John White et al. published a complete overview of all neuronal connections in the adult hermaphrodite [68]. This was possible, because neuronal connections in *C. elegans* are invariant. Additionally in 2012 the male connectome was published [69].

All in all, the *C. elegans* nervous system comprises 302 neurons, which can be grouped into 120 neuronal classes according to their topology and synaptic connectivity. Neurons are connected with around 6400 synapses and further 900 gap junctions. Neurons and muscles are connected with around 1500 neuromuscular junctions. Most of the neuronal cell bodies are clustered together into ganglia, which are located either in the head or tail of the worm [70]. Neurotransmitters used by the *C. elegans* nervous system are classical ones like acetylcholine, dopamine, GABA, glutamate and serotonin. However, special to the *C. elegans* nervous system is the use of tyramine instead of noradrenaline and octopamine instead of histamine [68,71]. One neuron can make use of more than one neurotransmitter. Also neuropeptides are used for signal transduction within the nervous system. The *C. elegans* genome encodes in total 113 neuropeptide precursor genes, which are processed to potentially 250 neuropeptides [72]. Out of the 113 neuropeptide precursor genes 40 encode insulin-like peptides [73,74], 31 genes encode FMRFamide-related peptides (short FLP's) [75,76] and 42 genes encode non-insulin and non-FMRFamide-related peptides (short: NLP's) [77,78].

Regarding the physiology of neurons, *C. elegans* was long believed to be an exception because of its lack of classical action potentials. There was rather experimental proof that *C. elegans* neurons function via graded electrical potentials and graded synaptic transmission [79–87]. Nevertheless, very recently Liu, Kidd, Dobosiewicz and Bargmann claimed that they were able to show the presence of an all-or-none action potential in the AWA olfactory neurons in *C. elegans* [88].

1.2.4 Developmental sleep in *C. elegans*

One type of sleep in *C. elegans* is connected to its development. As descript earlier, larvae enter a lethargus phase after each of their four larval stages. Lethargus fulfills all behavioral criteria to be classified as sleep [4,6,55,66,89–94]. The most important criteria worms display during lethargus are shown here:

1. behavioral quiescence [4,89]
2. specific and relaxed body posture [94]
3. increased arousal threshold and overall reduction of neuronal activities [93,95]
4. reversibility [92]
5. homeostatic regulation [4].

In lethargus, worms go through alternating sequences of motion (wake) and quiescence (sleep) bouts. Quiescence bouts are characterized by increased immobility and increased arousal thresholds. During motion bouts, worms are less immobile and show decreased arousal thresholds [89,90,96].

1.2.4.1 Genetic control of developmental sleep in *C. elegans*

The timing of larval molts and therefore, indirectly, the timing of lethargus is controlled by gene oscillation [97]. The heterochronic gene *lin-42* is one of the genes oscillating with the molting cycle. *lin-42* mRNA levels peak during intermolt phases but decline dramatically in temporal proximity to the molt. LIN-42 function is particularly interesting, because it is the protein in *C. elegans* with the highest similarity to the PERIOD protein family of circadian clock regulators in insects and mammals [98]. LIN-42 regulates the expression of the neuropeptide NLP-22, which was shown to be sleep-regulatory by Nelson et al. in 2013 [53] . *nlp-22* mRNA levels cycle in synchrony with lethargus. Ectopic *nlp-22* overexpression in active worms leads to cessastion of locomtion and feeding.

Not all sleep-regulating elements oscillate in their expression, as it is the case for EGL-4. It is a cGMP-dependent protein kinase (PKG) and its function in sensory neurons promotes quiescence. *egl-4* (lf) mutants show an overall reduction of

quiescence during the L4/YA lethargus. *egl-4*(gf) mutants however, undergo ectopic sleep phases both in larval and in the adult stage [4]. EGL-4 signaling partly overlaps with EGF (epidermal growth factor) signaling to induce sleep. In 2007, van Buskirk and Sternberg descript a role for the EGF ligand LIN-3 in sleep induction [50]. They could show that ectopic expression of LIN-3 at any stages induces the reversible cessation of feeding and locomotion. The cessation of locomotion due to LIN-3 overexpression was abolished in the *egl-4*(lf) mutant background.

Singh et al. described in 2011 that EGL-4 activity is also required to induce quiescence via Notch signaling [51]. They could show that the overexpression of *osm-11*, a gene encoding a co-ligand of Notch receptors, causes anachronistic quiescence in adults. This quiescence was suppressed in the *egl-4*(lf) mutant background. Furthermore, they proposed a model, in which Notch signaling levels represent arousal levels during the L4/YA lethargus. Increased Notch signaling leads to an increased arousal threshold and consequently to increased quiescence. Huang, Zhu, Skuja, Hayden, and Hart identified in 2017 genes acting downstream of Notch signaling by screening for suppressors of the *osm-11* overexpression induced anachronistic quiescence in adults [99]. They found the $G\alpha_0$ protein GOA-1 and the $G\beta_5$ protein GBP-2. Both of them function in G protein signaling pathways. Very recently, in 2018, the same group described a role for gap junction innexins in sleep-regulation [100]. UNC-7 and UNC-9 function together to build gap junctions. Single loss-of-function mutants and the double mutant show dramatically reduced amounts of quiescence in L4/YA lethargus. Despite sleep quantity, these mutations also impact sensory neuron responses in lethargus and that way they determine arousal thresholds [100].

1.2.4.2 RIS as a sleep-active neuron

On the neuronal level the single interneuron RIS plays a major role in sleep regulation. In 2013, it was shown by Turek et al. to be a direct sleep-active neuron [57]. Direct sleep-active neurons strongly depolarize at the sleep onset and release inhibitory neurotransmitters, like GABA or neuropeptides. The name “sleep active” resides from the fact that the depolarization of these neurons coincides with the sleep

onset. In agreement to that RIS is GABAergic and peptidergic, it strongly depolarizes at the sleep onset and it releases the FLP-11 neuropeptide to actively induce sleep [55,57]. The expression of FLP-11 in RIS is regulated by the AP2 transcription factor APTF-1. *aptf-1* mutants also show RIS depolarization at the sleep onset. However, in these mutants RIS depolarization does not cause immobilization. At the sleep onset, *aptf-1* mutants stop feeding as it is seen in Wild-type worms but do not immobilize [57].

To date the neuronal regulation of RIS is only barely understood. As published in the *C. elegans* connectome by White, Southgate, Thomson and Brenner in 1986, RIS receives synaptic input from six upstream neurons, which is little compared to other interneurons [68]. A schematic overview of chemical synapses and gap junction between RIS and its upstream neurons is shown in **Figure 3.**

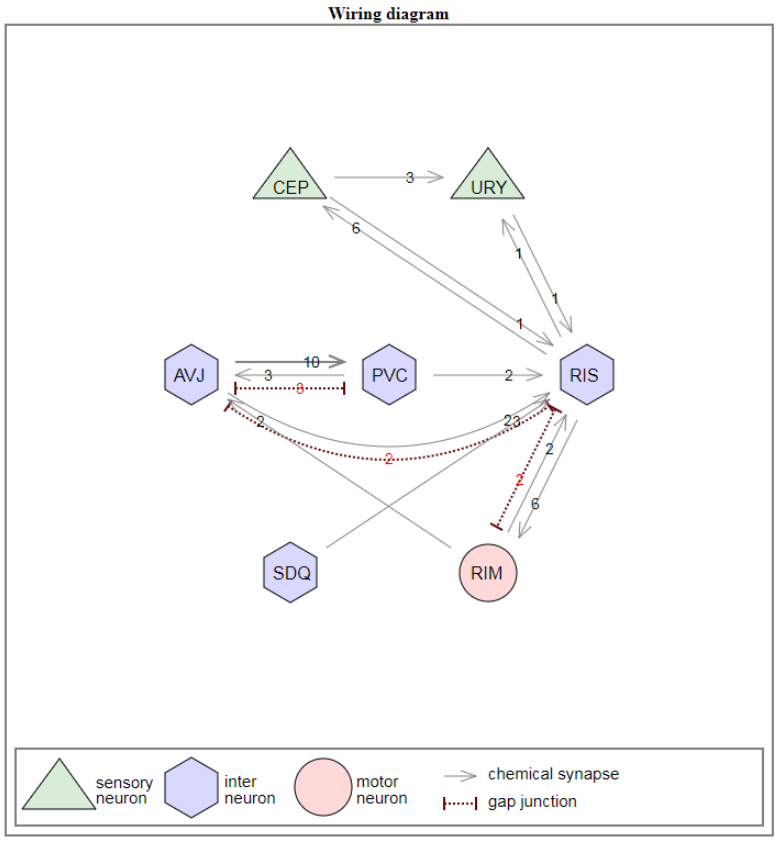

Figure 3. Wiring diagram of RIS and presynaptic neurons.

According to the White connectome, RIS is postsynaptic to six neurons [68]. Different neuron classes are indicated in the figure as well as the presence of chemical synapses and gap junctions between neurons including numbers. The scheme was designed using the online tool: Connectivity of *C. elegans* for computation [114].

1.2.5 Other types of quiescence in *C. elegans*

Starvation can induce quiescence in *C. elegans* larvae. As described previously, larvae enter a developmentally arrested state if there is no food available when they are freshly hatched. Colleagues of mine were able to show very recently that 1d-old starved L1 arrest larvae go through phases of behavioral quiescence and that the quiescence seen in those larvae fulfills all criteria to be considered as sleep. Under those conditions sleep does not necessarily occur to save energy but to limit the progression of aging processes [101]. Similarly to the L1 arrest state, dauer larvae also display a strong overall reduction of locomotion. Again colleagues of mine detected the occurrence of sleep bouts in dauer larvae. Both for L1 arrested larvae and dauer larvae, they correlated sleep bout onsets with increased RIS activity [66,101,102]. This again underlies the importance of RIS in sleep induction not only throughout lethargus but also in starvation induced quiescence.

However, behavioral quiescence also occurs in the adult worm. There it can be induced by food related cues, as for example by high quality food. The so-called "satiety quiescence" requires signals from the intestine and is mediated by insulin and transforming growth factor beta (TGFβ) signaling [103]. Other cues inducing quiescence in adult worms are environmental stressors, like heat stress. Heat stress activates the ALA interneuron and leads to the release of the neuropeptide FLP-13. Despite releasing FLP-13, ALA mediates sleep induction via EGF and Notch signaling [50,51,54].

2 Thesis aims

Throughout its life cycle, *C. elegans* displays three different kinds of quiescence behavior. Two of them were proven to be present in the adult worm: 1) satiety quiescence, which is induced by high quality food or a high food amount; 2) stress-induced sleep, which can be caused by heat stress or cellular damage [50,51,54,103]. However, in my thesis I focused on the quiescence behavior, which is directly connected to the development of *C. elegans*. It occurs after each of its four larval stages. This quiescence behavior was shown by Raizen et al. in 2008 to be sleep [4]. From this point onwards I refer to it as sleep or lethargus.

Around five years later, in 2013, Turek et al. confirmed the presence of a sleep-active neuron in *C. elegans*, which is the RIS neuron[57]. RIS functions as motor for sleep induction and is specified by its inactivity outside of lethargus. However, at the sleep onset it undergoes an astonishing increase in activity. This contrasts the behavior of all other neurons of the *C. elegans* nervous system, whose activities are dampened in lethargus.

When I started my thesis in 2015, RIS was well established as a sleep-active neuron in *C. elegans*. What was not known, were the neuronal circuits regulating the activity of RIS. The same was true for RIS downstream targets.

Taking all of that into consideration, I chose my thesis aims as follows:

1. **Identify sleep-regulating pathways upstream of RIS.**
   All RIS presynaptic neurons are known from the *C. elegans* connectome [68]. RIS presynaptic neurons were either optogenetically depolarized or hyperpolarized and RIS activity was measured simultaneously. Experiments were done both outside of and in lethargus.

2. **Identify sleep-regulating neurotransmitters and neuropeptides in *C. elegans*.**

   Sleep-regulating neurotransmitters or –peptides were already known from other systems. It is well established that the neurotransmitter GABA and other neuropeptides regulate sleep in humans. In 2013, Turek et al. showed that also RIS uses GABA and neuropeptides to induce sleep [57]. It was my task to test for the potential presence of further sleep regulating neurotransmitters and neuropeptides. To do so, I repeated the screening experiments described in Aim 1 in neurotransmitter and neuropeptide mutants. The results from Aim1 were used as indication of which neurotransmitters and neuropeptides could possibly be of interest.

3. **Design a circuit model for RIS regulation in lethargus.**

   Using the results from Aim 1 and 2, a circuit model for the regulation of RIS in lethargus was designed. This model, additionally, presents ideas of how sleep and therefore RIS regulation function in a feedback, to mediate arousal levels and sleep homeostasis.

4. **Find a suppressor of the *aptf-1* mutant phenotype.**

   RIS fails to induce quiescence in lethargus of *aptf-1* mutants. To understand more about potential downstream targets of RIS, I did an EMS mutagenesis of *aptf-1* mutants. After the mutagenesis I successfully isolated two candidate lines, which regained the ability to immobilize in lethargus. Potential candidate lines were subjected to whole genome sequencing and to EMS-based mapping.

3 Material and methods

3.1 *C. elegans* maintenance

C. elegans were grown on plates made out of nematode growth medium (NGM). These plates were seeded with OP50 *E. coli* bacteria [63]. Plates were placed at 15, 20 or 25°C as needed.

3.2 *C. elegans* strains

Throughout this work the following strains were used **Table 1**.

Table 1: List of used *C. elegans* strains throughout this work.

Strain name	Genotype	Back crosses
N2	Wild-type (Bristol)	
HBR227	*aptf-1*(gk794) II.	10x
HBR531	*yxIs1[pglr-1::GCaMP3.35, punc-122::gfp], aptf-1(gk794) II.*	
HBR560	*goeIs120[ptdc-1::SL1-GCaMP3.35-SL2::mKate2-unc-54-3'utr,unc119(+)].*	2x
HBR1118	*aptf-1(gk794) II,goeIs120[ptdc-1::SL1-GCaMP3.35-SL2::mKate2-unc-54-3'utr,unc119(+)].*	
HBR1151	*unc-119(ed3) III, goeIs268[aptf-1-5'utr::SL1-GCaMP3.35-SL2::aptf-1-3'utr,unc-119(+)].*	
HBR1161	*unc-119(ed3) III, goeIs273[tdc-1::ReaChR::mKate2-unc-54-3'utr,unc-119(+)].*	
HBR1177	*goeIs268[aptf-1-5'utr::SL1-GCaMP3.35-SL2::aptf-1-3'utr,unc-119(+)]; egl-3(ok979) V.*	
HBR1228	*goeIs268[aptf-1-5'utr::SL1-GCaMP3.35-SL2::aptf-1-3'utr,unc-119(+)].*	2x
HBR1361	*goeIs304[pflp-11::SL1-GCaMP3.35-SL2::mKate2-unc-54-3'UTR, unc-119(+)].*	2x
HBR1374	*goeIs307[flp-11 prom::ArchT::SL2mKate2-unc-54-3'utr,unc-119(+)], goeIs304[pflp-11::SL1-GCaMP3.35-SL2::mKate2-unc-54-3'UTR, unc-119(+)].*	
HBR1391	*goeIs268[aptf-1-5'utr::SL1-GCaMP3.35-SL2::aptf-1-3'utr,unc-119(+)]; goeIs273[tdc-1::ReaChR::mKate2-unc-54-3'utr,unc-119(+)]*	

HBR1394	*tdc-1 (n3420) II;goeIs268[aptf-1-5'utr::SL1-GCaMP3.35-SL2::aptf-1-3'utr,unc-119(+)]; goeIs273[tdc-1::ReaChR::mKate2-unc-54-3'utr,unc-119(+)]*	
HBR1463	*goeIs307[flp-11 prom::ArchT::SL2mKate-2-unc-54-3'utr,unc-119(+)].*	2x
HBR1464	*goeIs315[pflp-11::ReaChR::mKate2-unc-54-3'UTR, unc-119(+)].*	2x
HBR1465	*goeIs120[ptdc-1::SL1-GCaMP3.35-SL2::mKate2-unc-54-3'utr,unc119(+)]; goeIs315[pflp-11::ReaChR::mKate2-unc-54-3'UTR, unc-119(+)].*	
HBR1472	*goeIs268[aptf-1-5'utr::SL1-GCaMP3.35-SL2::aptf-1-3'utr,unc-119(+)]; goeIs307[flp-11 prom::ArchT::SL2mKate-2-unc-54-3'utr,unc-119(+)]*	
HBR1478	*goeIs268[aptf-1-5'utr::SL1-GCaMP3.35-SL2::aptf-1-3'utr,unc-119(+)]; goeEx557[pgcy-13-ArchT-mkate-2-unc-54-3´-utr,unc-119(+)]*	
HBR1482	*goeIs268[aptf-1-5'utr::SL1-GCaMP3.35-SL2::aptf-1-3'utr,unc-119(+)]; goeEx561[pgcy-13-ReaChr-mkate-2-unc-54-3´-utr,unc-119(+)]*	
HBR1533	*goeIs268[aptf-1-5'utr::SL1-GCaMP3.35-SL2::aptf-1-3'utr,unc-119(+)]; goeIs273[tdc-1::ReaChR::mKate2-unc-54-3'utr,unc-119(+)]; flp-18(db99) X*	
HBR1537	*goeIs268[aptf-1-5'utr::SL1-GCaMP3.35-SL2::aptf-1-3'utr,unc-119(+)]; goeIs308[dat-1 prom::ReaChR::mKate2-unc-54-3'UTR, unc-119(+)].*	
HBR1572	*goeIs268[aptf-1-5'utr::SL1-GCaMP3.35-SL2::aptf-1-3'utr,unc-119(+)]; goeIs273[tdc-1::ReaChR::mKate2-unc-54-3'utr,unc-119(+)]; flp-18(db99) X.; tdc-1(n3420) II.*	
HBR1589	*goeIs268[aptf-1-5'utr::SL1-GCaMP3.35-SL2::aptf-1-3'utr,unc-119(+)], goeIs330[pnmr-1::ArchT::mKate-2-unc-54-3'utr,unc-119(+)].*	
HBR1597	*unc-119(ed3) III, goeIs268[aptf-1-5'utr::SL1-GCaMP3.35-SL2::aptf-1-3'utr,unc-119(+)], goeIs332[pnmr-1::ReaChr::mKate2-unc-54-3'utr,unc-119(+)].*	
HBR1793	*goeIs268[aptf-1-5'utr::SL1-GCaMP3.35-SL2::aptf-1-3'utr,unc-119(+)]; goeIs293[tol-1 prom::ReaChr::mKate2-unc-54-3'utr,unc-119(+)].*	
HBR1799	*unc-119(ed3) III, goeIs402[ptol-1::ArchT2::SL2-mKate2-unc-54-3'UTR, unc-119(+)].*	
HBR1844	*goeIs268[aptf-1-5'utr::SL1-GCaMP3.35-SL2::aptf-1-3'utr,unc-119(+)], goeIs340[dat-1 prom::ArchT::SL2mKate2unc-54-3UTR].*	
HBR1845	*goeIs268[aptf-1-5'utr::SL1-GCaMP3.35-SL2::aptf-*	

	1-3'utr,unc-119(+)], goeIs370[plad-2::ReaChR::mKate2-unc-54-3'UTR, unc-119(+)].	
HBR1873	*goeIs268[aptf-1-5'utr::SL1-GCaMP3.35-SL2::aptf-1-3'utr,unc-119(+)]; goeIs373[plad-2::ArchT::SL2-mKate2-unc-54-3'UTR, unc-119(+)].*	
HBR1982	*goeIs402[ptol-1::ArchT2::SL2-mKate2-unc-54-3'UTR, unc-119(+)]; goeIs304[pflp-11::SL1-GCaMP3.35-SL2::mKate2-unc-54-3'UTR, unc-119(+)].*	
HBR02019	*akIs11[pnmr-1::ICE], goeIs307[flp-11 prom::ArchT::SL2mKate2-unc-54-3'utr,unc-119(+)], goeIs304[pflp-11::SL1-GCaMP3.35-SL2::mKate2-unc-54-3'UTR, unc-119(+)].*	
HBR2021	*goeIs307[flp-11 prom::ArchT::SL2mKate2-unc-54-3'utr,unc-119(+)], goeIs304[pflp-11::SL1-GCaMP3.35-SL2::mKate2-unc-54-3'UTR, unc-119(+)], nmr-1(ak4) II.*	
HBR2039	*goeIs307[flp-11 prom::ArchT::SL2mKate2-unc-54-3'utr,unc-119(+)], goeIs120[ptdc-1::SL1-GCaMP3.35-SL2::mKate2-unc-54-3'utr,unc119(+)]*	
HBR2058	*goeIs304[pflp-11::SL1-GCaMP3.35-SL2::mKate2-unc-54-3'UTR, unc-119(+)]; goeEx716[ptbh-1::ReaChR::mKate2unc-54 3'UTR, unc119(+); unc-122::RFP]*	
HBR2103	*yxIs1[Pglr-1::GCaMP3.35.3, Punc-122::gfp].; nmr-1(ak4) II.*	
HBR2105	*aptf-1(gk794) II.; rod-1 (syb414) IV*	
HBR2128	*eat-4(ky5) III; goeIs304[pflp-11::SL1-GCaMP3.35-SL2::mKate2-unc-54-3'UTR, unc-119(+)].*	6x
HBR2169	*goeEx718[phlh-34::ReaChR::mKate2-unc-54-3'UTR, unc-119(+); myo-2::mCherry]; goeIs304[pflp-11::SL1-GCaMP3.35-SL2::mKate2-unc-54-3'UTR, unc-119(+)].*	
HBR2180	*goeEx725[phlh-34::ArchT::SL2mKate2-unc-54-3'UTR,unc-119(+); myo-3::mCherry]; goeIs304[pflp-11::SL1-GCaMP3.35-SL2::mKate2-unc-54-3'UTR, unc-119(+)].*	
AX1410	*flp-18(db99) X.*	
MT10661	*tdc-1(n3420) II.*	
MT6308	*eat-4(ky5) III.*	
PHX414	*rod-1 (syb414) IV*	
VC671	*egl-3(ok979) V.*	
VM487	*nmr-1(ak4) II.*	12x

ZC1148	*yxIs1[Pglr-1::GCaMP3.35.3, Punc-122::gfp].*	

3.3 Generation of transgenic strains

3.3.1 MultiSite Gateway cloning (Invitrogen)

All constructs were cloned using the MultiSite Gateway system (Invitrogen). LR reactions were performed following the protocol in the MultiSite Gateway User Manual with slight adjustments [104]. The plasmid pCG150 (Addgene plasmid #17247) was used as destination plasmid. Entry plasmid concentrations were calculated using the following formula:

$$\frac{size\ of\ entry\ plasmid\ (bp)}{size\ of\ destination\ plasmid\ (bp)} * 150\ ng * 3 = ng\ entry\ plasmid$$

The reaction mix, consisting of all entry plasmids and the destination plasmid, was filled up to a volume of 8 µL using 1x TE buffer, pH 8.0.

Before use, all constructs were sequenced to confirm their correctness. As sequencing method Sanger sequencing was used. A list of generated constructs is given in **Table 2**.

Table 2: List of generated constructs.

Construct number	Construct
K345	ptbh-1::ReaChR::mKate2-unc-54-3'UTR, unc-119(+)
K355	phlh-34:: ReaChR::mKate2-unc-54-3'UTR, unc-119(+)
K356	phlh-34::ArchT::SL2-mKate2-unc-54-3'UTR, unc-119(+)

3.3.2 Transformation of *E. coli*

3.3.2.1 Transformation of One Shot® TOP10 competent *E. coli* cells

One Shot® TO10 competent cells were transformed with the LR reaction mix following the description in the MultiSite Gateway User Maunal [104].

3.3.2.2 Transformation of *Dh5α E. coli* competent cells

For retransformations *Dh5α* competent cells were used. The amount of plasmid used was between 0.2-0.5 µL. The transformation was done as descripted for the One Shot® TOP10 competent cells.

3.3.3 Transformation of *C. elegans*

3.3.3.1 Transformation by microparticle bombardment

To generate stable low-copy integrated lines, *unc-119(ed3)* mutants were transformed following the ballistic transformation protocol described by Wilm, Demel, Koop, Schnabel, & Schnabel in 1999 [105]. Throughout the selection of successfully transformed worms, the unc-119 rescue fragment of the pCG150 plasmid was used as a selection marker [106].

3.3.3.2 Transformation by microinjection

To generate extrachromosomal arrays, worms were transformed by microinjection. Microinjections were done in Wild-type, mutant or transgenic strains. The injection mix was set up as follows:

construct: 30-100 ng/ µL
co-injection marker: 5–50 ng/ µL

If required, DNA concentration was raised to 100 ng/ µL with the pCG150.

Positively transformed worms were selected according to the presence of the co-injection marker.

3.4 Crossing of *C. elegans*

Crosses of *C. elegans* were performed following the standard procedure described by Brenner in 1974. The presence of mutated alleles was verified by PCR. Template DNA was isolated by lysing worms with ProteinaseK. A list of used primers is given in **Table 3**. The presence of transgenes was confirmed using fluorescent markers.

Back crosses were done against N2 Wild-type. Mutants or transgenic strains were back crossed at least 2 times.

Table 3: List of used primers.

Gen	Primer sequence
aptf-1(gk794)	5'-CGACAATCTTCCCAAAGACC-3' 5'-CGGATCGATTGCTAGAGAGG-3' 5'-GCTTGGACGGCTTTAGTTGA-3'
ArchT	5'-ACTTCATCGTCAAGGGATGG-3' 5'-CATGCAGATGGTGGAGAAGA-3'
eat-4(ky5)	5'-GGGGCGTTTCCTTTTCTTTA-3' 5'-AAAATGCTCCGACTCCGATT-3' 5'-ACAGATCCATACGGAAAAGTTC-3'
egl-3(ok979)	5'-TGGTCTGCGGGAAAGAATCA-3' 5'-CCTTTCGTCTCGTCTTTCCG-3' 5'-CACTCCGTCATCCATAATCGC-3'
flp-18(db99)	5'-CGAACGAATCAGCCATGTAA-3' 5'-GAGATTCGACGATGACACGA-3' 5'-GGCTTGGGAGGAAGATTTTT-3'
mKate	5'-AGTCAACTTCCCATCCAACG-3'

	5’-GCTCGACGTAGGTCTCCTTG-3’
nmr-1(ak4)	5’-TGCTGGTGACTTATGAGCCT-3’ 5’-TGCTGGCGATCTTACTGGAA-3’ 5’-CAACACCGATGCAGAGCTC-3’
rod-1(syb414)	5’-TTGCTGTCTGGAGCTGACAT-3’ 5’-AACGCATCCTACATCCCATC-3’
tdc-1(n3420)	5’-GAGGATCCACGCCAGAATGA-3’ 5’-CATGTGAATCCGCCCAGAAG-3’

3.5 Freezing of *C. elegans*

For long-term storage, *C. elegans* L1/ L2 larvae can be kept at -80°C [63]. Worms were washed off from freshly starved NGM plates with a freezing solution. The freezing solution contained glycerol up to 15% of the final volume. Washed off worms were transferred in cryovials and put in a Styrofoam, in which they gradually cooled down to -80°C. After 24 h the vials were transferred to their final freezer positions.

3.6 Imaging of *C. elegans*

Imaging was done at 20°C. Experiments were controlled either by an Andor or NIS software. Cameras used were an Andor iXon EMCCD camera, an Andor iXon Ultra EMCCD camera, an Andor Neo camera or a Nikon DS Qi2 camera. Worms were cultured in individual microchambers and scanned repeatedly using an automated stage (Prior Proscan 2/ 3).

3.6.1 Agarose hydrogel microchambers

For long-term imaging worms were placed in agarose hydrogel microchambers according to the procedure described previously [107,108]. L1 and L4 larvae were imaged both in and outside of lethargus. For L1 larvae, the chamber size was 190 x 190 x 15 μm. For L4 larvae, the chamber size was 370 x 370 x 25 μm. For L1 larvae imaging, 3-fold stage eggs were placed together with OP50 food bacteria in the

microchambers. For L4 larvae imaging, L3 larvae were placed together with food bacteria into the microchambers.

3.6.2 Differential interference contrast (DIC) imaging

A 100 W Halogen lamp or a CoolLED pE-100 was used as light source. Light was filtered through a standard infrared filter (Chroma) to generate infrared light. Protocols were designed either in a continuous or in a burst mode. For continuous imaging, a frame rate between 1 frame/4 seconds up to 1 frame /10 seconds was chosen. L1 and L4 larvae were imaged using a 10 or 20 x objective. For imaging in burst mode, 40 frames with a rate of 2 frames/ seconds in an interval of 10-15 minutes were taken. Burst mode imaging was only done for L1 larvae using a 40x oil objective.

3.6.2.1 Sleep bout analysis of *C.elegans*

Continuous DIC imaging was used for sleep bout analysis. Movies were selected from 3-4 hours before worms were completely out of molt (COM) up to the COM time point. Within the selected time period, worms were both in and outside of lethargus. Their amount of movement was quantified by frame subtraction. Frame subtraction was performed as described previously [4,89,90,109,110]. Sleep bout detection was done using MATLAB scripts written by my colleague Jan Konietzka (see paragraph **10.1.2**). A sleep bout was detected, if the worm was slower than 10-20 % of its wake speed and stayed immobile for at least 2 minutes. Sleep bout frequency, sleep bout duration and total time spend in quiescence were quantified. For comparison, mutants or transgenic worms were imaged in the same chambers as control animals.

3.6.3 Calcium imaging of *C. elegans*

Protocols for calcium imaging in *C. elegans* were described previously [57,93,94,111]. Calcium imaging was performed using genetically encoded calcium sensors. In this study, the calcium-sensitive probe GCaMP3.35 was used. It is derived from GCaMP3 and lacks the first 35 amino acids of GCaMP3. GCaMP3.35 was codon-optimized for

the use in *C. elegans*. mKate2 was co-expressed with GCaMP3.35 to control expression levels. GCaMP3.35 and mKate were expressed under neuron-specific promoters or promoters specific for a certain subset of neurons [93].

GCaMP3.35 was imaged using LED illumination (CoolLED, intensities ranged between 0.006 mW/ mm^2-2.24 mW/ mm^2 for 20 x magnification). Worms were only illuminated while exposure. For light filtering, a standard set of GFP and Texas Red filters was used. In the GFP channel exposure times were set to 5–30 ms to enable imaging of moving worms without getting blurry images. The EM Gain was set to values between 100-200. Fluorescent images were taken every 4–10 seconds. DIC images were taken in the same interval to evaluate the behavior and developmental state of the worm. Worms were imaged using a 20 x objective and a 0.7 lens in front of the camera.

3.6.3.1 Extraction of neuronal activities

To extract neuronal activities, movies were selected using DIC images. The selection was done either starting 2 hours before sleep until the end of sleep or COM-4 hours until the COM time point. Worms were scored as awake, if they were pumping. Fluorescent signals were cut out manually or automatically using homemade MATLAB routines (for MATLAB scripts see paragraph **10.1.1)**. Both intensity values and signal xy coordinates were extracted. The xy coordinates were used to calculate speed values. During analysis, data was normalized to calculate activity levels over baselines. Normalization was done for every individual worm. Afterwards, data was averaged for all worms of the same genotype.

3.6.4 Optogenetics in *C. elegans*

Optogenetic experiments using microchambers were described previously [55]. To excite neurons, a red-shifted variant of channelrhodopsin (ReaChR) was used. Channelrhodpsins are non-selective cation channels [112]. To inhibit neurons, ArchT was used. ArchT stands for archaerhodopsin from the *Halorubrum* strain TP009 and is an outward rectified proton pump [113]. Both ReaChR and ArchT were expressed

using neuron-specific promoters or promoters specific for a group of neurons. For optogenetic imaging, worms were prepared the evening before. In case of experiments performed with L1 larvae, L4 larvae or young adult worms were placed on NGM plates supplemented with 0.2 mM all-*trans* Retinal (ATR, Sigma) the night before. Plates were incubated overnight on 25°C. In case of optogenetic experiments using L4 larvae, a chunk of worms was transferred to ATR-containing plates and placed overnight on 25°C. Next day, either eggs or L3 larvae were placed in microchambers the without any additional supplementation of ATR. During the imaging process, ReaChR and ArchT were stimulated using a LED at 585 nm with intensities between 0.017 mW/ mm^2-3.54 mW/ mm^2 for a 20 x objective (intensities were measured with an optical power meter).
The standard optogenetic protocol was repeated for individual worms every 15 or 30 minutes and is described in the following:

1. Baseline measurements for 1-3 minutes
2. Optogenetic stimulation for 1minute; tools were stimulated in 2 second intervals
3. After stimulation measurements for 1-3minutes

L1 larvae were imaged using a 20 x objective and an additional 0.7 lens in front of the camera. L4 larvae were imaged using a 20 x objective.

Optogenetic experiments were also performed with fixed worms (fixation of worms is described in paragraph **3.6.6**). Protocols and procedures were the same as described above. Measurements were performed 2-4 times per animal. The time interval between each measurement was 2-5 minutes. The animal status was scored on the plate before fixation. For experiments, in which PVC neurons were optogenetically manipulated (**Figure 7** and **Figure 9**), two positions were defined during the imaging process. In one position a fluorescent image was taken and in the other position the optogenetic tool was stimulated.

3.6.5 Spinning disc imaging of *C. elegans*

To study expression patterns, an Andor Revolution spinning disc system was used. The system was equipped with two lasers (488 and 565 nm) and a Yokogawa X1 spinning disc head. For imaging, 60 x or 100 x oil objectives were used. Images were taken with an iXon EMCCD or an iXon Ultra EMCCD camera. For z-stack measurements, maximum intensity projections were calculated using the Andor software.

3.6.6 Fixation of *C. elegans*

Worms were fixated using three different methods and always directly picked into a drop of the fixating agent.

1. **Fixation using levamisol:**
   250 µL of 2 % high melting agarose were used to cast a thin agarose pad. Worms were fixated on this pad using 2 µL of 25 mM levamisol.

2. **Fixation using polystyrene beads:**
   Worms were fixated using 2 µL of polystyrene beads (Polysciences, polybead microspheres 0.10 µm #00876-15). The beads were used in combination with 10 % agarose.

3. **Fixation using levamisol and polystyrene beads:**
   For optogenetic experiments performed in the fixated L1 larvae, both fixation methods were combined. A thin agarose pad was cast out of 10 % agarose. 0.3 µL of polystyrene beads were pipetted on the pad. The drop with the worm in it was allowed to dry for 1-2 minutes. Next, a drop of 0.6 µL levamisol was added.

3.7 Statistical analysis

Statistical analysis was done using statistical tools implemented in the Origin software. To compare neuronal activities of the same genotype under different

conditions, the Wilcoxon-signed rank test was used. To compare data between two different genotypes, samples were tested for a normal distribution using a Shapiro-Wilk test. If samples were normally distributed, a student's t-test was done. In case of unequal variance of both samples, a Welsh-correction was performed. Not normally distributed data was statistically tested with a Kolmogorov-Smirnov test. For Figures 6 B, C and D no correction for multiple comparisons (Bonferroni correction or false discovery rate) was performed due to the small amount of comparisons. In the case of a very small amount of comparisons these corrections would rather lead to the elimination of correct positive results than the elimination of false positive results. Figure descriptions specify, which statistical testing was performed. Error bars represent SEM.

3.8 EMS mutagenesis of *C. elegans*

aptf-1 L4 larvae or young adult worms were mutagenized using standard protocols with a final EMS concentration of 47 mM [114]. Around 7000 worms were used and incubated 3.5 hours with the mutagenizing agent. After mutagenesis, each 2 viable hermaphrodites were picked on fresh plates. Starting from the next day, adult hermaphrodites were transferred every day on fresh plates for a duration of 3 days. Their offspring was screened by eye for immobilization in lethargus on plates. Immobilizing worms were separated on single plates. Worms were allowed to self-fertilize and the next generation was again scored for immobilization in lethargus on plates and in microchambers.

3.8.1 Back crossing of mutagenesis candidates

Potential candidate lines were back crossed 4 times with *aptf-1* mutants. The back crossing scheme was as follows:

1. Hermaphrodites of candidates were crossed with *aptf-1* homozygous mutant males, which additionally carried *aptf-1::GCaMP3.35*. These males were produced by heat shock following standard protocols [114].

2. F1 offspring was imaged in microchambers and scored according to their sex and quiescence behavior in lethargus. Immobilization in lethargus of heterozygous candidates indicated dominant mutations and missing immobilization in lethargus indicated recessive mutations in the gene of interest in the mutagenesis candidates.

3. Heterozygous males of step 1 were crossed with homozygous *aptf-1* mutant hermaphrodites, which did not carry *aptf-1::GCaMP3.35*.

4. Step 3 F1 offspring were scored for GCaMP positive worms. GCaMP positive worms were separated on fresh plates. Choosing GCaMP positive worms, ensured the successful crossing of worms in step 3.

5. F2 offspring of crossing step 3 were scored for their quiescence behavior in lethargus on plates. Immobilizing worms were separated on single plates.

6. To check for the homozygosity of genes of interest in candidate worms after back crossing, F3 offspring of crossing step 3 were scored for their quiescence behavior on plates and in microchambers. Candidate lines were assumed as homozygous after back crossing if all, out of at least 10, worms analyzed immobilized in lethargus in microchambers.

7. Homozygous worms were subjected to another round of the procedure described above (steps 1-6).

3.8.2 Complementation assays of mutagenesis candidates

Successfully back crossed candidates were subjected to complementation assays. Complementation assays allowed for the verification, whether 2 mutagenesis candidates carried a mutation in the same gene of interest. To do so, homozygous males of one candidate were crossed with hermaphrodites of the second candidate. Heterozygous F1 offspring were imaged in microchambers and scored according to their sex and quiescence behavior in lethargus. In complementation assays only those candidates were used, which carried recessive mutations in their genes of interest.

3.8.3 Isolation of genomic DNA

Genomic DNA was extracted from 4 x back crossed mutagenesis candidates 1 and 9. For genomic DNA extraction, worms were starved on NGM plates. Starved worms were washed off the plates with M9 buffer and washed in total 3 times using M9 buffer. Afterwards, worms were incubated at room temperature on a rotator. 2 hours later, worms were washed again 3 times using M9 buffer. In the last washing step, supernatants were removed and pellets were frozen overnight on -80°C.

Next day, genomic DNA was extracted using the Qiagen Gentra Purgene Kit following manual instructions. Optional steps 2 and 10a were omitted. Step 9 was modified. Centrifugation was performed 2 times as indicated in the protocol. Then supernatants were transferred in Eppendorf tubes and centrifugation was performed in a table centrifuge at 16000 g for a duration of 3 minutes. DNA quality was verified and DNA concentrations were measured using a Nanodrop. Additionally, DNA quality was verified using agarose gel electrophoresis.

3.8.4 Whole genome sequencing and statistical analysis

Procedures of whole genome sequencing and statistical analysis of sequencing results are described in chapter **4.9** in the results part.

4 Result

Results described in the paragraphs **4.1** to **4.7** are part of the manuscript we are currently writing with my colleague Inka Busack. The manuscript is entitled "A wake-active command interneuron circuit controls sleep-active neuron depolarization to govern sleep".

4.1 RIS activity outside of and in lethargus

The lethargus of *C. elegans* is divided into periods of increased and decreased mobility. They will be referred to as sleep and wake bouts, respectively. In spite of increased immobility, sleep bouts are connected to an increased arousal threshold. On the contrary, wake bouts are connected to lowered arousal. To characterize the role of RIS in sleep bout induction, we quantified RIS activity and mobility of worms in and outside of lethargus (**Figure 4**).

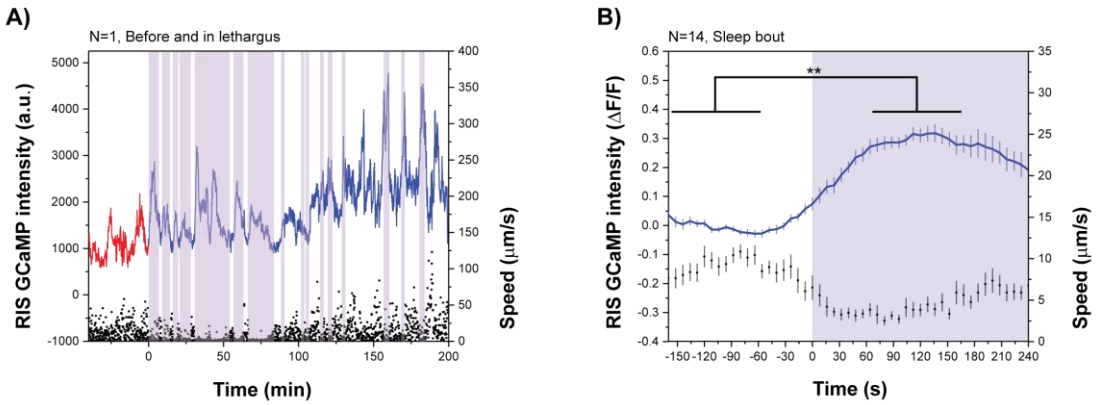

Figure 4. RIS activates at sleep bout onsets.

Worms were imaged in microchambers in and outside of lethargus. RIS activity was measured using GCaMP3.35. Speed data was extracted from neuron positions.

A) Sample trace of RIS activity and mobility of worms in and outside of lethargus. Red color indicates RIS activity outside of lethargus and blue color indicates RIS activity in lethargus. Speed data is depicted in black. Violet shading indicates sleep bouts. 0 denotes lethargus onset.

B) RIS activity in sleep bouts. Sleep bouts were extracted using the following criteria: 1) speed is lower than 10 % of the maximum speed of the worm and 2) the duration of low speeds is at least 2 minutes. RIS activity is shown in blue and speed data is shown in black. Violet shading indicates sleep bouts and 0 denotes sleep bout onsets. Error bars indicate SEM. Significance was calculated using a Wilcoxon-signed rank test. ** denotes statistical significance at $p < 0.01$.

RIS activity peaks correlated with the occurrence of sleep bouts in lethargus. Outside of lethargus no sleep bouts were detected. RIS activity levels in a sleep bout were significantly increased compared to levels before sleep bout onsets (**Figure 4**).

4.2 RIS optogenetic hyperpolarization

Sleep is subject to homeostatic control [66]. Hence we tested, whether RIS activity is also subject to homeostatic regulation. To do so we optogenetically hyperpolarized RIS, using a cell-specifically expressed ArchT. ArchT is a light-driven proton pump that gets activated by green light [113]. RIS activity was measured simultaneously using GCaMP3.35. (**Figure 5**).

The following data was generated by my former colleague Dr. Judith Besseling. She performed the imaging, extracted neuronal activities and speed data. I did the data averaging, quantification and statistical calculations on her data.

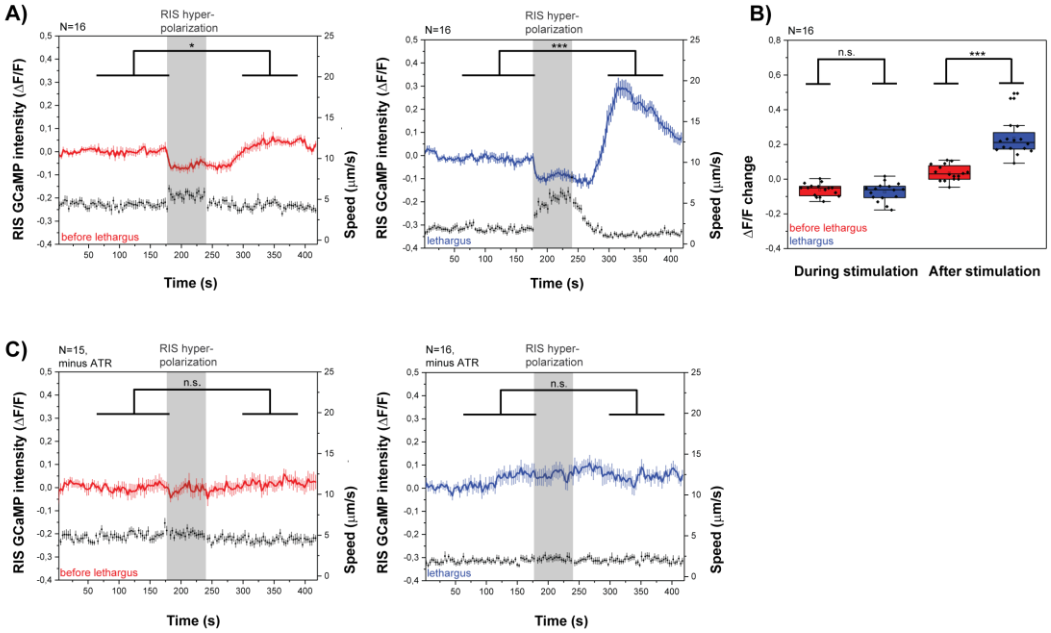

Figure 5. RIS activity is homeostatically regulated.

Worms were cultured overnight on ATR-containing plates and grown at 25°C. Imaging was done in microchambers in and outside of lethargus. RIS activity was measured using GCaMP3.35. RIS was hyperpolarized using ArchT. ArchT was stimulated with green light. Optogenetic measurements were repeated every 15 minutes.

A) RIS optogenetic hyperpolarization in and outside of lethargus. Red color indicates RIS activity outside of lethargus. Blue color indicates RIS activity in lethargus. Speeds are shown in black. Gray shading indicates stimulation periods. Error bars indicate SEM. Significance was calculated using the Wilcoxon-signed rank test. * denotes statistical significance at $p < 0.05$ and *** denotes statistical significance at $p < 0.001$.

B) Quantification of RIS activity levels during and after RIS optogenetic hyperpolarization in and outside of lethargus. To quantify RIS activity levels during the stimulation period, GCaMP data was averaged for the interval from 180 to 240 seconds. After the stimulation period, GCaMP data was averaged for the interval from 300 to 387 seconds. To compare levels during the stimulation period, a student's t-test was performed. To compare activity levels after the stimulation period, a Kolmogorov-Smirnov test was performed. *** denotes statistical significance at $p < 0.001$.

C) Control experiments. Same as in A, but worms were cultured on plates without ATR.

Optogenetic RIS inhibition led to a drop in its activity throughout the whole stimulation period. RIS activity levels during the stimulation period were comparable in and outside of lethargus. In both cases, the drop in RIS activity induced mobility. After the stimulation period, RIS activity rose above baseline levels. This effect, which I will be referring to as rebound activation, was six times stronger in lethargus than outside of lethargus (**Figure 5A and B**).

Control animals, which were grown without ATR supply, showed no significant change in their RIS activity levels (**Figure 5C**).

Data presented in **Figure 5** indicate that RIS depolarization is under homeostatic control outside of and in lethargus. However, the propensity for a rebound activation was increased in lethargus.

4.3 Dose-response curve of RIS optogenetic hyperpolarization

The next question was, whether the rebound activation is an acute or a chronic phenomenon. To answer this question, I did a dose-response curve and optogenetically inhibited RIS for different time intervals. I quantified the strength as well as the timing of the rebound activation (**Figure 6**). This experiment was a collaboration with my former colleague Dr. Judith Besseling. She imaged the worms, extracted neuronal activities and speed data for the 1-minute time point. I did the averaging, quantification and statistical analysis on her data and measured and analyzed the other time points.

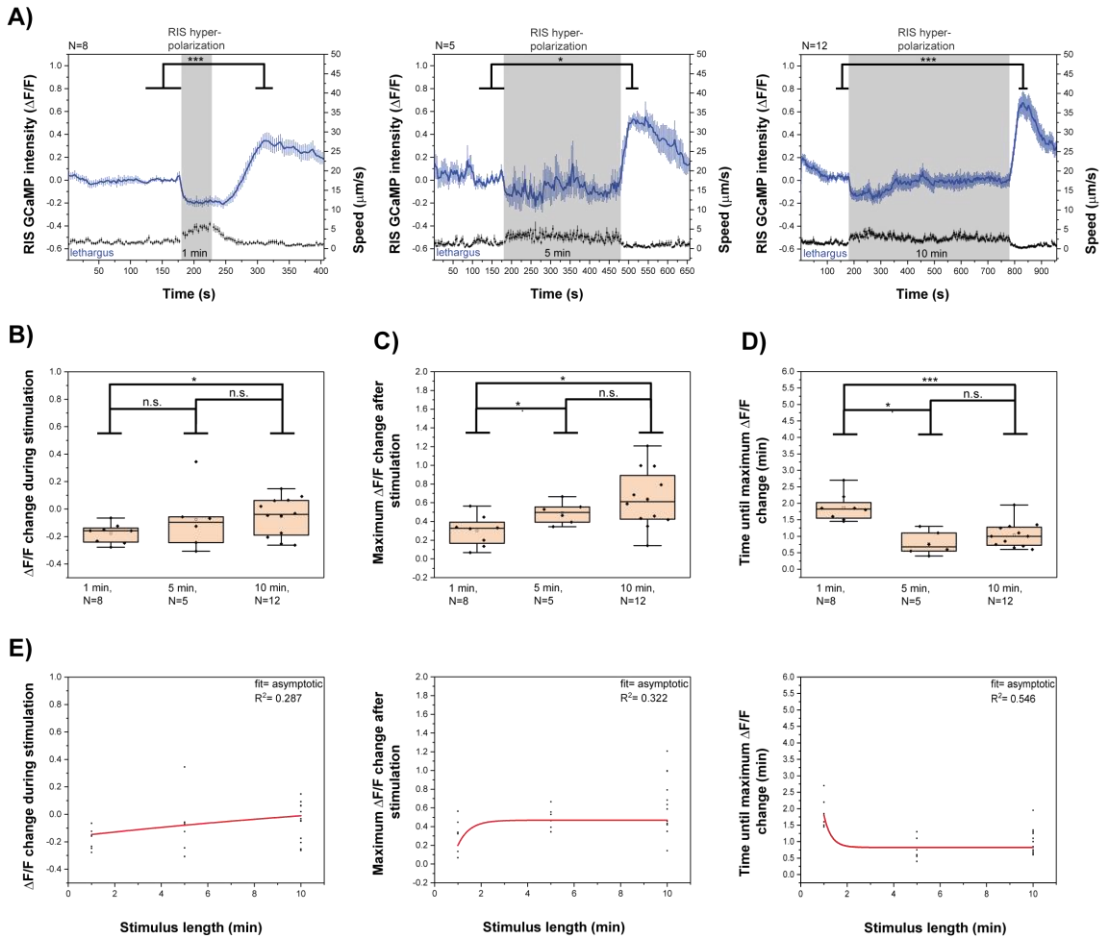

Figure 6. RIS rebound activation represents acute sleep homeostasis.

Worms were cultured overnight on ATR-containing plates at 25°C. For imaging, worms were cultured in microchambers. Optogenetic experiments were performed in and outside of lethargus. RIS activity was measured using GCaMP3.35. For optogenetic RIS inhibition, ArchT was used. ArchT was stimulated by green light. The stimulation lasted for 1, 5 or 10 minutes. In case of 1-minute stimulation, experiments were repeated every 15 minutes. In cases of 5 and 10 minutes stimulation, experiments were repeated every 30 minutes. Worms not showing rebound activation were excluded from the analysis.

A) Optogenetic RIS inhibition. Blue color indicates RIS activity in lethargus. Speed is shown in black. Gray shading indicates optogenetic stimulation and numbers indicate the duration of the stimulation period. Error bars indicate SEM. Significance was calculated using the Wilcoxon-signed rank test. * denotes statistical significance at $p < 0.05$ and *** denotes statistical significance at $p < 0.001$.

B) Quantification of the inhibition strength. Inhibition strength was calculated as difference between RIS levels during the stimulation period and RIS baseline levels. Significance was calculated using a student's t-test. * denotes statistical significance at $p < 0.05$.

C) Quantification of the rebound activation strength. Maximum values of RIS activity were extracted from the after stimulation period with a homemade MATLAB routine. RIS GCaMP data was averaged starting 15 seconds before up to 15 seconds after the maximum was reached. Significance was calculated using a student's t-test. * denotes statistical significance at $p < 0.05$.

D) Quantification of the timing of the rebound activation. Time points of maximum RIS activities after the stimulation were extracted using a homemade MATLAB routine. Significance was calculated using a student's t-test. * denotes statistical significance at $p < 0.05$ and *** denotes statistical significance at $p < 0.001$.

E) Data fitting. The data from B), C) and D) were successfully fitted with an asymptotic fit. R^2 values are indicated in the figures.

In all cases, optogenetic RIS hyperpolarization led to a drop in RIS activity levels below baseline. During 1 minute of optogenetic hyperpolarization, RIS levels dropped constantly to one level. The same was true for 5 minutes of optogenetic RIS inhibition. During 10 minutes of optogenetic inhibition, RIS activity levels returned back to baseline after 350 seconds. However, in all cases, worms stayed mobile throughout the whole stimulation period and strongly immobilized with rebound activation onsets (**Figure 6A and B**).

Within a limited time interval, I saw a correlation between a longer RIS inhibition and a stronger rebound activation following the inhibition. The quantification of the rebound strength resulted in a significantly stronger rebound activation after 5 compared to 1 minute of optogenetic RIS inhibition. In median, RIS activity levels were raised to 0.50 after 5 minutes of stimulation compared to 0.33 after 1 minute of stimulation. Contrary to that, rebound activation levels did not significantly increase after 10 compared to 5 minutes of optogenetic RIS inhibition. In conclusion, the strength of the rebound activation reached saturation levels after 5 minutes of optogenetic RIS inhibition (**Figure 6A, C and E**).

Furthermore, rebound activation occurred faster with increasing optogenetic stimulation period length. After 1 minute of stimulation, the highest rebound peak was reached in median after 1.8 minutes. Following 5 minutes of optogenetic hyperpolarization, RIS activity reached maximum levels after in median 0.675 minutes. There was no significant difference to the condition, in which RIS was hyperpolarized for 10 minutes. In agreement to rebound activation levels, saturation was reached after 5 minutes of RIS inhibition (**Figure 6A, D and E**).

Taking everything into consideration, the dose-response curve suggests that RIS rebound activation represents acute rather than chronic homeostasis.

4.4 Optogenetic manipulations of RIS presynaptic neurons

In 2013, former lab members established that RIS is sleep-inducing [57]. However, neuronal circuits regulating RIS are not known. Therefore, we analyzed RIS

presynaptic neurons with regard to their ability to change RIS activity. All RIS presynaptic neurons were identified according to the *C. elegans* connectome [68].

4.4.1 Optogenetic depolarization of RIS presynaptic neurons

All presynaptic neurons were optogenetically depolarized using ReaChR, which is a non-selective cation channel and which can be activated by green light [112]. RIS activity was measured simultaneously. Experiments were performed in microchambers or in immobilized worms. Immobilization allowed for the specific illumination of neurons of interest (**Figure 7)**.

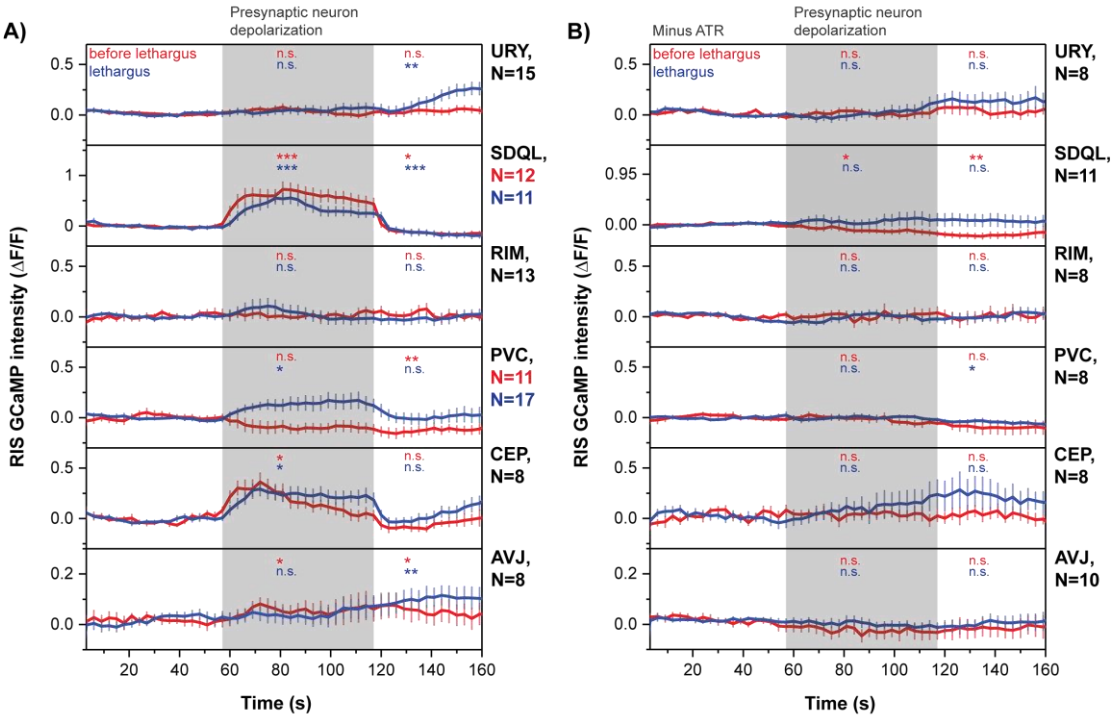

Figure 7. Presynaptic neurons can activate RIS.

A) Optogenetic depolarization of all RIS presynaptic neurons. Worms were cultured overnight at 25°C on ATR-containing plates. Next day, experiments were performed as follows: AVJ) L1 larvae in microchambers, CEP) L4 larvae in microchambers, PVC) L1 larvae immobilized with 10 % agarose, microbeads and 250 µM levamisol, RIM) L1 larvae in microchambers, SDQL) L4 larvae immobilized with 10 % agarose and microbeads and URY) L1 larvae in microchambers. Presynaptic neurons were stimulated using ReaChR. ReaChR was activated by green light, whereas in case of immobilized worms green light illumination was restricted to the neurons of interest. RIS activity was measured simultaneously, using GCaMP3.35. Per worm optogenetic experiments were repeated as follows: AVJ) every 15 minutes, CEP) every 30 minutes, PVC) 1 measurement per worm, RIM) every 30 minutes, SDQL) 4 measurements per worm and URY) every 15 minutes. Red color indicates RIS activity outside of lethargus and blue color indicates RIS activity in lethargus. Gray shading represents optogenetic stimulation periods. Error bars indicate SEM. Significance was calculated using the Wilcoxon-signed rank test. * denotes statistical significance at $p < 0.05$, ** denotes statistical significance at $p < 0.01$ and *** denotes statistical significance at $p < 0.001$.

B) Control experiments. Same as in A, but experiments were performed without the addition of ATR.

The response of RIS to the optogenetic depolarization of its directly presynaptic neurons differed for the single neurons. For a subset of neurons RIS responded differently outside of and in lethargus (**Figure 7).**

AVJ optogenetic depolarization induced RIS activation outside of lethargus, both during and after the optogenetic stimulation period. In lethargus, AVJ optogenetic stimulation had no direct effect on RIS, but RIS activity levels were increased following the optogenetic stimulation period. In case of optogenetic CEP

depolarization, I observed, both in and outside of lethargus, RIS activation. Optogenetic PVC stimulation resulted in a state-dependent RIS activation, which was exclusively present in lethargus. After the stimulation period, RIS activity dropped below baseline levels outside of lethargus and back to baseline levels in lethargus. Upon RIM depolarization no net change was induced in RIS activity. In experiments, in which SDQL was optogenetically stimulated, RIS was consistently activated in and outside of lethargus. In both cases, following the stimulation period, RIS activity dropped below baseline levels. Finally, optogenetic URY depolarization had no direct effect on RIS. However, in lethargus RIS was activated following the optogenetic URY stimulation.

To sum up, outside of lethargus optogenetic depolarization of presynaptic neurons either led to RIS activation or did not cause any changes in RIS activity. The same was true in lethargus. However, PVC neurons were the only neurons, which showed a state- dependent, lethargus specific input on RIS activity. As a second exception, RIM neurons had no net effect on RIS activity, neither outside of nor in lethargus.

Control experiments, which were performed without the addition of ATR and in which AVJ, CEP, RIM and URY neurons were stimulated, resulted in no significant changes in RIS activity levels. However, PVC depolarization without the supply of ATR caused a drop in RIS activity levels after the stimulation period in lethargus. In experiments, in which SDQL was optogenetically activated without the supply of ATR in worms outside of lethargus, RIS activity significantly dropped below baseline during and after the stimulation period. These effects might be due to photo bleaching (**Figure 7B**).

4.4.1.1 Optogenetic depolarization of RIM

Because of previous experimental data (see paragraph **4.8**), we hypothesized that RIM neurons are able to both activate and to inhibit RIS. Thereby, RIM might act differently depending on different incoming stimuli. The capacity of both activating and inhibiting RIS could explain why, in sum, RIM had no net input on RIS activity in the optogenetic depolarization experiment.

I split the data from **Figure 7A** into responsive and non-responsive experimental trials (**Figure 8**). Experimental trials were classified as responsive, if RIS activity changes correlated with stimulation period onsets.

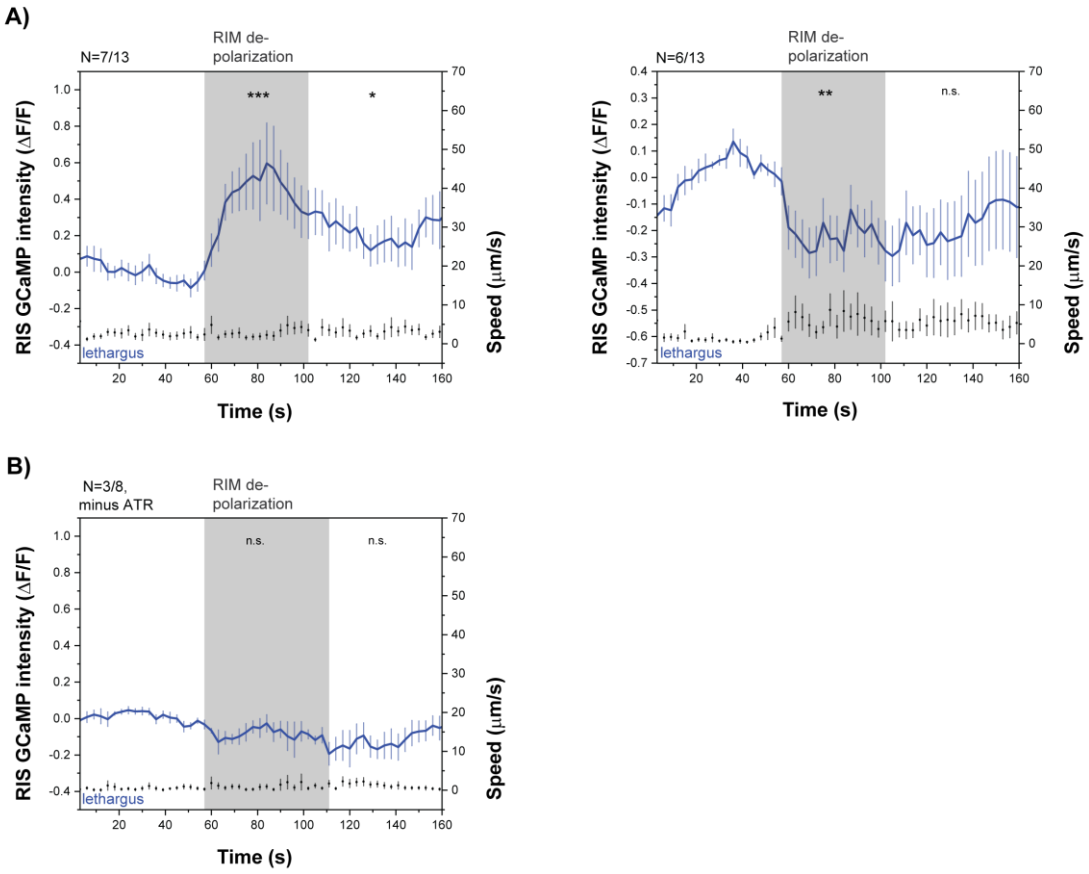

Figure 8. RIM can activate and inactivate RIS.

A) Optogenetic RIM depolarization in lethargus. Worms were cultured overnight on ATR-containing plates and grown at 25°C. Next day, L1 larvae were imaged in microchambers. RIS activity was measured using GCaMP3.35. RIM neurons were optogenetically activated using ReaChR. ReaChR was stimulated with green light. Optogenetic experiments were repeated every 30 minutes. Single experimental trials were selected according to the presence of an RIS response or no RIS response. RIS was classified as responding, if a change in its activity correlated with stimulation period onsets. In total 7 out of 13 animals showed RIS activation and 6 out of 13 animals showed RIS inhibition. 2 animals showed both RIS activation and inhibition. In blue RIS activity in lethargus is shown and in black speed data. Error bars represent SEM. Statistical significance was calculated using the Wilcoxon-signed rank test. * denotes statistical significance at $p < 0.05$, ** denotes statistical significance at $p < 0.01$ and *** denotes statistical significance at $p < 0.001$.

B) Control experiments. Same as in A, but experiments were performed without the addition of ATR. Selection of experimental trials was done as described in A. Figure B shows the selection of experimental trials, in which RIS showed a drop in its activity at stimulation period onsets. This was the case in 3 out of 8 animals tested.

Outside of lethargus, RIS activity in single trials did not change significantly (data not shown). In lethargus in a first set of trials, optogenetic RIM activation led to a significant increase in RIS activity levels, although this did not induce a stronger immobilization of worms. After the optogenetic stimulation period, RIS activity remained significantly above baseline levels and the speed of the worms remained unchanged.

In a second set of trials, optogenetic RIM activation caused RIS to significantly drop in its activity below baseline levels. This drop in RIS activity caused the worms to mobilize. After the stimulation period, RIS activity levels went back to baseline, but worms remained mobile (**Figure 8A**).

Trials, which were recorded without the addition of ATR, showed no significant changes in RIS activity for any condition (**Figure 8B** and data not shown).

In agreement to what was hypothesized before, RIM indeed activates or inhibits RIS. For RIM to induce RIS activation or inhibition, the status of RIS before optogenetic RIM depolarization could be decisive. Because baseline activity levels were higher, RIM might inhibit RIS, if RIS is active (**Figure 8A**). Accordingly, RIM might activate RIS, if RIS is inactive. In agreement to this, optogenetic RIM activation can lead to RIS activation or inhibition in the same worm.

Among all presynaptic neurons, RIM neurons were the only ones, which could induce a RIS inhibition. Comparable to PVC, RIM neurons optogenetic depolarization had a lethargus-specific input on RIS.

4.4.2 Optogenetic hyperpolarization of RIS presynaptic neurons

We were aiming to identify presynaptic neurons, which are required to activate RIS in lethargus. We expressed ArchT in all presynaptic neurons and simultaneously measured RIS activity using GCaMP3.35. For optogenetic experiments, L1 and L4 larvae were used and worms were imaged in microchambers or immobilized.

Immobilization of worms was required to ensure sufficient specificity of illumination of only neurons of interest during the optogenetic stimulation (**Figure 9**).

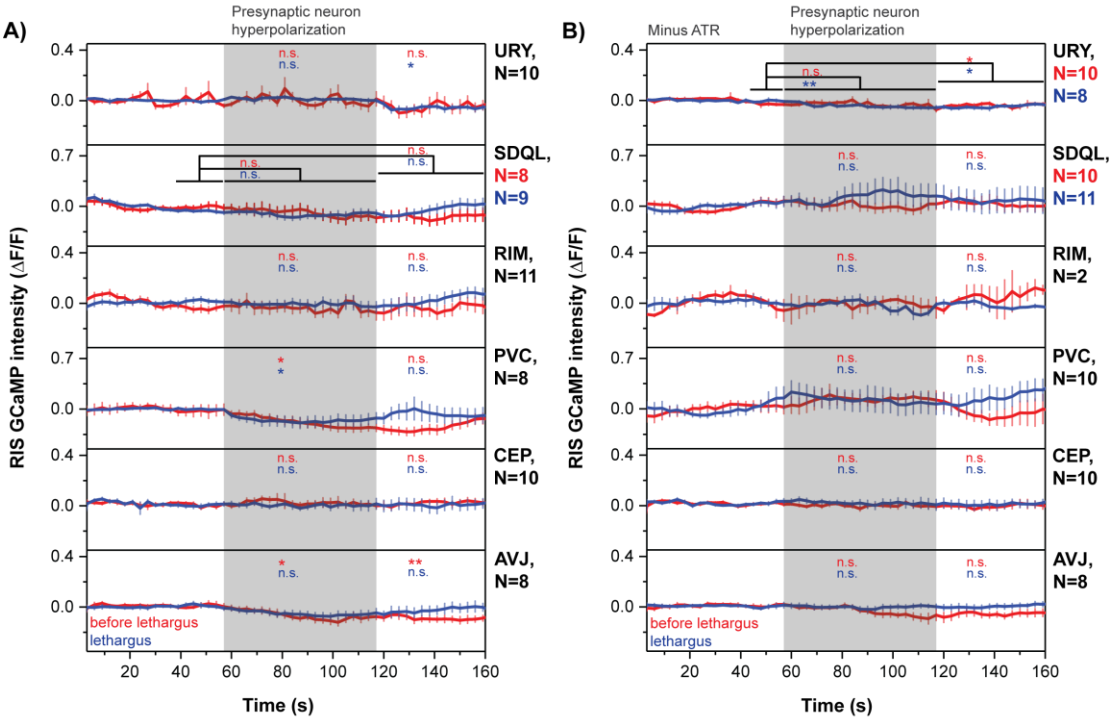

Figure 9. Identification of RIS activators in lethargus.

A) Optogenetic hyperpolarization of RIS presynaptic neurons. Worms were cultured overnight at 25°C on ATR-containing plates. Next day, experiments were performed as follows: AVJ) L1 larvae in microchambers, CEP) L1 larvae in microchambers, PVC) L1 larvae immobilized with 10 % agarose, microbeads and 250 µM levamisol, RIM) L1 larvae in microchambers, SDQL) L4 larvae immobilized with 10 % agarose and microbeads and URY) L4 larvae in microchambers. RIS presynaptic neurons were hyperpolarized using ArchT and ArchT was stimulated with green light. RIS activity was measured simultaneously using GCaMP3.35. Optogenetic experiments were repeated as follows: AVJ) every 15 minutes, CEP) every 15 minutes, PVC) 1 measurement per worm, RIM) every 30 minutes, SDQL) 4 measurements per worm and URY) every 30 minutes. Red color shows RIS activity outside of lethargus. Blue color represents RIS activity in lethargus. Gray shading indicates the optogenetic stimulation period. Neurons of interest are indicated in the figure. Error bars indicate SEM. In experiments, in which SDQL was optogenetically hyperpolarized, RIS baseline activity was calculated over the interval from 36 to 60 seconds. Before second 36 the baseline in the lethargus condition was unstable. Significance was calculated using the Wilcoxon-signed rank test. * denotes statistical significance at $p < 0.05$, ** denotes statistical significance at $p<0.01$ and *** denotes statistical significance at $p < 0.001$.

B) Control experiments. Same as in A, but experiments were repeated without the addition of ATR. In experiments, in which URY was optogenetically stimulated, RIS baseline activity was calculated over the interval from 42 to 60 seconds, because before this interval the baseline was unstable.

Comparable to experiments, in which presynaptic neurons were optogenetically depolarized (**Figure 7**), RIS activity was changed differently upon the optogenetic hyperpolarization of these neurons. For some presynaptic neurons, induced changes in RIS activity differed outside of and in lethargus (**Figure 9A**).

AVJ optogenetic hyperpolarization outside of lethargus, induced a long lasting drop in RIS activity below baseline levels, which also remained present after the optogenetic stimulation period. However, in lethargus optogenetic AVJ hyperpolarization induced no changes in RIS activity. The optogenetic hyperpolarization of CEP neurons failed to induce any changes in RIS activity, both outside of and in lethargus. Contrary to this, optogenetic PVC hyperpolarization induced a drop in RIS activity outside of and in lethargus during the stimulation period. In both cases, RIS activity returned back to baseline levels after the stimulation period. In agreement to depolarization experiments, optogenetic RIM hyperpolarization had no net input on RIS activity. The same was true for experiments, in which SDQL was optogenetically hyperpolarized. Finally, URY optogenetic inhibition had an impact on RIS only in lethargus. After the stimulation period, RIS activity levels dropped significantly below baseline.

Control experiments, which were performed without the addition of ATR, revealed no significant changes in RIS activity upon the optogenetic stimulation of presynaptic neurons, despite URY. In the control experiments, RIS activity dropped significantly below baseline levels after the stimulation period outside of lethargus. However, in lethargus RIS activity dropped significantly below baseline levels during and after the optogenetic stimulation period. Amplitudes of changes in RIS activity in the control experiments were not significantly smaller than changes measured in experiments, which were done with the supply of ATR. For that reason the change in RIS activity, following the optogenetic hyperpolarization of URY with the supply of ATR, might be light induced and not due to optogenetic manipulations (**Figure 9B**).

To sum up, optogenetic hyperpolarization of upstream neurons outside of lethargus either induced a drop or no change in RIS activity. The same was true for lethargus. Outside of lethargus, optogenetic hyperpolarization of AVJ and PVC inactivated RIS. In lethargus, only optogenetic hyperpolarization of PVC inactivated RIS.

Based on results of optogenetic manipulation experiments, PVC is important in RIS regulation in lethargus. There are 2 reasons for that:

1. PVC had a lethargus-specific ability to activate RIS (**Figure 7**).
2. Only optogenetic PVC hyperpolarization induced a drop in RIS activity outside of lethargus and in lethargus (**Figure 9**).

4.4.2.1 Optogenetic hyperpolarization of RIM

In analogy to the optogenetic depolarization of RIM in **Figure 8**, I split the data of optogenetic RIM hyperpolarization from **Figure 9** into RIS responsive and RIS non-responsive trials (**Figure 10**).

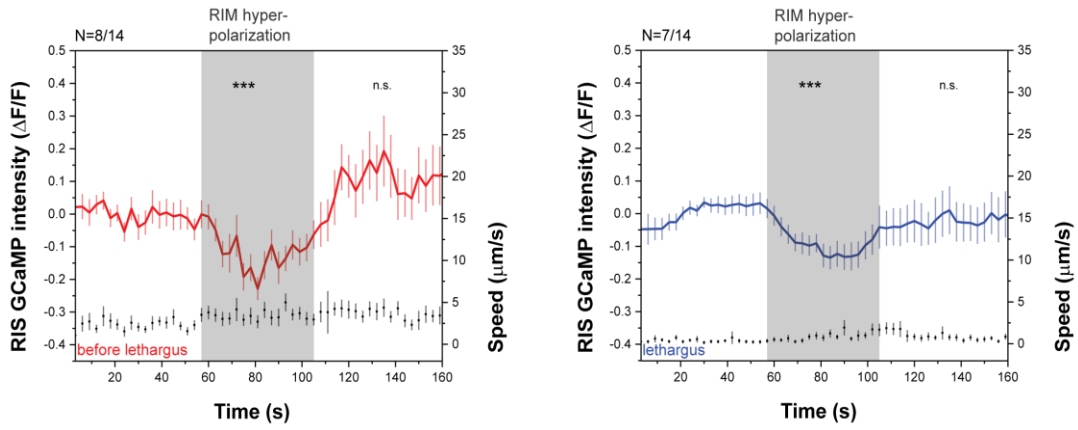

Figure 10. RIM hyperpolarization can induce a drop in RIS activity.

Worms were cultured overnight on ATR-containing plates and grown at 25°C. Next day, worms were imaged in microchambers. RIM neurons were optogenetically hyperpolarized using ArchT. ArchT was stimulated with green light. Simultaneously RIS activity was measured. Optogenetic experiments were repeated every 30 minutes. Data was separated into RIS responsive or non-responsive trials. RIS was classified as responsive, if a change in its activity correlated with stimulation period onsets. Outside of lethargus 8 out of 14 worms showed changes in RIS activity upon the optogenetic manipulation of RIM. In lethargus, this was the case for 7 out of 14 animals. Worms were responsive exclusively outside of lethargus or exclusively in lethargus or both outside of and in lethargus. In red RIS activity outside of lethargus is depicted. Blue color represents RIS activity in lethargus. In black the speed is shown. Gray shading indicates optogenetic stimulation periods. Error bars represent SEM. Statistical significance was calculated using the Wilcoxon-signed rank test. *** denotes statistical significance at $p < 0.001$.

Both outside of lethargus and in lethargus, optogenetic RIM hyperpolarization could induce a significant drop in RIS activity. This drop was connected to a slight increase in mobility outside of lethargus. In lethargus, worms mobilized towards the end of the stimulation period. The fact that optogenetic RIM inhibition did not always activate RIS, strengthens the hypothesis of RIM having a modulatory rather than an active function in RIS regulation. However, except for PVC, RIM neurons were the only neurons, which optogenetic hyperpolarization caused a drop in RIS activity in L1 lethargus (**Figure 10**).

4.4.3 Sleep bout analysis and RIS activity in sleep bouts of *nmr-1::ICE* mutants

To study the role of PVC, the *nmr-1* promoter was used. The *nmr-1* promoter triggers expression in all locomotion command interneurons. For simplicity, locomotion command interneurons will be referred to as command interneurons in the following. Thereby, PVC and RIM are the only command interneurons, which are directly presynaptic to RIS. In an *nmr-1::ICE* strain all command interneurons, except AVB, are genetically ablated. ICE stands for interleukin-1β-converting enzyme and is a human caspase. Its expression in the command interneurons causes their apoptotic cell death [115].

If command interneurons are responsible for RIS activation in L1 lethargus, *nmr-1::ICE* mutants should display a low quiescence phenotype in lethargus. To test this hypothesis, I analyzed sleep bouts in these mutants in regard to their length, frequency and RIS activity. Finally, I repeated the optogenetic hyperpolarization of RIS in *nmr 1::ICE* mutants to determine, whether the RIS rebound activation is also controlled by command interneurons (**Figure 11**).

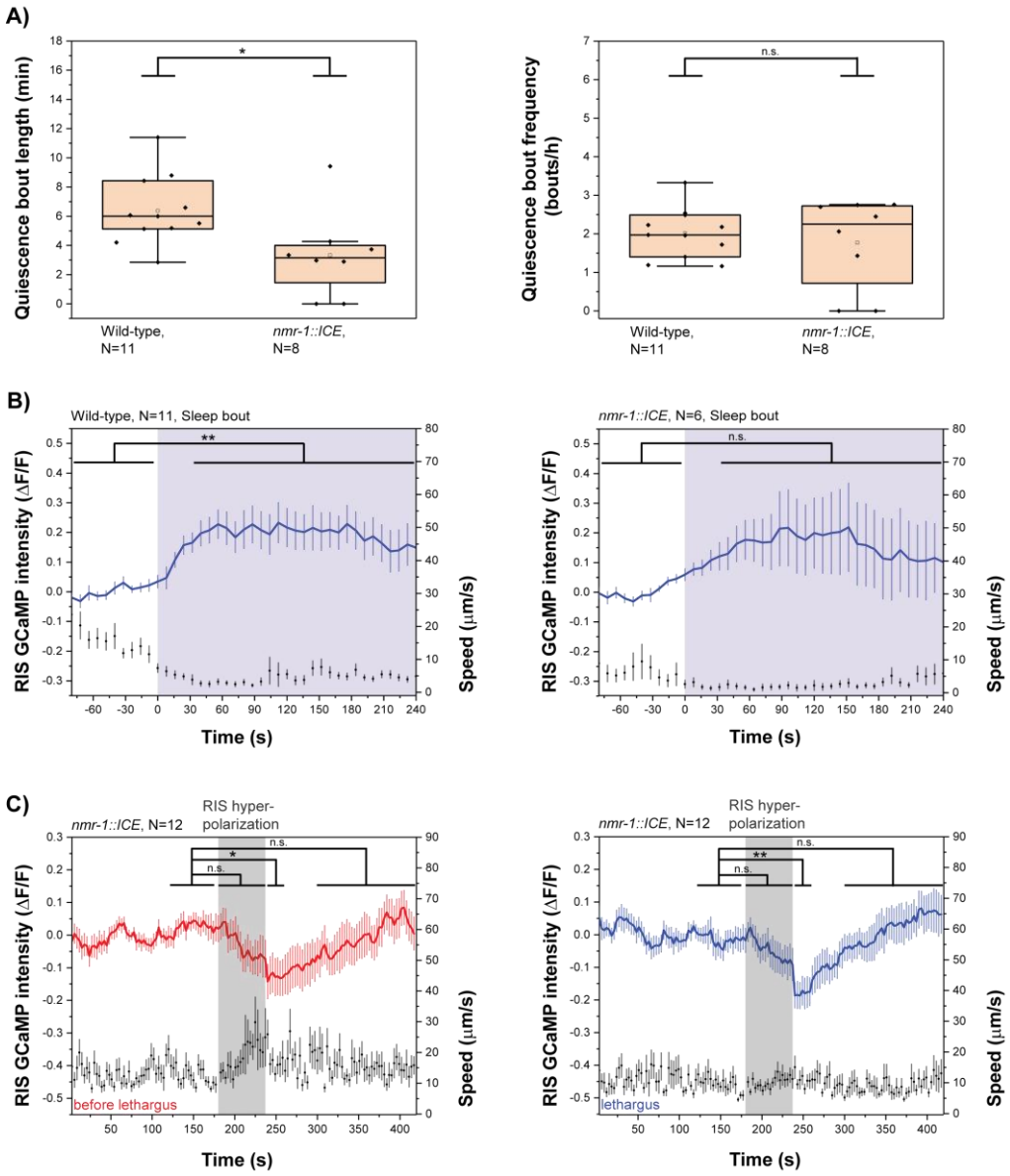

Figure 11. ***nmr-1::ICE*** **mutants display a low quiescence phenotype in L1 lethargus.**

A) Sleep bout analysis of *nmr-1::ICE* mutants. Worms were grown at 20°C and imaged in microchambers. RIS activity was measured using GCaMP3.35. Fluorescent images were taken every 8 seconds. Speed data was calculated from neuron positions. Sleep bouts were extracted using the following criteria: 1) lower speeds than 10 % of the maximum speed of the individual worm and 2) low speeds lasted for at least 2 minutes. Statistical significance was calculated using a student's t-test for the quantification of the quiescence bout lengths. Statistical significance for the quiescence bout frequencies were calculated using a Kolmogorov-Smirnov test. * denotes statistical significance at $p < 0.05$.

B) RIS activity in sleep bouts in *nmr-1::ICE* mutants. RIS data was extracted based on the bout analysis displayed in A. Dark blue color represents RIS activity in sleep bouts. Violet shading indicates sleep bouts. Error bars represent SEM. Statistical significance was calculated using a Wilcoxon-signed rank test. ** denotes statistical significance at $p<0.01$.

C) The RIS rebound activation is abolished in *nmr-1::ICE* mutants. Worms were grown at 25°C overnight on ATR-containing plates. RIS activity was measured using GCaMP3.35. RIS was optogenetically hyperpolarized with ArchT. ArchT was stimulated by green light. Optogenetic experiments were repeated every 30 minutes. In red RIS activity outside of lethargus is shown. In blue is shown the RIS activity in lethargus. Black color represents speed. Gray shading marks the optogenetic stimulation period. Error bars represent SEM. Statistical significance was calculated using a Wilcoxon-signed rank test. * denotes statistical significance at $p < 0.05$.** denotes statistical significance at $p<0.01$.

As hypothesized, sleep bout analysis of *nmr-1::ICE* mutants resulted in a low quiescence phenotype (**Figure 11A**). The mutants showed significantly shorter sleep bouts than Wild-type worms. However, sleep bouts occurred at the same frequency as for Wild-type worms.

Compared to Wild-type worms, mutants showed a similar amount of RIS activation in sleep bouts. However, the effect was not significant in *nmr-1::ICE* mutants. 2 out of 6 animals displayed RIS activation in sleep bouts. Eventually, command interneurons were not completely ablated in these worms. The 4 remaining animals lacked RIS activation in sleep bouts completely. To confirm this result, more mutant worms should be analyzed. However, a lack of RIS activity in sleep bouts, agrees with the low quiescence phenotype of *nmr-1::ICE* mutants in lethargus (**Figure 11B**).

Finally, **Figure 11C** shows that command interneurons are involved in the RIS rebound activation following optogenetic RIS hyperpolarization. In contrast to Wild-type worms (**Figure 5A**), there was no significant increase in RIS activity measurable in *nmr-1::ICE* mutants in any condition.

4.5 Optogenetic RIS manipulations and simultaneous measurements of RIM activities

To further dissect, how presynaptic neurons regulate RIS activity in lethargus, I tested for a possible feedback regulation between RIM and RIS. The equivalent experiments, in which we tested for a feedback regulation between PVC and RIS were done by my colleague Inka Busack and are not shown in this work.

To test for a feedback mechanism, I optogenetically manipulated RIS activity using ReaChR and ArchT. Simultaneously, I measured RIM activity using GCaMP3.35 (**Figure 12**).

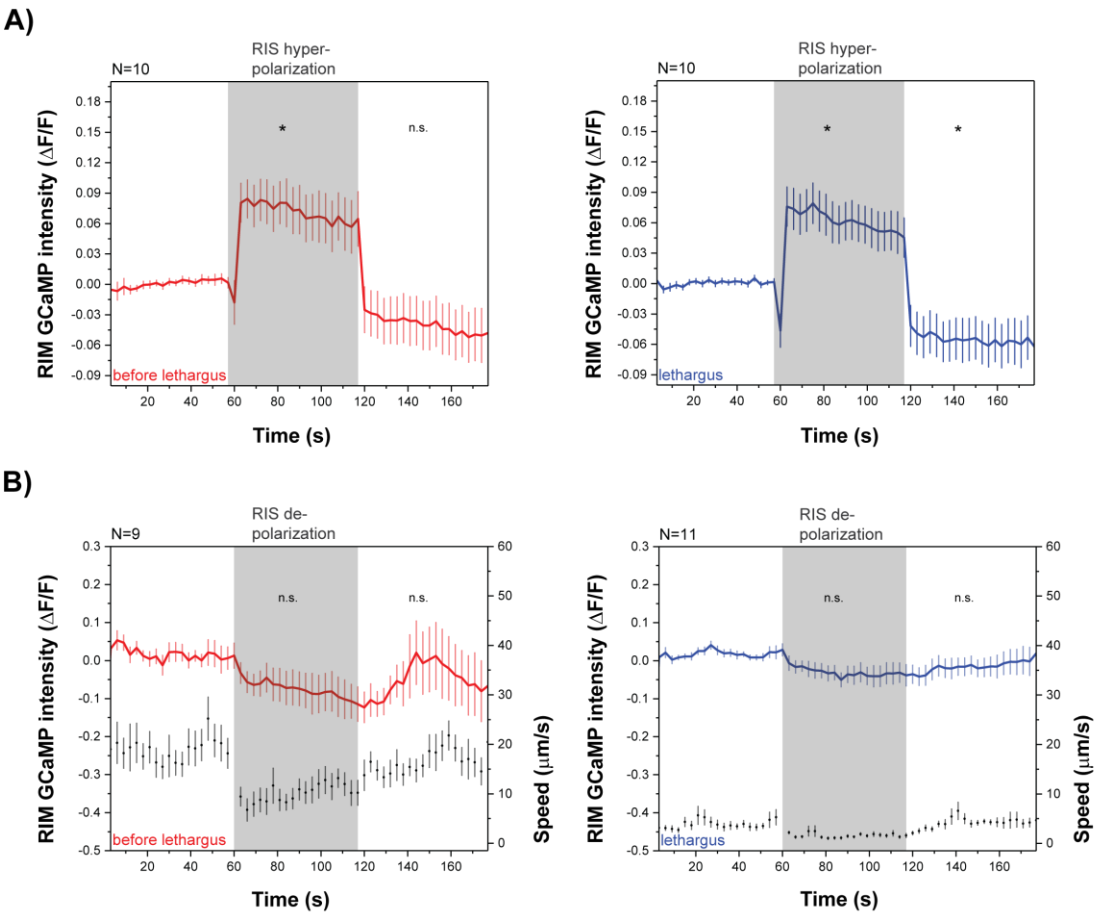

Figure 12. Optogenetic RIS hyperpolarization activates RIM.

Worms were grown at 25°C for one night and cultured on ATR-containing plates.

A) Optogenetic hyperpolarization of RIS and simultaneous measurement of RIM activities. ArchT was stimulated with green light. RIM activities were measured using GCaMP3.35. Activities of the left and right RIM neuron were extracted together as one signal. L1 larvae were immobilized with 10 % agarose, 250 µM Levamisol and microbeads. 2 measurements were done per worm. In red is shown RIS activity outside of lethargus. Blue represents RIS activity in lethargus. Gray shading indicates the optogenetic stimulation period. Error bars represent SEM. Statistical significance was calculated using a Wilcoxon-signed rank test. * denotes statistical significance at $p < 0.05$.

B) Optogenetic RIS depolarization and simultaneous measurement of RIM activites. ReaChR was stimulated with green light. RIM activities were measured and extracted as described in A. Only worms, which immobilized upon optogenetic RIS depolarization, were taken into account during the analysis. L1 larvae were imaged in microchambers. Optogenetic experiments were repeated every 15 minutes. In red is shown RIS activity outside of lethargus. Blue represents RIS activity in lethargus. Gray shading indicates the optogenetic stimulation period. Error bars represent SEM. Statistical significance was calculated using a Wilcoxon-signed rank test.

RIM activity significantly increased upon optogenetic RIS hyperpolarization, both outside of and in lethargus. In lethargus, RIM activity levels dropped significantly below baseline following the stimulation period (**Figure 12A**).

However in net, RIM activities did not change upon optogenetic RIS depolarization in any condition (**Figure 12B**). Nevertheless, splitting data into RIM responsive and non-responsive trials might reveal significant effects.

The fact that RIM activates upon optogenetic RIS depolarization proves, that there is a feedback between RIS and RIM. However, this feedback was restricted to low RIS activity.

4.6 Command interneuron activities outside of and in lethargus

RIS activity is subjected to dynamic changes outside of and in lethargus (**Figure 4A**). Consequently, circuits, which regulate RIS activity, should also be subjected to changes outside of and in lethargus. To study this, I measured command interneuron activities outside of and in lethargus.

The activity of command interneurons was measured using the *glr-1* promoter. *glr-1* is expressed in the same subset of command interneurons as *nmr-1*, despite AVB. I compared neuronal activities outside of and in lethargus and outside of and in sleep bouts. To analyze RIS dependent and RIS independent changes in command interneurons, I repeated the experiments in *aptf-1* mutants. In these mutants, RIS lost its ability to induce sleep [57] (**Figure 13**).

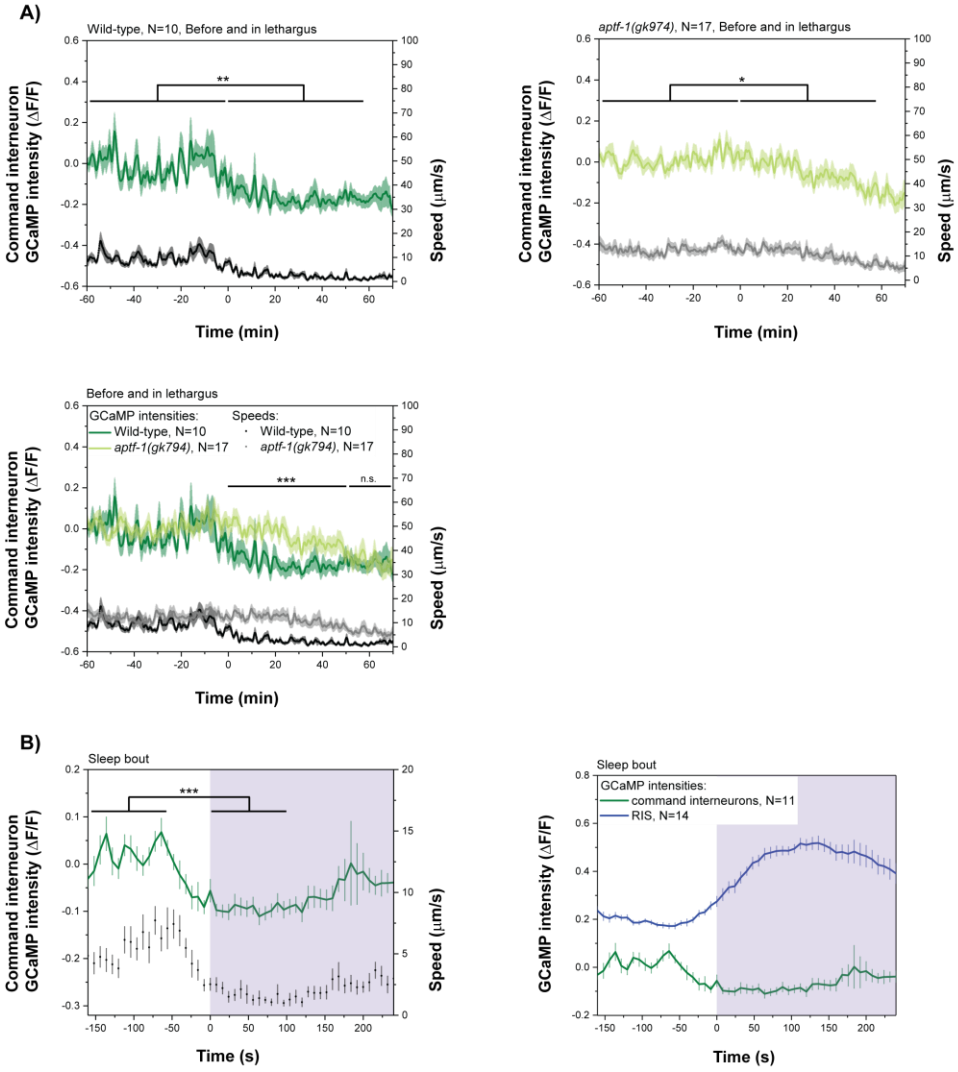

Figure 13.Command interneuron activities are dampened in lethargus.

Worms were grown at 20°C and imaged in microchambers. To measure command interneuron activities, GCaMP3.35 expressed under the *glr-1* promoter was used. Fluorescent images were taken every 8 seconds. The GCaMP signal of all head command interneurons was analyzed as one signal. Speeds were extracted from neuronal positions.

A) Command neuron activities outside of and in lethargus. Data was smoothed using Rloess smoothing and a span of 20 frames. Dark green indicates command interneuron activities in Wild-type worms. Light green represents command interneuron activities in *aptf-1* mutants. Black indicates Wild-type speed data. Gray indicates *aptf-1* mutant speed data. 0 indicates sleep onsets. Error bars represent SEM. Activity levels outside of and in lethargus were statistically compared performing a Wilcoxon-signed rank test. * denotes statistical significance at $p<0.05$ and ** denotes statistical significance at $p<0.01$. Activity levels in the time interval from 0–50 minutes in lethargus were compared using a student's t-test. Activities in the interval from 50–70 minutes in lethargus were compared using a Kolmogorov-Smirnov test. *** denotes statistical significance at $p<0.001$.

B) Activity levels of command interneurons in sleep bouts. Data from A was supplied to a bout analysis. The following criteria were applied for sleep bout identification: 1) worms were slower than 10 % of their own maximum speed and 2) kept low speeds for at least 2 minutes. Command interneuron activities were extracted according to the bout analysis. Dark green indicates command interneuron activities. Black represents the speed data. Violet shading indicates sleep bouts. 0 marks sleep bout onsets. Blue color represents RIS activity in bouts. RIS activities were taken from another experiment. In this experiment worms were imaged and bouts and RIS activities were extracted under the same conditions as described above. Error bars indicate SEM. Statistical significance was calculated using the Wilcoxon-signed rank test. *** denotes statistical significance at $p<0.001$.

Command interneuron activities were significantly lowered in lethargus, compared to activity levels outside of lethargus. The same was true for *aptf-1* mutants, although the dynamics of command interneuron activity reduction were altered in the mutant background. During the first 50 minutes in lethargus, command interneurons were significantly more active in the mutant than in Wild-type worms. After 50 minutes of lethargus, command interneuron activity levels in the mutant reached Wild-type levels (**Figure 13A**). The level of command interneuron activities correlated with the amount of movement of mutant and Wild-type worms in all conditions.

In analogy to the sleep onset, command interneuron activities dropped significantly below baseline levels upon the onset of sleep bouts. Command interneuron activities were lowered simultaneously with the RIS activity increase at the onset of sleep bouts (**Figure 13B**).

Taken together, these results indicate that command interneuron activities are indeed subjected to dynamic changes outside of and in lethargus. Furthermore, the dampening of command interneuron activities in lethargus happens partly upstream of RIS, but RIS strongly accelerates this process throughout the first 50 minutes of lethargus.

4.6.1 RIM activities outside of and in lethargus in Wild-type worms and *aptf-1* mutants

To be more specific, I repeated the above-described experiments using the *tdc-1* promoter to image RIM activities. I compared RIM activities outside of and in lethargus and I compared RIM activities in Wild-type worms and *aptf-1* mutants. Wild-type data was generated by my colleague Inka Busack. She imaged the worms. I did the signal extraction and data analysis (**Figure 14**).

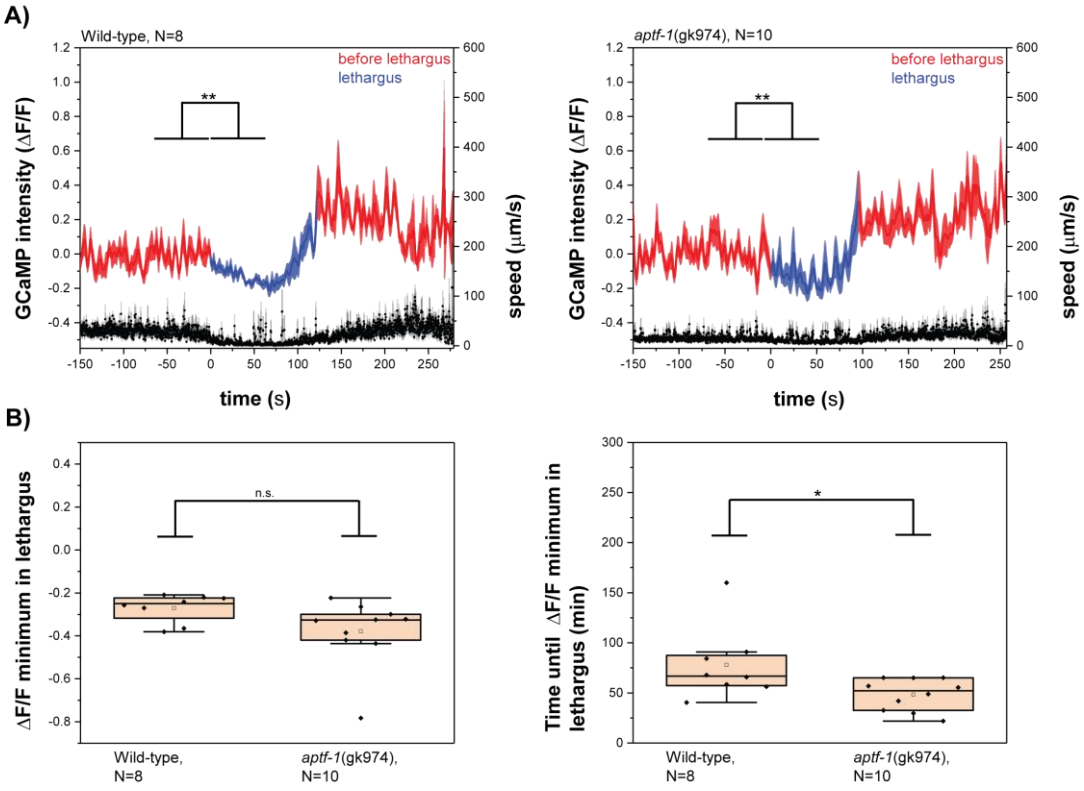

Figure 14. RIM activities are dampened in lethargus in Wild-type worms and *aptf-1* mutants.

Worms were cultured at 20°C and imaged in microchambers. GCaMP3.35 was used to measure RIM activities. Fluorescent images were taken every 10 seconds. The left and right RIM neuron were extracted as one signal. Speed data was extracted from neuron positions. GCaMP data was smoothed using Rloess smoothing and a span of 40 frames.

A) RIM activities outside of and in lethargus in Wild-type worms and *aptf-1* mutants. Red shows RIM activities outside of lethargus. Blue indicates RIM activity in lethargus. Black represents speed data. Error bars represent SEM. RIM activity levels were statistically compared using a Wilcoxon-signed rank test. ** denotes statistical significance at $p<0.01$.

B) Global minimum of RIM activity in lethargus. The global minimum of RIM activity as well as its time point of occurring, was extracted with a homemade MATLAB routine. Statistical significance was calculated by the Kolmogorov-Smirnov test. * denotes statistical significance at $p<0.05$.

RIM activity levels were significantly decreased in lethargus compared to conditions outside of lethargus. The same was true for *aptf-1* mutants (**Figure 14A**). The dampening of RIM activity in lethargus in both genotypes, agrees to the dampening of the activity of all command interneurons in lethargus (**Figure 13**). Nevertheless, the reduction of RIM activity in lethargus was not delayed in *aptf-1* mutants in comparison to Wild-type worms, as it was the case for the activity of all command interneurons. RIM level reached the global minimum in lethargus in *aptf-1* mutants in median after 52.08 minutes. In Wild-type worms, the global minimum was reached

after in median 66.75 minutes. Absolute levels of the global minima of RIM activities were not significantly different between both genotypes.

As a second important feature of RIM activity, I analyzed RIM peak frequencies in Wild-type worms and in *aptf-1* mutants outside of and in lethargus (**Figure 15**).

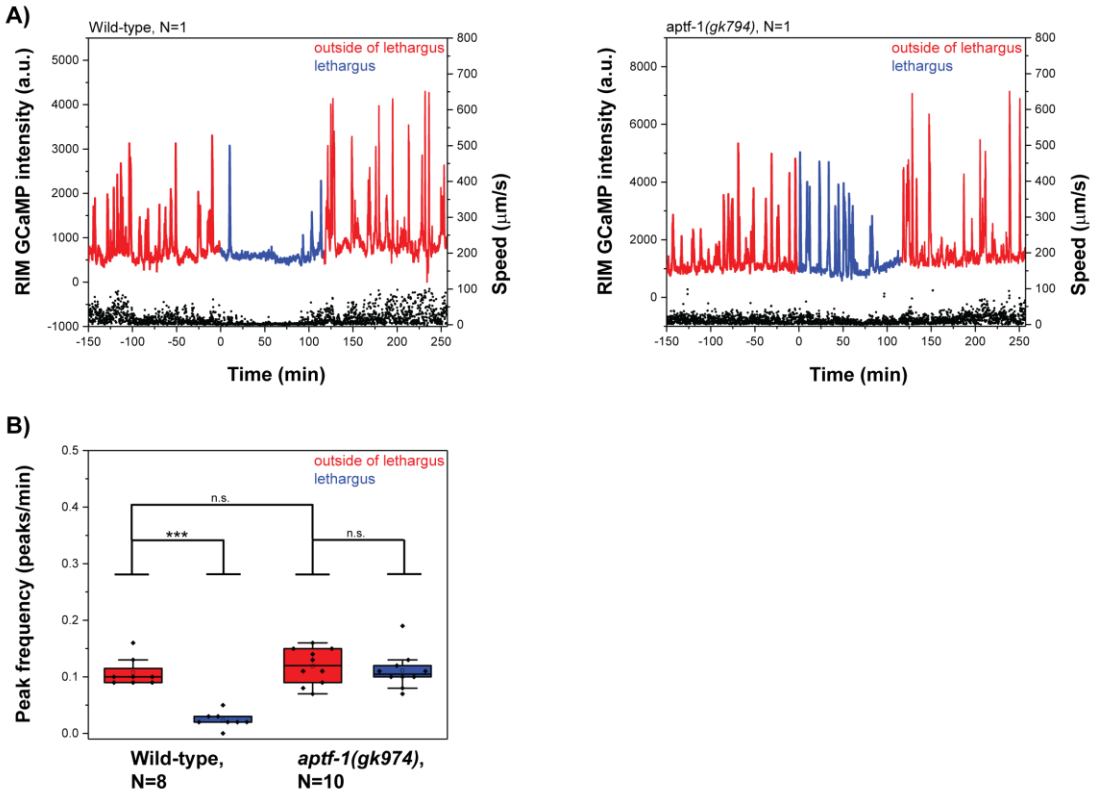

Figure 15. RIM peak frequency is not reduced in lethargus in *aptf-1* mutants.

Worms were grown at 20°C. Imaging was done in microchambers. RIM activity was tracked using GCaMP3.35. Fluorescent images were taken every 10 seconds. The left and right RIM neuron were extracted as one signal. Speeds were calculated from neuronal positions.

A) Sample traces. RIM activity outside of lethargus is depicted in red. RIM activity in lethargus is depicted in blue. Speed data is given in black.0 denotes lethargus onsets.

B) Quantification of RIM peak frequencies in Wild-type worms and *aptf-1* mutants. RIM peaks were defined by a minimum activity, which had to be at least twice as high as RIM baseline activity outside of lethargus. The baseline was defined for every worm individually. Statistical calculations were done as follows: 1) quantification of peak frequencies outside of and in lethargus in Wild-type worms: Kolmogorov-Smirnov test, 2) as in 1, but in *aptf-1* mutants: student's t-test, 3) comparison of peak frequencies outside of lethargus in Wild-type worms and *aptf-1* mutants: Kolmogorov-Smirnov test. *** denotes statistical significance at $p<0.001$.

RIM peaks were strongly reduced in lethargus compared to conditions outside of lethargus in Wild-type worms. Contrary to Wild-type worms, *aptf-1* mutants displayed no significant reduction of RIM peaks in lethargus. However, both genotypes showed the same amount of RIM peaks outside of lethargus (**Figure 15B**).

4.6.2 Command interneuron activities in *nmr-1* mutants

As mentioned in paragraph **4.6**, command interneurons are subjected to dynamical changes in their activity across lethargus. *nmr-1* is expressed in all command interneurons and encodes an NMDA-type ionotropic glutamate receptor subunit. Glutamate is an excitatory neurotransmitter. For that reason it is conceivable, that *nmr-1* function as plasticity factor in command interneurons [116–119].

To verify this idea, I quantified the activity levels of command interneurons in Wild-type worms and *nmr-1* mutants outside of and in lethargus. Furthermore, I studied the command interneuron activities in sleep bouts in Wild-type worms and *nmr-1* mutants (**Figure 16**).

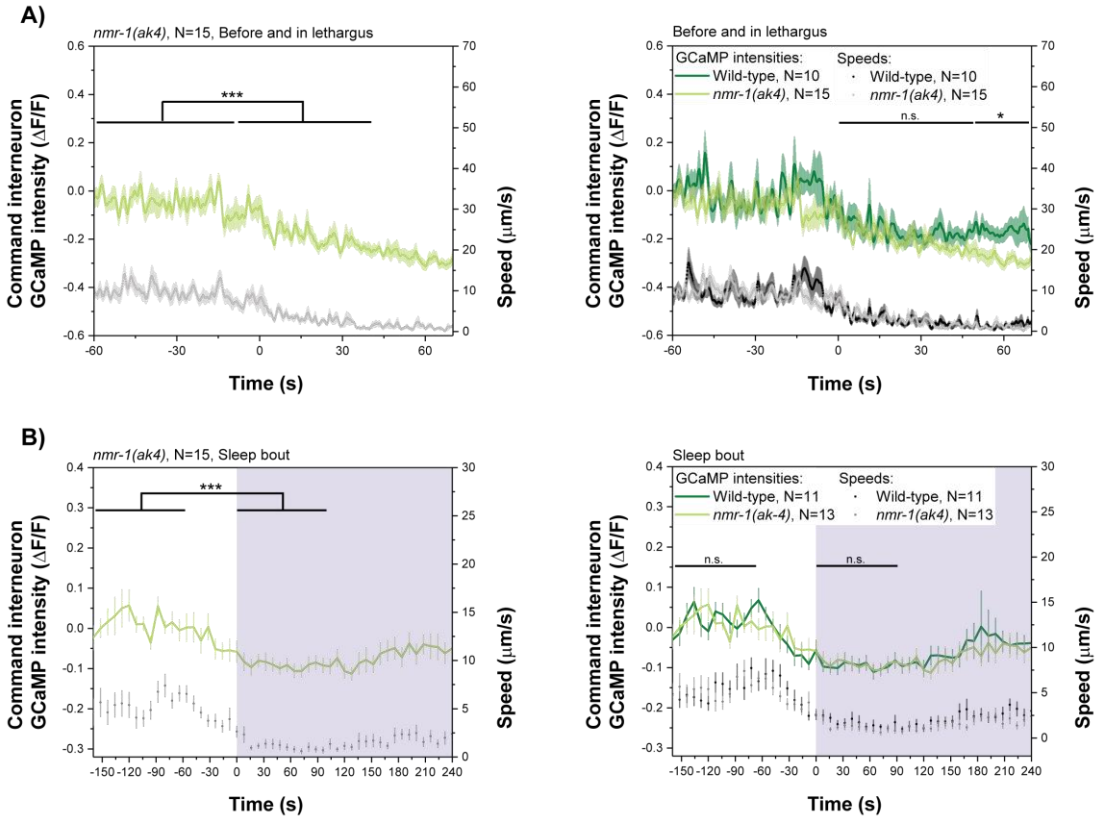

Figure 16. Command interneuron activities are more strongly reduced in lethargus in *nmr-1* mutants.

Worms were grown at 20°C and imaged in microchambers. Command interneuron activities were measured using GCaMP3.35. Fluorescent images were taken every 8 seconds. Speed data was extracted from neuron positions.

A) Command interneuron activities in Wild-type worms and *nmr-1* mutants outside of and in lethargus. Data was smoothed using Rloess and a span of 20 frames. In light green command interneuron activities in *nmr-1* mutants are shown. Dark green color indicates neuronal activities in Wild-type worms. In light gray, mutant speed data is depicted. Black indicates Wild-type speed data. 0 marks sleep onsets. Error bars represent SEM. Activity levels outside and in lethargus were statistically compared using a Wilcoxon-signed rank test. Neuronal activates between genotypes were compared using a student's t-test. * denotes statistical significance at $p<0.05$ and *** denotes statistical significance at $p<0.001$.

B) Command interneuron activities in Wild-type worms and *nmr-1* mutants in sleep bouts. Sleep bouts were extracted using the following criteria: 1) the worm displayed less than 10 % of its maximum speed outside of lethargus and 2) the worm kept the low speed at least for 2 minutes. GCaMP data was extracted based on the results of the bout analysis. Light green color represents command interneuron activities in *nmr-1* mutants and dark green color indicates neuronal activities in Wild-type worms. In light gray the mutant speeds are shown and in black Wild-type speeds are shown. 0 marks the onset of sleep bouts, which are indicated by violet shading. Neuron activity levels before and after onsets of sleep bouts were statistically compared using a Wilcoxon-signed rank test. To compare neuronal activities between genotypes a Kolmogorov-Smirnov test was performed. *** denotes statistical significance at $p<0.001$.

In agreement to Wild-type data, command interneuron activities dropped significantly below baseline levels in lethargus in *nmr-1* mutants. However, after 50 minutes in lethargus, neuron activity levels were significantly more strongly reduced in the mutant background (**Figure 16A**). In sleep bouts, there was no significant difference in neuronal activities of command interneurons detectable between Wild-type worms and *nmr-1* mutants (**Figure 16B**).

From these results we concluded, that *nmr-1* acts as plasticity factor in command interneurons. However, *nmr-1* function is only required later in lethargus.

4.6.2.1 Sleep bout analysis and RIS activity in sleep bouts in *nmr-1* mutants

I continued to analyze *nmr-1* mutant behavior with performing a sleep bout analysis. Thereby, I quantified the length and frequency of sleep bouts as well as the total amount of time worms spend in sleep bouts. Additionally, I extracted the RIS signal in sleep bouts (**Figure 17**).

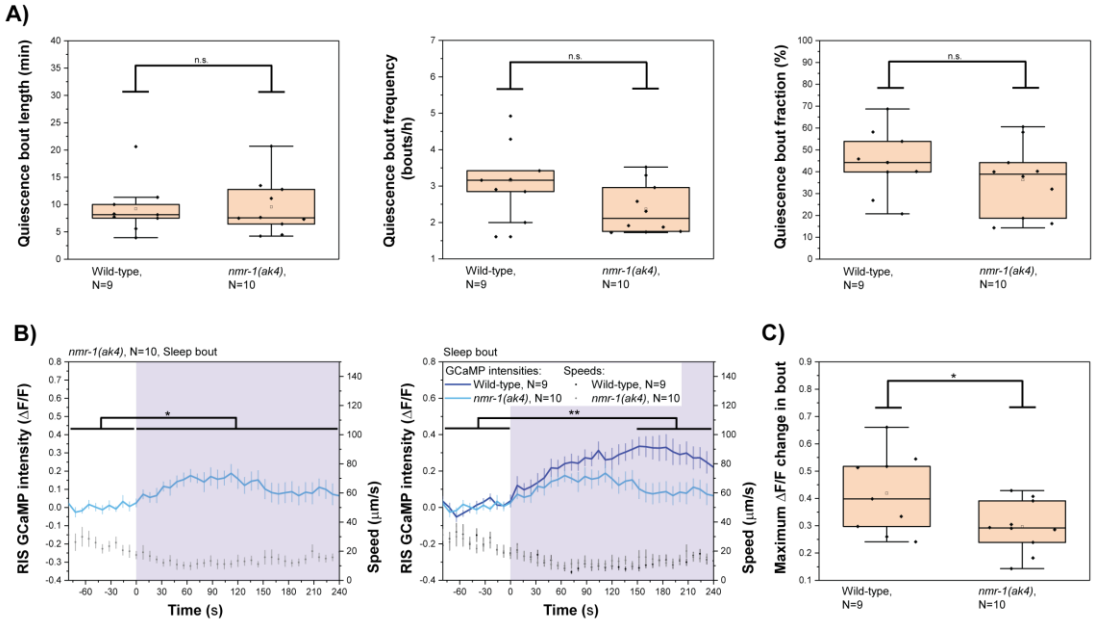

Figure17. *nmr-1* mutants show reduced RIS transients in sleep bouts.

Worms were cultured at 20°C. Imaging was done in microchambers. Fluorescent images were taken every 8 seconds. RIS activity was measured using GCaMP3.35. Speed data was generated using neuron positions.

A) Quantification of bout length, bout frequency and total time spend in sleep bouts of Wild-type worms and *nmr-1* mutants. Speed data was subjected to a bout analysis. Sleep bouts were defined by speeds lower than 10 % of the maximum speed of the individual worm for at least 2 minutes and were extracted using a homemade MATLAB routine. Significances were calculated as follows: 1) bout frequencies and total times spend in bouts were compared between genotypes using a student's t- test. 2) bout lengths were compared using a Kolmogorov-Smirnov test.

B) Quantification of RIS activity in sleep bouts in Wild-type worms and *nmr-1* mutants. RIS data was extracted according to the results in A. In light blue RIS activity in *nmr-1* mutants is shown. Dark blue color represents RIS activities in Wild-type worms. Speed data of the mutant is depicted in light gray. Speed data of Wild-type worms is depicted in black. Violet shading indicates sleep bouts and 0 denotes their onsets. Error bars represent SEM. Neuronal activity levels before and after sleep bout onsets were statistically compared doing a Wilcoxon-signed rank test. Neuronal activities between genotypes were compared using a student's t-test. * denotes statistical significance at $p<0.05$ and ** denotes statistical significance at $p<0.01$.

C) Quantification of RIS activity maxima in sleep bouts in Wild-type worms and *nmr-1* mutants. Using a homemade MATLAB routine, global RIS activity maxima in sleep bouts were extracted from Wild-type worms and *nmr-1* mutants. Genotypes were statically compared using a student's t-test. * denotes statistical significance at $p<0.05$.

With regard to sleep bout characteristics, *nmr-1* mutants and Wild-type worms showed no significant differences (**Figure 17A**). Analysis of RIS activities showed that RIS gets activated in sleep bouts in *nmr-1 mutants*. This agrees to the Wild-type like quiescence behavior in lethargus of *nmr-1* mutants. However, RIS transients in sleep bouts were significantly smaller and shorter in the mutant background (**Figure 17B and C**).

4.7 Sleep bout analysis and RIS activity in sleep bouts in *eat-4* mutants

Because we saw reduced RIS activity in sleep bouts of glutamate receptor mutants, we studied the sleep behavior and RIS activity in *eat-4* mutants. *eat-4* encodes a glutamate transporter and glutamate levels in these mutants are presumably too low to sustain neurotransmission [120–122]. I performed a sleep bout analysis of *eat-4* mutants and additionally extracted RIS activities in sleep bouts (**Figure 18**).

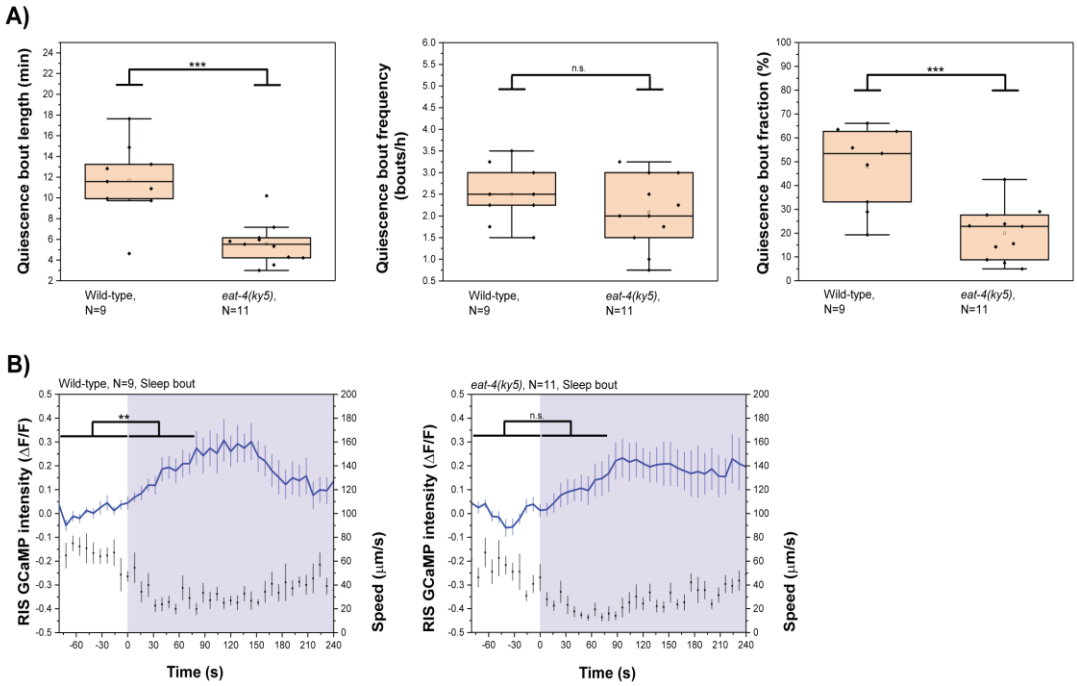

Figure 18. *eat-4* mutants display strongly reduced quiescence and RIS transients in L1 lethargus.

Worms were grown at 20°C. Imaging was performed in microchambers. Fluorescent images were taken every 8 seconds. RIS activity was tracked using GCaMP3.35. Speed data was generated from neuron positions.

A) Quantification of bout length, frequency and total time spend in quiescence bouts in Wild-type worms and *eat-4* mutants. Speed data was subjected to a bout analysis. Sleep bouts were defined by speeds lower than 10 % of the maximum speeds of individual worms and maintenance of these speeds for at least 2 minutes. Bouts were extracted using a homemade MATLAB routine. Genotypes were statistically compared performing a student's t-test. *** denotes statistical significance at $p<0.001$.

B) RIS activity levels in sleep bouts in Wild-type worms and *eat-4* mutants. RIS activities were extracted using a homemade MATLAB routine according to the results in A. Dark blue color represents RIS activities in sleep bouts. Speed data is depicted in black. Violet shading represents sleep bouts. Sleep bout onsets were at time point 0. Error bars represent SEM. RIS activity levels before and in sleep bouts were compared doing a Wilcoxon-signed rank test. ** denotes statistical significance at $p<0.01$.

eat-4 mutants showed a strong reduction of quiescence in lethargus compared to Wild-type worms. Mutants displayed significantly shorter quiescence bouts but with a Wild-type like frequency. In agreement to this, *eat-4* mutants lack RIS activation at sleep bout onsets (**Figure 18B**). Therefore, glutamate might be released at sleep bout onsets to activate RIS.

4.8 Optogenetic depolarization of *tdc-1*-expressing neurons

Because it was state of the art in 2015, we first used the *tdc-1* promoter to study RIM. The *tdc-1* promoter is expressed in RIC as well as in RIM neurons. For that reason, we later used the *gcy-13* promoter, which is RIM specific. The results generated with the *gcy-13* promoter are described in paragraph **4.4.**

To study the role of *tdc-1*-expressing neurons in the regulation of RIS activity, I optogenetically depolarized these neurons and simultaneously measured RIS activity (**Figure 19**).

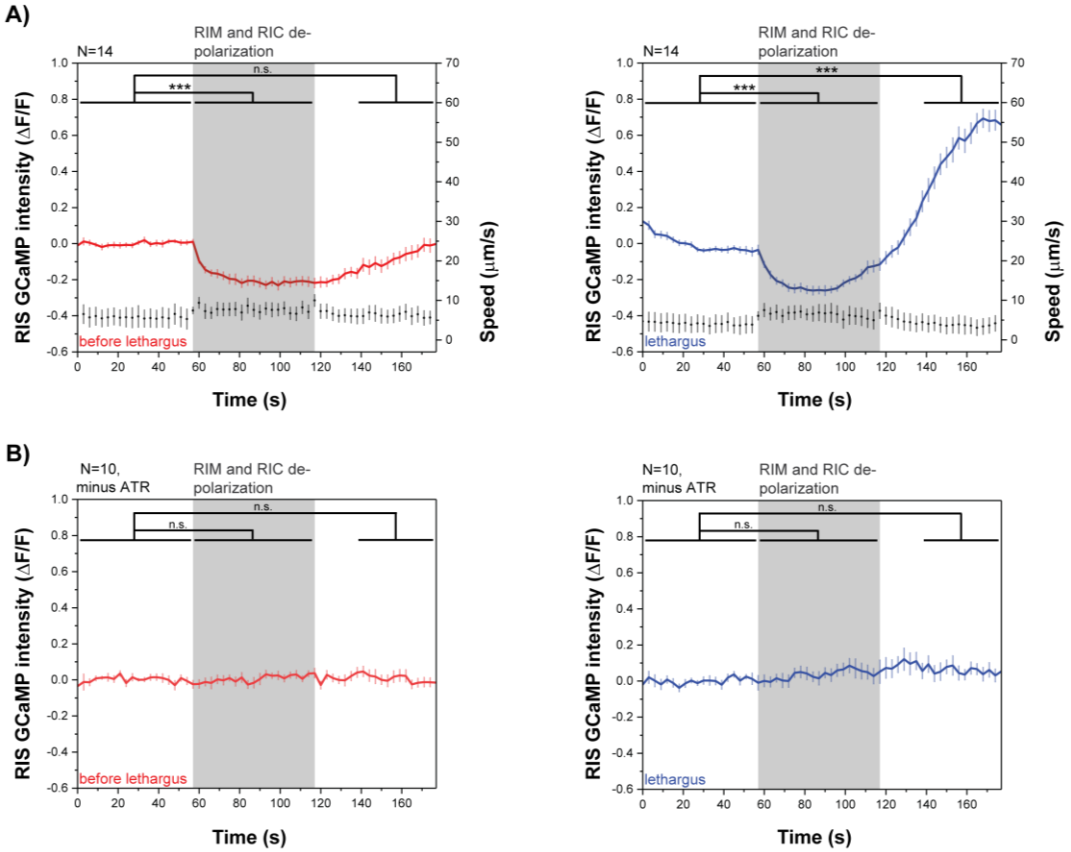

Figure 19. Optogenetic depolarization of *tdc-1* expressing neurons inactivates RIS.

A) Optogenetic depolarization of *tdc-1*-expressing neurons. Worms were cultured overnight on ATR-containing plates at 20°C. Next day, L1 larvae were imaged in microchambers. *tdc-1* expressing neurons were optogenetically depolarized using ReaChR. ReaChR was stimulated by green light. Optogenetic stimulation was repeated every 15 minutes. RIS activity was measured using GCaMP3.35. Speed data was generated from neuron positions. RIS activity outside of lethargus is shown in red. Blue indicates RIS activity in lethargus. Speed data is shown in black. Gray shading represents the optogenetic stimulation period. Error bars represent SEM. Neuron activity levels were compared performing a Wilcoxon-signed rank test. *** denotes statistical significance at $p<0.001$.

B) Control experiments. Same as in A, but without the addition of ATR.

As indicated in **Figure 19A,** optogenetic depolarization of *tdc-1* expressing neurons strongly inactivated RIS outside of and in lethargus. In lethargus, RIS displayed a massive rebound activation following the stimulation period. In agreement to RIS activity changes, worms mobilized during the stimulation periods, both outside of and in lethargus. Following the stimulation periods, worms did not change their speeds outside of lethargus and immobilized in lethargus.

This was the only experiment, in which the optogenetic depolarization of RIS upstream neurons led to a strong and robust net RIS inhibition followed by a state-dependent rebound activation in lethargus.

The control experiments in **Figure 19B**, showed no significant changes in RIS activities without the addition of ATR in any conditions.

4.8.1 Optogenetic depolarization of *tdc-1*-expressing neurons in *flp-18, tdc-1* double mutants

I aimed to identify neurotransmitters and neuropeptides, which are involved in the interactions between *tdc-1*-expressing neurons and RIS. A neurotransmitter candidate was tyramine. Tyramine is produced out of the amino acid tyrosine by the enzyme tyramine decarboxylase 1 (TDC-1). In 2014, Singh et al. reported an increase of total quiescence in L4 lethargus in *tdc-1* mutants and they reported that mutations in *tdc-1* orthologous genes caused an increase in rest in *Drosophila* [48]. Except for tyramine, the neuropeptide FLP-18 was an interesting candidate. FLP-18 was previously shown to be involved in the microhomeostasis of lethargus in *C. elegans* [96].

I repeated the optogenetic experiments shown in **Figure 19**, in single mutants as well as double mutants.

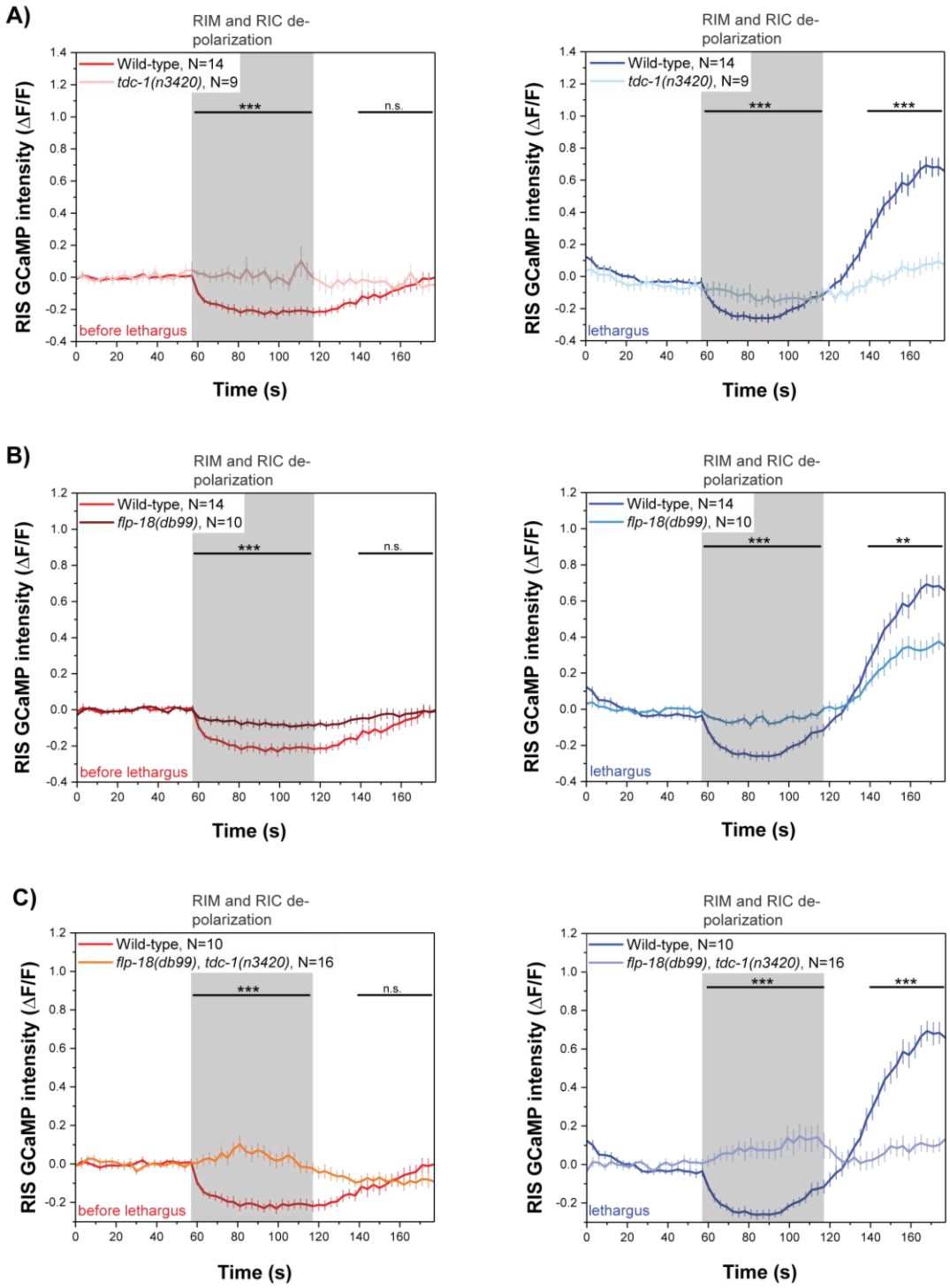
A)
RIM and RIC de-polarization
Wild-type, N=14
tdc-1(n3420), N=9
***
n.s.
before lethargus
RIS GCaMP intensity (ΔF/F)
Time (s)
RIM and RIC de-polarization
Wild-type, N=14
tdc-1(n3420), N=9
***
***
lethargus
RIS GCaMP intensity (ΔF/F)
Time (s)
B)
RIM and RIC de-polarization
Wild-type, N=14
flp-18(db99), N=10
***
n.s.
before lethargus
RIS GCaMP intensity (ΔF/F)
Time (s)
RIM and RIC de-polarization
Wild-type, N=14
flp-18(db99), N=10
***
**
lethargus
RIS GCaMP intensity (ΔF/F)
Time (s)
C)
RIM and RIC de-polarization
Wild-type, N=10
flp-18(db99), tdc-1(n3420), N=16
***
n.s.
before lethargus
RIS GCaMP intensity (ΔF/F)
Time (s)
RIM and RIC de-polarization
Wild-type, N=10
flp-18(db99), tdc-1(n3420), N=16
***
***
lethargus
RIS GCaMP intensity (ΔF/F)
Time (s)

Figure20. Tyramine and/or octopamine and FLP-18 mediate the RIS hyperpolarization by *tdc-1*-expressing neurons.

Worms were grown at 20°C and cultured overnight on ATR-containing plates. Next day, L1 larvae were imaged in microchambers. RIS activity was measured using GCaMP3.35. *tdc-1*-expressing neurons were stimulated using ReaChR. ReaChR was activated by green light. Optogenetic experiments were repeated every 15 minutes. Speed data was generated from neuron positions.

A) Optogenetic depolarization of *tdc-1*-expressing neurons in Wild-type worms and *tdc-1* mutants. Light red color indicates RIS activities outside of lethargus in mutants and red color indicates RIS activities outside of lethargus in Wild-type worms. Light blue color indicates RIS activities in lethargus in the mutant background. Dark blue color indicates RIS activities in lethargus in Wild-type worms. Gray shading represents the optogenetic stimulation period. Error bars represent SEM. Statistical calculations were done as follows: 1) a student's t-test was used to compare RIS activity levels during the optogenetic stimulation period. 2) a Kolmogorov-Smirnov test was used to compare RIS activity levels between genotypes after the optogenetic stimulation period. *** denotes statistical significance at $p<0.001$.

B) Optogenetic stimulation of *tdc-1*-expressing neurons in *flp-18* mutants and Wild-type worms. Same as in A, but experiments were done in *flp-18* mutants. Statistical calculations to compare genotypes were done using a student's t-test. ** denotes statistical significance at $p<0.01$ and *** denotes statistical significance at $p<0.001$.

C) Optogenetic stimulation of *tdc-1*-expressing neurons in *flp-18, tdc-1* double mutants and Wild-type worms. Same as in A, but experiments were performed in *flp-18, tdc-1* double mutants.

In *tdc-1* mutants, RIS was not inhibited upon optogenetic depolarization of *tdc-1*-expressing neurons outside of lethargus. In lethargus, the optogenetic depolarization of *tdc-1*-expressing neurons still inhibited RIS activity in the mutant background. However, inhibition levels were strongly reduced. In the mutant, depolarization of *tdc-1*-expressing neurons in lethargus led to a median reduction of RIS activity to -0.08. With contrast to that, the same experiments in Wild-type worms led to a median drop in RIS activity to -0.18. Consequently, inhibition levels were reduced to 43 % in the mutant background. Following the stimulation period, RIS activity levels in Wild-type worms rose in median to 0.53. In the mutant background, RIS activity levels increased to 0.03 after the stimulation period. Therefore, in the mutant background, RIS rebound activation levels resembled 6 % of Wild-type levels (**Figure 20A**).

A similar behavior was seen for *flp-18* mutants. Outside of lethargus, RIS was only very weakly inhibited upon optogenetic depolarization of *tdc-1*-expressing neurons. In median, RIS levels dropped to -0.06 compared to -0.16 in Wild-type worms. This equals a reduction to 40 % in the mutant background. In lethargus, the experimental outcome was different. During the optogenetic stimulation period, RIS was still inactivated in *flp-18* mutants. In median RIS levels dropped down to -0.04. This equals 25 % of the Wild-type effect. With regard to the rebound activation, *flp-18*

mutants resembled 65 % of the Wild-type effect. In median, RIS levels after the stimulation period rose to 0.34 in the mutant (**Figure 20B**).

Finally, in *flp-18, tdc-1* double mutants the effect of optogenetic depolarization of *tdc-1*-expressing neurons on RIS activity was completely abolished in all conditions (**Figure 20C**).

4.8.2 Optogenetic depolarization of RIC

The results in **Figure 19** revealed a discrepancy to the results in **Figure 8**. The difference between both experiments was, that the optogenetic depolarization of *tdc-1*-expressing neurons also includes RIC. Therefore, RIC might play a role in RIS regulation, although it is not directly presynaptic to RIS. 2 out of the 3 shortest connections between RIC and RIS, either via chemical synapses or gap junctions, include RIM [68,124].

To test for a potential role of RIC, I optogenetically activated RIC neurons using ReaChR. ReaChR was cell-specifically expressed in RIC neurons using the *tbh-1* promoter. Simultaneously, RIS activity was measured using GCaMP3.35 (**Figure 21**).

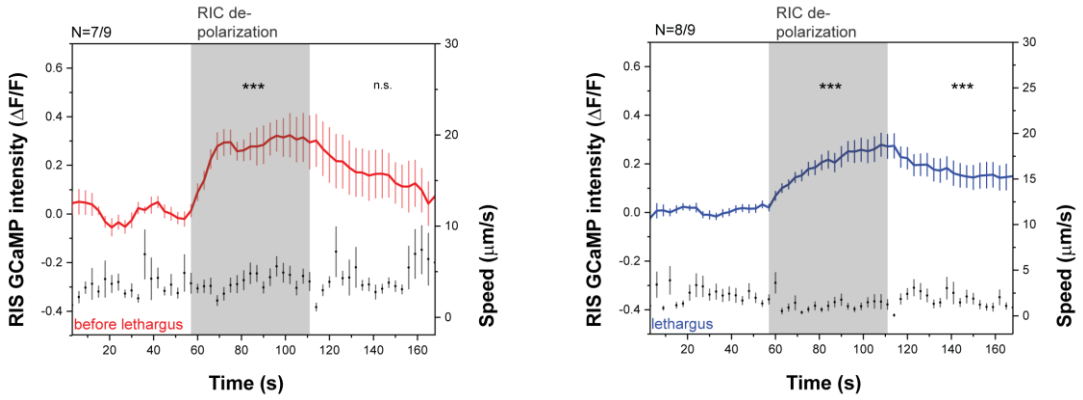

Figure 21. RIC optogenetic depolarization can activate RIS.

Worms were grown at 25°C overnight on ATR-containing plates. Next day, L1 larvae were imaged in microchambers. RIC neurons were optogenetically depolarized using ReaChR. ReaChR was activated by green light. RIS activity was measured using GCaMP3.35. Optogenetic experiments were repeated every 15 minutes. Speed data was extracted from neuron positions. RIS data was separated into RIS responsive and non-responsive trials. RIS was classified as responsive, if a change in its activity correlated with the onset of the optogenetic stimulation period. Outside of lethargus, RIS was activated in 7 out of 9 worms. In lethargus, 8 out of 9 worms showed RIS activation. Worms showed a change in RIS activity either exclusively outside of or in lethargus or in both conditions. Red color indicates RIS activity outside of lethargus. RIS activity in lethargus is shown in blue. Speed data is shown in black. Gray shading indicates the optogenetic stimulation period. Error bars indicate SEM. Neuron activities were statistically compared using a Wilcoxon-signed rank test. *** denotes statistical significance at $p<0.001$.

In agreement to experiments depicted in **Figure 8** and **Figure 10,** the data of **Figure 21** was generated by splitting GCaMP traces into RIS responsive and non-responsive trials. RIS was classified as responsive in a single trial, if RIS activity levels changed upon the onsets of the optogenetic stimulation periods.

In separated trials, RIC optogenetic depolarization could induce RIS activation, both outside of and in lethargus. However, outside of lethargus RIS activity levels went back to baseline after the stimulation period. In lethargus, RIS activity remained at levels significantly above baseline. Outside of lethargus, RIS activity changes did not cause any changes in the speed of worms. In lethargus, worms immobilized during the stimulation period. After the stimulation period, they returned to speed levels equal to those before the simulation.

To sum up, both separate RIM and separate RIC optogenetic depolarization can lead to RIS activation under certain conditions.

4.9 Identification of suppressors of the *aptf-1* mutant low quiescence phenotype

A side project of my thesis was the identification of suppressors of the *aptf-1* mutant low quiescence phenotype. To find *aptf-1* suppressors, I undertook an unbiased EMS mutagenesis. EMS stands for ethyl methanesulfonate. It is an alkylating agent, which predominantly introduces G:C to A:T single base pair exchanges in the DNA [125]. In *C. elegans* it has a forward mutation rate of $2.5*10^{-3}$ mutations per gene and generation for in total 23000 genes [126].

aptf-1 L4 larvae were treated with EMS according to standard protocols [114]. After mutagenesis, the direct offspring of the mutagenized worms were scored for their ability to immobilize in lethargus. Finally, 2 candidate lines were identified.

Speed data of candidate worms were extracted using a homemade worm tracker [127], were binned with a bin size of 1 and probabilities for each speed interval outside of and in lethargus were calculated. In **Figure 22** data of the mutagenesis candidate 1 and in **Figure 23** data of the mutagenesis candidate 9 is shown. Candidates were numbered according to their order in the selection process.

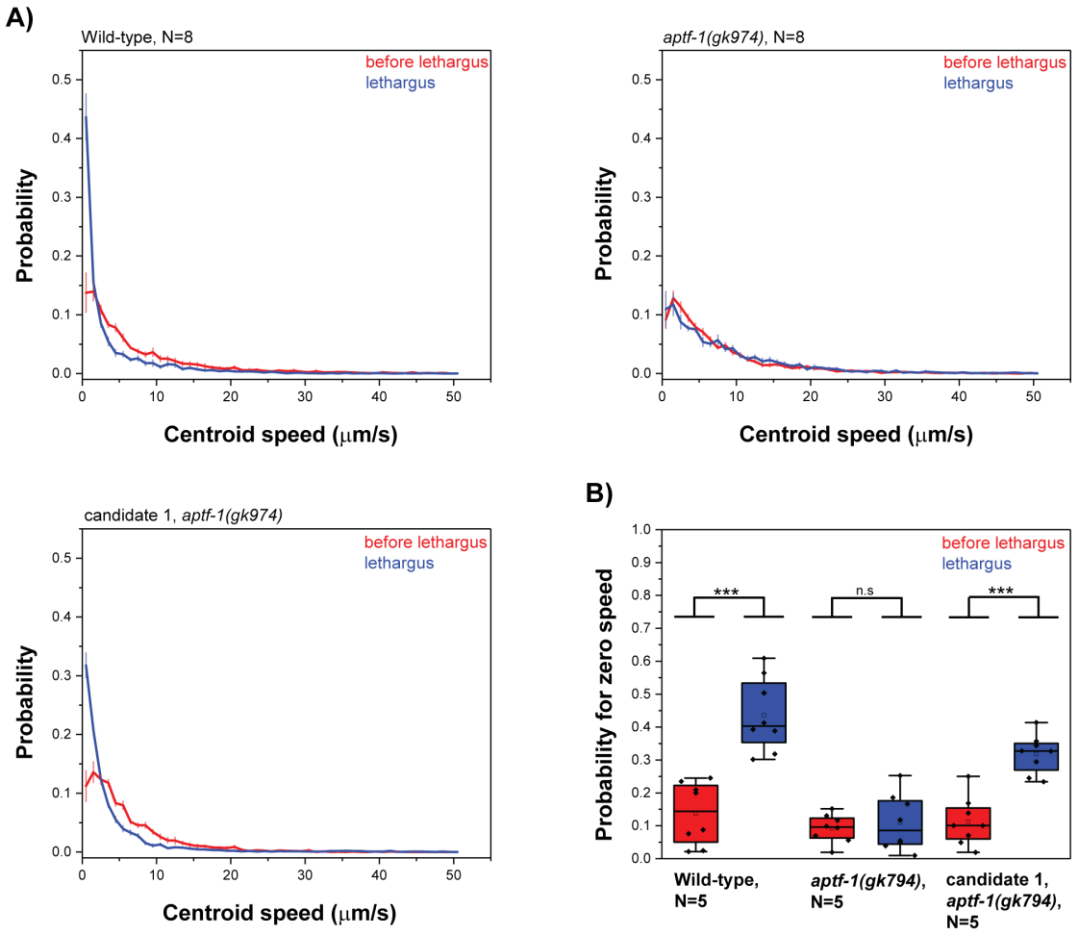

Figure 22. Worms of the mutagenesis candidate 1 immobilize in L1 lethargus.

Worms were grown at 20°C and L1 larvae were imaged in microchambers. Wild-type worms, *aptf-1* mutants and the mutagenesis candidate 1 worms were imaged in the same microchamber. The protocol was as follows: 40 DIC images in an interval of 500 ms were taken every 10 minutes. Centroid speeds were extracted using a homemade worm tracker [127]. Red color indicates speed interval probabilities outside of lethargus. Blue color indicates speed interval probabilities in lethargus.

A) Probability distribution of binned speeds outside of and in lethargus of Wild-type worms, *aptf-1* mutants and worms of the mutagenesis candidate 1. Speed data was binned with a bin size of 1. Probabilities were calculated for each binning interval individually. Speeds outside of and in lethargus were analyzed separately.

B) Quantification of probabilities of speeds of the first binning interval (from 0 to 1 µm/s) outside of and in lethargus of Wild-type worms, *aptf-1* mutants and worms of the mutagenesis candidate 1. Probabilities were statistically compared using a student's t-test. *** denotes statistical significance at $p<0.001$.

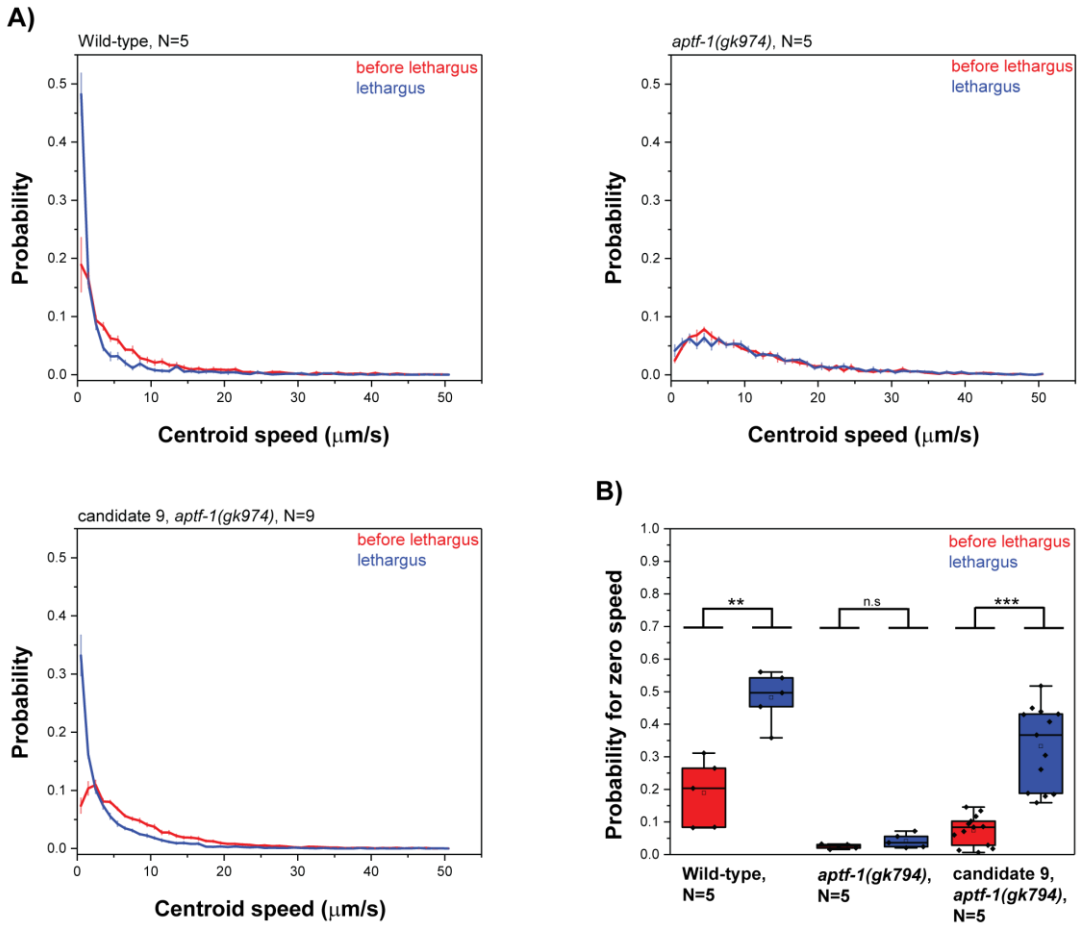

Figure 23. Mutagenesis candidate 9 worms immobilize in L1 lethargus.

Worms were grown at 20°C and L1 larvae were imaged in microchambers. Wild-type worms, *aptf-1* mutants and mutagenesis candidate 9 worms were imaged in the same microchamber. The protocol was as follows: 40 DIC images, with a frequency of 1 image per 500 ms, were taken every 10 minutes. Centroid speeds were extracted using a homemade worm tracker [127]. Red color indicates probabilities of binned speeds outside of lethargus. Blue color indicates probabilities of binned speeds in lethargus.

A) Probability distribution of binned speeds outside of and in lethargus of Wild-type worms, *aptf-1* mutants and worms of mutagenesis candidate 9. Speed data was binned with a bin size of 1. Probabilities were calculated for each binning interval individually. Speeds outside of and in lethargus were analyzed separately.

B) Quantification of probabilities of speeds of the first binning interval (0-1 μm/s) outside of and in lethargus of Wild-type worms, *aptf-1* mutants and mutagenesis candidate 9 worms. Probabilities were statistically compared using a student's t-test. *** denotes statistical significance at $p<0.001$.

As can be seen in **Figure 22**, probabilities of zero speeds (0-1 μm/s) were significantly different in Wild-type worms outside of and in lethargus. However, this was not true for *aptf-1* mutants. Their probabilities of zero speeds were equally low outside of and in lethargus. In candidate 1 worms, the *aptf-1* mutant phenotype was

suppressed, because probabilities for zero speeds were significantly different outside of and in lethargus. For comparison, Wild-type worms had zero speeds in lethargus with a median probability of 40 %, the *aptf-1* mutant had a median probability of 9 % and mutagenesis candidate 1 worms displayed zero speeds in lethargus with a median probability of 33 %. Therefore, mutagenesis candidate 1 worms did not fully resemble Wild-type immobilization levels.

Similarly to candidate 1, also in candidate 9 worms the *aptf-1* mutant phenotype was suppressed. In median, mutagenesis candidate 9 worms displayed zero speeds with a probability of 37 % which equals 74 % of Wild-type levels (**Figure 23**).

In subsequent experiments (data not shown) I characterized the mutations in the GOIs of candidate 1 and 9 as recessive. Furthermore, using complementation assays, I confirmed that both candidates do not carry the mutation in the same gene.

4.9.1 Whole genome sequencing of mutagenesis candidates

To identify genes of interest (GOI), genomic DNA from 4x back crossed mutagenesis candidates was extracted and was send for whole genome sequencing (WGS). WGS was done by the company GATC. For sequencing, the Illumina technology was used. Thereby, the paired end reads mode (2x 125 bp) was chosen with an ensured coverage rate of 30 per position. In total, the following amount of mutations was detected per candidate: mutagenesis candidate 1 carried 1919 INDELs (insertions and/or deletions) and 4721 SNPs (single nucleotide polymorphisms). Candidate 9 carried 1986 INDELs and 4721 SNPs. Altogether, there were 6630 mutations detected in candidate 1 and 6461 mutations detected in candidate 9.

To find GOIs, EMS-based mapping was applied. This method can be summarized as follows: EMS mutagenesis introduces randomly distributed mutations in the *C. elegans* genome. With back crossing, background mutations can be removed, except for those in very close proximity to the GOIs. Ideally, after back crossing, only one “Hot spot” should remain in the genome. Hot spot refers to a very strong enrichment

of mutations around the GOIs. The precision of this method equals an around 1 million base pair window in size [128,129].

The statistical department of the Universitätsmedizin Göttingen (UMG) identified the Hot spots in both candidates. We excluded all mutations from the Hot spot analysis, which were found in both candidates, because these mutations were presumably present in the original strain. Results of the Hot spot analysis are shown in **Figure 24.**

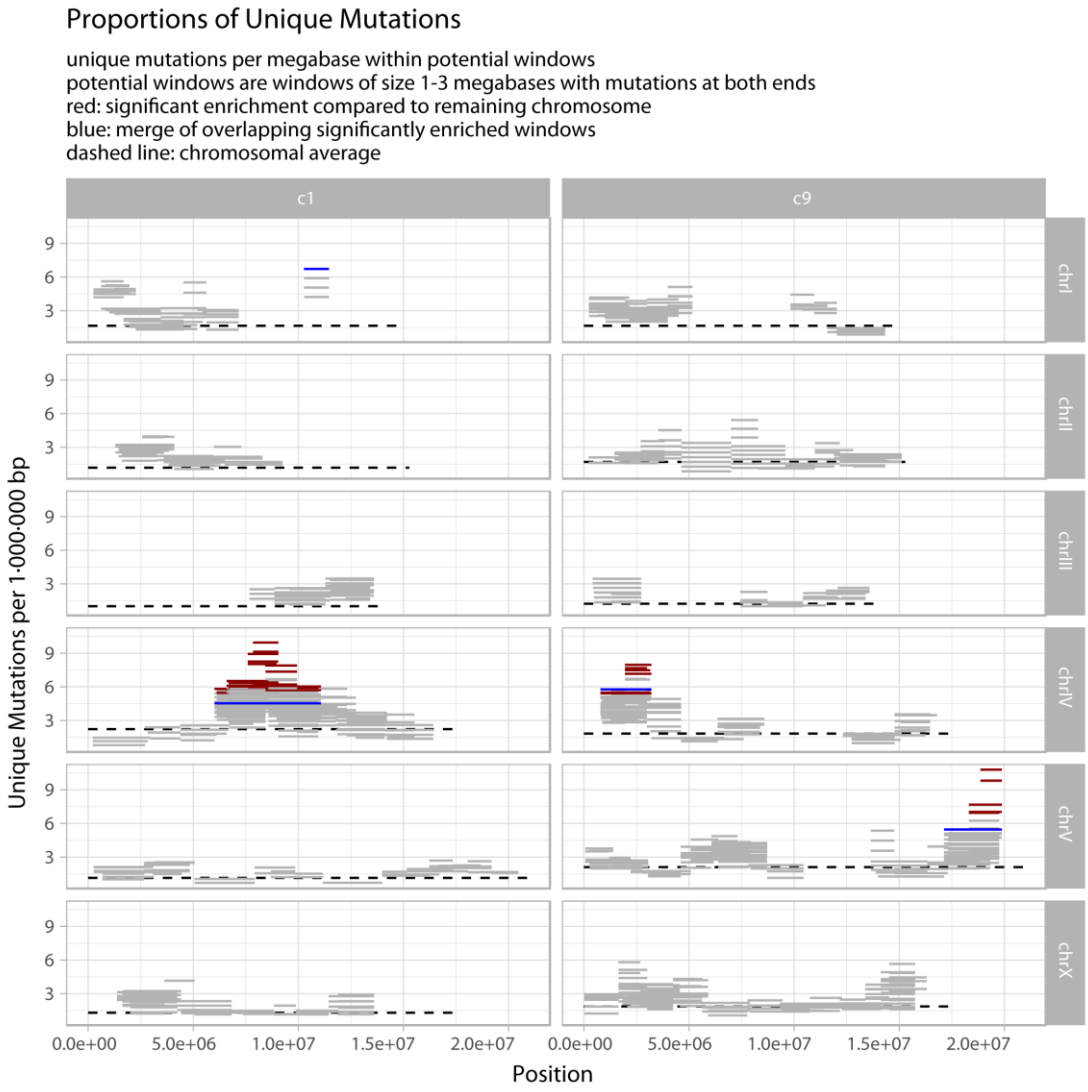

Figure 24. Distribution of mutations among all chromosomes of mutagenesis candidates 1 and 9.

WGS data of both candidates was subjected to a Hot spot analysis, which was performed by the UMG. Mutations, which were present in both candidates were excluded from the analysis. The distribution of remaining mutations over all chromosomes was plotted. This figure was taken from the UMG.

The Hot spot analysis showed 1 Hot spot on chromosome IV of candidate 1 and 2 Hot spots for candidate 9 on chromosome IV and V. Because there was only 1 Hot spot detected, we continued working with candidate 1. The aim was to establish a selection method first and then to apply this method also on candidate 9.

The Hot spot of candidate 1 contained 761 mutations. To further decrease the amount of possible GOIs, the following criteria were applied:

1. The mutation is unique for the candidate.
2. The mutation is homozygous.
3. All quality filters are passed.

These selection criteria shortened the list of possible GOIs to 8 (**Table 4**).

Table 4. List of possible GOIs in candidate 1 after filtering of Hot spot mutations.

Type	Effect	Impact	Gene name
insertion	codon insertion	moderate	*rod-1*
insertion	upstream	modifier	*F56H11.2*
insertion	upstream	modifier	*Y69E1A.2*
SNP	downstream	modifier	*Y59H11AM.1*
SNP	upstream	modifier	*Y73F4A.2*
SNP	downstream	modifier	*Y5F2A.3*
insertion	upstream	modifier	*Y73B6BL.47*
insertion/ SNP	upstream	modifier	*Y59H11AM.4*

From **Table 4** *rod-1* was the most promising candidate, because it carried the only mutation in a protein-coding region. Furthermore, it had the highest impact on protein levels.

rod-1 is a homolog of human KNTC1 (kinetochore-associated protein 1) and is involved in mitotic chromosome movement, localization of proteins to the kinetochore and in the organization of cell organelles [130–133].

4.9.2 Generation of a *rod-1* CRISPR mutant

We ordered a CRISPR mutant of the *rod-1* gene from the company SunyBiotech (strain name: PHX414, allele name: *syb414;* DNA sequence is provided in paragraph **10.3**). This CRISPR mutant rebuilt the mutation in the *rod-1* gene found in the mutagenesis candidate. In candidate 1 *rod-1* carried an insertion of 76 base pairs at chromosome position 7485261. The inserted base pairs replaced an adenosine at this position in the original sequence.

To use the CRISPR mutant as a second allele, I codon optimized the inserted sequence. I kept the exact same amino acid sequence but changed the DNA sequence. The codon optimization was done using the web page "*C. elegans* Codon Adapter" [134] (**Figure 25**).

Optimization Details

```
ORIGINAL    Codon Adaptation Index: 0.25   GC content: 37%
OPTIMIZED   Codon Adaptation Index: 0.86   GC content: 51%

ORIGINAL    AGT ATC GAA CAA GTG ATG ACA CGT CTA CAA ATT AGC AAA CAA TGG AAT ACA CTT CGT GCT CTA CTC AAC TAT GTT
OPTIMIZED   TCC ATC GAG CAA GTT ATG ACC CGC CTT CAG ATC TCT AAG CAA TGG AAC ACT CTC CGT GCC CTT CTC AAC TAC GTC
AMINO ACIDS Ser Ile Glu Gln Val Met Thr Arg Leu Gln Ile Ser Lys Gln Trp Asn Thr Leu Arg Ala Leu Leu Asn Tyr Val
```

Figure 25. Codon optimization of the DNA sequence, which was inserted in the *rod-1* gene in candidate 1.

The inserted DNA sequence in the *rod-1* gene was subjected to codon optimization using the web page "*C. elegans* Codon Adapter". This figure was taken from the web page. Before and after the codon optimization, the amino acid sequence of ROD-1 remained unchanged.

4.9.3 Sleep bout analysis of *aptf-1, rod-1* double mutants

The *rod-1* CRISPR mutant was crossed into *aptf-1* mutants. Thereafter, the double mutant was analyzed for its behavior in lethargus. If a mutation in *rod-1* could suppress the *aptf-1* low-quiescence phenotype, than the *aptf-1, rod-1* double mutant should display a Wild-type like lethargus behavior. Sleep bouts of double mutants were analyzed according to their frequencies and lengths. Additionally, total times spend in quiescence bouts were measured (**Figure 26**).

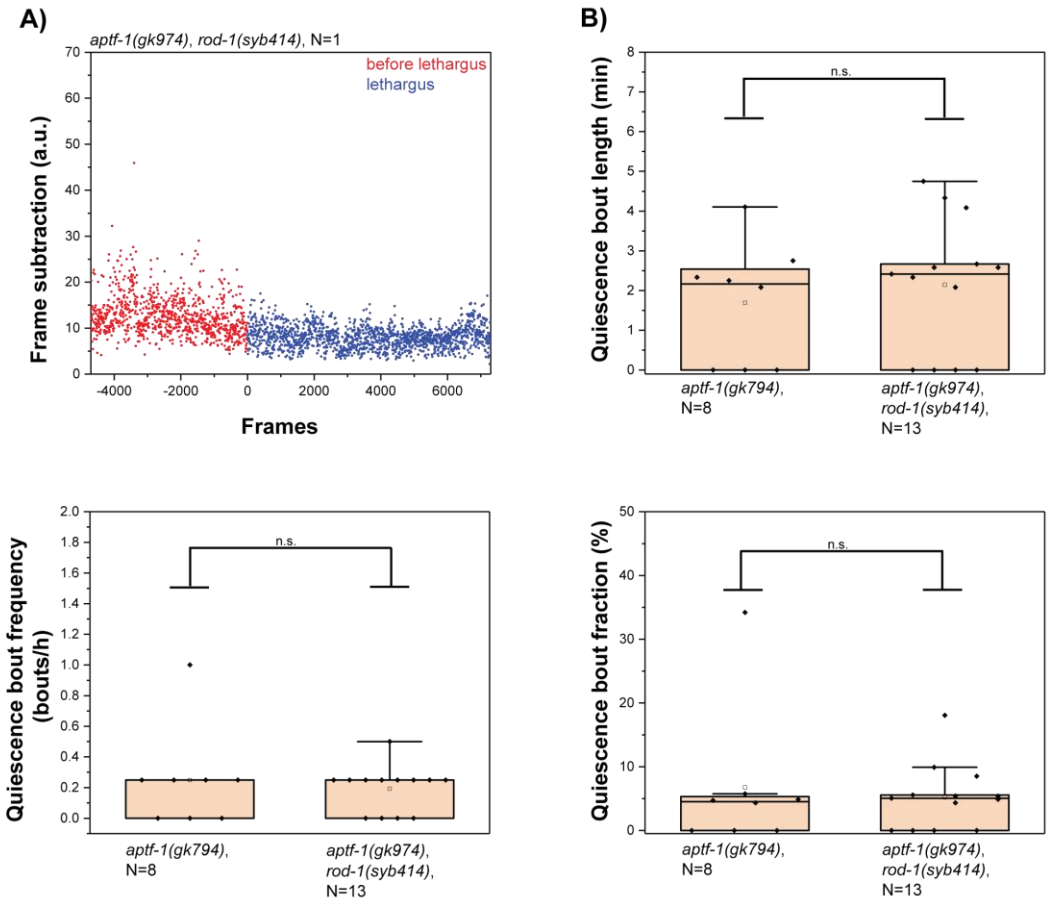

Figure 26. *aptf-1, rod-1* double mutants display an *aptf-1*-like lethargus behavior.

Worms were grown at 20°C and imaged in microchambers. *aptf-1* mutants and *aptf-1*, *rod-1* double mutants were imaged in the same microchamber. DIC images were taken every 5 seconds. Speeds were generated by frame subtraction.

A) Sample trace of *aptf-1, rod-1* double mutants outside of and in lethargus. Speeds outside of lethargus are shown in red and speeds in lethargus are shown in blue.

B) Sleep bout analysis of *aptf-1* and *aptf-1, rod-1* double mutants. Speed data was subjected to a bout analysis. Bouts were defined by speeds less than 10 % of the maximum speed of each individual worm and a minimum duration of least 2 minutes. Bouts were characterized with regard to their lengths and frequencies. Furthermore, total times worms spend quiescent were analyzed. Statistics were performed as follows: 1) to compare bout frequencies and total times spend in sleep bouts, a Kolmogorov-Smirnov test was used. 2) to compare bout lengths, a student's t-test was used.

In lethargus, *aptf-1*, *rod-1* double mutants displayed an *aptf-1*-like lethargus behavior. Therefore, the mutation in *rod-1* cannot suppress the *aptf-1* mutant phenotype (**Figure 26**).

5 Discussion and Outlook

5.1 RIS displays rebound activation after optogenetic hyperpolarization

The fact that all organisms which possess a nervous system have to sleep, led to the assumption that sleep regulating mechanisms are conserved amongst species [10,45–49]. According to that, both in humans and in *C. elegans*, sleep is controlled by sleep-active and sleep-promoting neurons [19,57]. Sleep-active neurons are characterized by their activity increase around sleep onset and that their activity causes an inhibition of wake-promoting circuits. For RIS, it was shown by Turek et al. in 2013 that it takes over this sleep-inducing function in *C. elegans* [57]. Furthermore, my former colleague Dr. Jan-Philipp Spies described in his thesis a function of RIS in sleep homeostasis and a function in the induction of quiescence after sleep deprivation [135]. Homeostatic regulation is one of the behavioral criteria, which define the sleep state [4]. To further study the role of RIS in sleep homeostasis, I collaborated with my former colleague Dr. Judith Besseling. The experimental set up was to optogenetically hyperpolarize RIS and track its activity during and after the stimulation period. In this experiment, we were able to detect a strong rise of RIS activity, above baseline levels, after the stimulation period. Rebound activation was six times stronger in lethargus than outside of lethargus. Taken together, these results prove that RIS activity is indeed subject to homeostatic regulation, which is much more tightly regulated in lethargus than outside of lethargus. The dose-response curve of optogenetic RIS hyperpolarization revealed, that the rebound activation is rather an acute than a chronic phenomenon. Experiments showed that the RIS rebound activation is only in a very limited range increasing with the time spent awake. Comparing the strength of the rebound activation after 1 and 5 minutes of optogenetic hyperpolarization, there was a significant increase in the rebound activation strength. Contrary to that, no further increase in the rebound activation strength was detectable after 10 minutes of optogenetic stimulation. This indicates that saturation levels were reached after 5 minutes.

5.2 PVC is a lethargus-specific activator of RIS

As described above, it is well established that RIS is sleep-inducing in *C. elegans* [57]. What is not characterized so far are the neuronal networks regulating RIS. To address this topic, we separately optogenetically depolarized or hyperpolarized neurons, which are directly presynaptic to RIS and simultaneously measured RIS activity (**Figure 7 and Figure 9**).

The response of RIS was quite diverse for the individual neurons but also for the conditions of lethargus and outside of lethargus.

1. AVJ had no effect on RIS in lethargus, because its optogenetic manipulation led only outside of lethargus to changes in RIS.
2. CEP depolarization caused a robust RIS activation outside of and in lethargus. However, the optogenetic hyperpolarization of CEP had no effect on RIS in any condition.
3. RIM optogenetic manipulations caused no net change in RIS activity, neither while optogenetically depolarizing nor while hyperpolarizing RIM. The role of RIM is discussed in more detail in the next paragraph.
4. Upon optogenetic depolarization of SDQL, RIS strongly activated outside of and in lethargus. Upon optogenetic SDQL hyperpolarization, RIS activity levels remained unchanged. However, SDQ synapses are not mature in the L1 larval stage (M. Turek, Mei Zhen, personal communication) [61].
5. Neither optogenetic depolarization nor hyperpolarization of URY caused a significant change in RIS activity levels, suggesting that URY might not have a direct effect on RIS.
6. PVC neurons were the only neurons with a robust lethargus-specific input on RIS upon their optogenetic depolarization. Furthermore, RIS reacted consistently with a drop in its activity to the optogenetic hyperpolarization of PVC, both outside of and in lethargus.

5.3 RIM can activate and inactivate RIS in lethargus

According to the results of optogenetic RIM manipulations, which are presented in **Figure 8** and **Figure**, RIM possesses a modulatory rather than active role in the regulation of RIS. Modulatory in the sense that, RIM is preferably reacting to stimuli it receives from other neurons than actively manipulating RIS activity. This conclusion was drawn from the fact that, both in optogenetic RIM depolarization and RIM hyperpolarization experiments, trials had to be selected according to the presence or absence of a significant effect in RIS. This modulatory function of RIM is further supported by the fact that its optogenetic depolarization can induce RIS activity increase as well as decrease. Thereby, it is conceivable that at least parts of the RIM effects are based on indirect mechanisms. A possible scenario for the inhibition of RIS by RIM would be that RIM inhibits PVC, and this PVC inhibition leads to a drop in RIS activity. A hypothetical mechanism of how RIM could inhibit PVC is provided in paragraph **5.4**.

Another point to the idea described above is added by experiments, in which RIS was optogenetically manipulated and RIM activity was measured simultaneously. Although RIM changed its activity upon optogenetic hyperpolarization of RIS, there was no change in RIM activity measurable upon optogenetic depolarization of RIS.

5.3.1Both excitatory and inhibitory neurotransmitters and neuropeptides are expressed in RIM

5.3.1.1 *tdc-1*-expressing neurons release tyramine and/ or octopamine and FLP-18 to inhibit RIS

According to the literature, RIM releases the neurotransmitter tyramine and the neuropeptide FLP-18 [71,123,136]. Tyramine is a biogenic neurotransmitter and is produced out of the amino acid tyrosine by the tyramine decarboxylase 1 (TDC-1). *tdc-1* is expressed in RIM and RIC neurons. Tyramine is in turn used as a precursor for the synthesis of the biogenic neurotransmitter octopamine. An enzyme called

tyramine beta hydroxylase (TBH-1) converts tyramine into octopamine. *tbh-1* is only expressed in the RIC neurons. Both neurotransmitters were shown to function independently [123]. Literature suggests that RIM is exclusively tyraminergic and RIC is octopaminergic [71,123]. To study a potential role of tyramine in sleep regulation the *tdc-1* mutant was used, which lacks both tyramine and octopamine. Therefore, effects seen in the *tdc-1* mutant could be additive effects of the lack of both neurotransmitters. To dissect tyraminergic and octopaminergic effects in sleep regulation, the optogenetic stimulation of *tdc-1*-expressing neurons should be repeated in *tbh-1* mutants.

The inhibitory effect of tyramine and/ or octopamine and FLP-18 on RIS activity differed outside of and in lethargus. Outside of lethargus, RIS inhibition by *tdc-1*-expressing neurons was completely abolished in *tdc-1* mutants but only decreased in *flp-18* mutants. This implies, at least partly, independent mechanisms of action for tyramine and/ or octopamine and FLP-18 in RIS regulation. However, the picture is different in lethargus. Both the *tdc-1* mutant as well as the *flp-18* mutant showed reduced RIS inhibition upon optogenetic depolarization of *tdc-1*-expressing neurons. Only in the double mutant background, RIS inhibition by the depolarization of *tdc-1*-expressing neurons was completely abolished. This indicates overlapping pathways for tyramine and/ or octopamine and FLP-18. The fact that RIS showed a state-dependent rebound activation after the optogenetic manipulations, further strengthen the hypothesis of mechanistic differences of RIS inhibition outside of and in lethargus.

5.3.2 RIM releases glutamate to potentially activate RIS

Despite releasing tyramine and FLP-18, RIM was also shown to be glutamatergic [71,137]. Glutamate is an excitatory neurotransmitter. Including the RIM neurons, glutamate is expressed in 38 different neuron classes and 78 neurons in total [114]. Among the directly presynaptic neurons of RIS, RIM and URY are glutamatergic [71]. Based on the fact that all command interneurons express the glutamate receptor *nmr-1*, we hypothesized that glutamate might be involved in sleep regulation [116]. Furthermore, we speculated that RIM could release glutamate to activate RIS.

Addressing the first point, it turned out that glutamate is indeed involved in sleep regulation. This can be concluded from the low quiescence phenotype in L1 lethargus of *eat-4* mutants. EAT-4 is a glutamate transporter and when absent glutamate levels are presumably too low to sustain neurotransmission [120–122,138]. Consistent with the function of glutamate in RIS activation, *eat-4* mutants lack RIS activation at the onset of sleep bouts. To prove the second point, that RIM releases glutamate to activate RIS, exclusive optogenetic depolarization of RIM in *eat-4* mutants should be repeated. Then, the prediction would be that RIM fails to activate RIS.

To sum up, RIM releases both inhibitory and excitatory neurotransmitters, what further supports the ambivalent function of RIM in RIS regulation.

5.4 A hypothetical circuit model for RIS regulation

In the following paragraphs, I present a hypothetical circuit model for the regulation of RIS. At first, this model establishes a general role for command interneurons in RIS regulation. All command interneurons function in either the forward or the backward locomotion circuit. Later, I specify which functions might be overtaken by the neurons of the forward and which by the neurons of the backward locomotion circuit.

5.4.1 Command interneurons are essential for RIS activation

Command interneurons have a fundamentally important function in the regulation of RIS. *nmr-1::ICE* mutants, in which command interneurons are ablated [115], display significantly less quiescence in L1 lethargus compared to Wild-type worms (**Figure 11**). The remaining sleep bouts in *nmr-1::ICE* mutants might be induced in a RIS-independent manner and might be caused by a general drop in neuronal activities in lethargus. A RIS-independent drop in the activity of command interneurons was seen in experiments, in which command interneuron activities were measured in the *aptf-1* mutant outside of and in lethargus (**Figure 13**). In agreement to the low quiescence phenotype, *nmr-1::ICE* mutants displayed only minimal RIS activation within sleep bouts. Finally, *nmr-1::ICE* mutants failed to display the RIS rebound activation after

optogenetic RIS hyperpolarization (**Figure 11**). This implies that the RIS rebound activation is neuronally regulated and that command interneurons also play a major role in the induction of the rebound activation. This links command interneurons to sleep regulation and sleep homeostasis.

5.4.2 A role for locomotion circuits in sleep regulation

PVC belongs to the forward locomotion circuit. RIM belongs to the backward locomotion circuit. Single neurons of the forward and the backward locomotion circuits are all connected via gap junctions. The activity of one locomotion circuit inhibits the activity of the other and vice versa. The decision for which direction the worm is moving in, is made by the relative activity of both systems to one another. The system which is more active determines the direction of movement [115,116,139–141]. The mutual inhibition of locomotion circuits bears a quite striking similarity to the working principle of wake-active wake-promoting circuits and sleep-active sleep-promoting circuits in mammals. Sleep-regulating circuits in mammals function in a so-called flip-flop switch. If wake-active wake-promoting circuits are active, sleep-active sleep-promoting circuits are inactive and vice versa [19].

Furthermore, Zheng et al. showed in 1999 that even small changes in arousal could change the equilibrium of forward and backward locomotion circuits [115]. This links command interneuron activity to arousal and consequently RIS regulation to arousal. A change of arousal thresholds at the lethargus onset is induced by the dampening of command interneuron activities (**Figure 13**). This change in arousal might be potent enough to cause an imbalance in the locomotion circuits, which favors the activity of either one of these. Data from Nichols, Eichler, Latham, and Zimmer in 2017 suggests that the forward locomotion circuit would be the one in favor, because in their studies worms induced a forward locomotion program before they go to sleep [142]. If the forward locomotion circuit is active, PVC is also active. Consequently, PVC activation can trigger RIS activation. RIS activity would send the worm to sleep and further dampen the activity of the neurons of the locomotion circuits. With the dampening of command interneuron activities, RIS could further establish the imbalance in the locomotion circuits, favor the active state of the forward locomotion

circuit including PVC, strengthen its own active state and therefore sleep. However, high RIS activity would ultimately lead to the inhibition of its own activator, because it induces a dampening of all command interneurons including PVC. This limits RIS activity to a certain strength and a certain duration. A restricted RIS activity agrees with the observation that the lethargus period is split into periods of higher and lower RIS activity and therefore increased or decreased arousal and mobility (**Figure 4**).

5.4.3 Sleep-specific activity of the backward circuit

The model described before supposes that the backward locomotion circuit is off in lethargus, but it is also off if worms make a forward movement. The difference, which makes the worm go backwards or go to sleep, might be how strongly the activity of the backward locomotion circuit is reduced. The hypothesis is that the neurons of the backward locomotion circuit are more inactive in lethargus than they are during a forward movement. To test this idea, neuronal activities of the backward circuit in a freely moving worm during forward and backward movement outside of lethargus as well as neuronal activities in lethargus should be measured. Methods to image multiple neurons in freely-behaving worms are described in the literature [143–145].

In 2011, Kawano et al. described *unc-7*, *unc-9* double mutants. Both genes are required to build functional gap junctions in the locomotion circuits. Kawano et al. characterized the backward locomotion circuit in the double mutant as overall more active than in Wild-type worms [139]. In a paper published in 2018, these mutants were proven to display almost no quiescence during L4 lethargus [100]. Maybe because of their overactivated backward circuit, the forward circuit including PVC cannot activate RIS around sleep onset in *unc-7*, *unc-9* double mutants. A lack in PVC activity causes a lack in RIS activation. As a consequence, these mutants display a severely diminished quiescence behavior during L4 lethargus. To test this idea, a possible experimental design would be to measure RIS activity in these mutants. The prediction would be that RIS activity peaks can be barely detected and therefore the same holds true for sleep bouts. Another interesting experiment would address the question, whether PVC is able to activate RIS, although the backward locomotion circuit is active. Optogenetic depolarization of PVC in the gap junction mutant and

simultaneous measurement of RIS activity should give an answer to that question. However, one caveat would be that optogenetic manipulations are stronger than naturally occurring transients. This might allow PVC activity to dominate the overactivation of the backward circuit.

5.4.4 How RIS and its regulatory network respond to waking stimuli

The control of RIS activity by command interneurons provides an elegant link between lethargus and arousal levels, homeostatic maintenance of sleep, and the translation of locomotion into increased sleep-active neuron depolarization.

It was shown before, that arousing stimuli trigger escape responses in lethargus. The escape response manifests as a backwards movement and is accompanied by the inhibition of sleep-active neurons [57,101,146]. The inhibition of RIS during the escape response might be caused by an activity increase of the backward locomotion circuit. Because the backward locomotion circuit is active, PVC and the forward locomotion circuit are inactive and no RIS activation can take place. When the waking stimulus stops, the escape response stops as well. The backward locomotion circuit becomes less active and therefore the forward locomotion circuit reactivates and consequently PVC reestablishes a higher RIS activity state.

Additional data were provided in the PhD thesis of my former colleague Dr. Florentin Masurat [147]. He optogenetically activated the ASH neurons and simultaneously measured RIS activity. ASH neurons are the most important arousal neurons in *C. elegans*. Activation of the ASH neurons induces an escape response [95,124,148]. During the escape response RIS activity was significantly decreased in lethargus. The drop in RIS activity is abolished in *tdc-1::egl-1* mutants. EGL-1 activates programmed cell death [149]. Therefore, its expression under the *tdc-1* promoter leads to programmed cell death of the RIM and RIC neurons. Consequently, the important factor for RIS inhibition is the connection of the ASH neurons to RIM and therefore the connection of the backward locomotion circuit to RIS.

5.4.5 *nmr-1* regulates command interneuron activity levels in lethargus

To identify plasticity factors, which function in the command interneurons, activity levels of these neurons in *nmr-1* mutants were analyzed. As mentioned before, *nmr-1* is expressed in all command interneurons and encodes a glutamate receptor subunit [116-118]. Mutants display Wild-type activity levels of command interneurons up to 50 minutes during lethargus. After 50 minutes, activity level dropped significantly below Wild-type levels in the mutant, which indicates that *nmr-1* function is required later in sleep to maintain command interneuron activity (**Figure 16**). For this reason, *nmr-1* mutants display only a small but significant reduction in RIS activity in sleep bouts. Because RIS activity is still present in sleep bouts, *nmr-1* mutants do not display abnormalities in their sleep bout behavior (**Figure 17**). The behavior of RIS in *nmr-1* mutants was consistent with the behavior of RIS in *eat-4* mutants (**Figure 18**). This, further suggests a function for glutamate in the regulation of command interneurons and therefore in RIS regulation.

5.5 The *aptf-1* mutant phenotype can be suppressed

The EMS mutagenesis of *aptf-1* mutants, which is presented in **Figure 22** and **Figure 23**, prove that it is possible to suppress the *aptf-1* mutant low quiescence phenotype in lethargus. Two promising candidates were isolated. Speed probability distribution analysis outside of and in lethargus showed their ability to immobilize in lethargus and therefore to suppress the mutant phenotype.

To identify potential GOIs the method of EMS-based mapping was chosen [128,129]. The plan was to optimize the selection criteria first and to use candidate 1 as a proof-of principle. Then the next step would be to apply the optimized selection criteria on candidate 9. However, the selection procedure did not lead to a successful identification of the GOI in candidate 1, in which a mutation in *rod-1* did not suppress the low quiescence phenotype in L1 lethargus.

To progress with this project, *aptf-1* mutants should be crossed with mutants for the seven remaining candidate GOIs in the Hot spot of candidate 1.The huge amount of

available mutants for almost all genes in *C. elegans*, allows for screening through all potential GOIs without previous selection. Successful identification of a suppressor could prove, that the applied filtering criteria to identify the Hot spot in candidate 1 were correct. A negative result would suggest repeating the identification of the Hot spot and thereby only consider EMS-typical mutations.

5.6 Perspectives

5.6.1 Does every RIS activation necessarily lead to sleep induction?

It is possible that not every RIS activation necessarily leads to sleep induction. This hypothesis is, amongst others, supported by the fact that the AVJ neurons only induce RIS activation outside of lethargus (**Figure 7**).

Another example are the CEP neurons. Optogenetic depolarization of CEP neurons leads to RIS activation both outside of and in lethargus. However, optogenetic inhibition of CEP neurons did not induce changes in RIS (**Figure 7 and 9**). Probably, interactions between CEP neurons and RIS are important to regulate feeding behaviors. Dopaminergic neurons (CEP, ADE and PDE) in general were shown to be involved in the so-called “basal slowing response”. Basal slowing response describes a behavior in which worms decrease their locomotion speed if they enter a lawn of food bacteria [150]. It would be conceivable that this reduction in speed is achieved through RIS activation by the CEP neurons. This would also imply, that RIS does not exclusively serve a sleep-inducing function, but it also fulfills a function in speed regulation.

One way to understand when RIS activation leads to sleep induction and when RIS activation slows worms down would be to analyze how PVC is itself regulated. To investigate PVC regulation, an optogenetic screening through its directly presynaptic neurons should be performed. However, the analysis of PVC is subject to certain restrictions. Naturally occurring transients in PVC are very small [151]. In order to study PVC function in a freely-behaving, instead of an immobilized, worm an option would be to use more-sensitive GCaMP sensors.

Finally, the idea that not every RIS activation leads to sleep induction, can also explain why not all interactions of RIS with its upstream neurons induce a rebound.

5.6.2 Which RIS interactions can trigger a rebound activation?

Whenever we optogenetically hyperpolarized RIS, we observed a robust rebound activation. As described in paragraph **4.3**, within a distinct time interval, the strength of the rebound activation depends on the duration of the stimulus. Rebound activation was stronger and occurred faster the longer the optogenetic stimulus was applied, up to the threshold of 5 minutes.

Despite optogenetic manipulation of RIS, the occurrence and the strength of the rebound activation was difficult to predict. There were cases when RIS activity went back to baseline levels, both after activation and inhibition. In other cases, RIS activity stayed significantly above baseline levels following RIS activation. In all cases of RIS inhibition, we could not observe a significant drop of activity levels after the stimulation period, in analogy to the previously described RIS activation condition. In another subset of experiments, RIS activation resulted in a rebound activation only outside of lethargus or there was only a very short rebound activation detectable in lethargus, with a duration of around 30 seconds. Finally, in the last subset of experiments, RIS activation induced both outside of and in lethargus a rebound activation. However, the strength of the rebound activation was not state-dependent.

One possible explanation for the absence of a rebound activation after RIS inhibition, could be that the waking stimulus was very strong. A very strong stimulus would keep the worms awake longer, therefore requiring extended measurement time of RIS activity, after the stimulation period. Thereby, it would be of high importance to track the behavior of the worms to identify the time point of immobilization.

This explanation does not hold true when RIS activation can be seen. Therefore, the induction of a rebound activation might depend on the presynaptic neuron interacting with RIS. Another factor could be the age of the worms. Worms probably respond

differently in L1 compared to L4 lethargus, because neuronal networks for RIS regulation change between these stages. SDQ synapses are not mature in the L1 larvae [61] (M. Turek, Mei Zhen, personal communication). Amongst all presynaptic neurons, SDQL forms the highest amount of chemical synapses (3) with RIS [68,124].

5.6.3 Further analysis of *tdc-1*-expressing neurons function in RIS regulation

Because RIM and RIC neurons behave differently when they are separately stimulated, we can conclude that it is their simultaneous activation, which produces an inhibitory input on RIS. To test for that, the optogenetic lines for the single neurons should be crossed together to resemble the situation in which the *tdc-1* promoter was used. However, the expression levels of the single ReaChR lines differ. That means, even if the same amount of light is used to perform the optogenetic experiments, the magnitude of activation would be different for the RIM and RIC neurons. Because activation levels would not be comparable, RIM-induced effects and RIC-induced effects might overlay each other and therefore results would not be conclusive.

Nevertheless, the optogenetic depolarization of *tdc-1*-expressing neurons, was the only condition in which upstream neurons induced a robust RIS inhibition outside of and in lethargus. To understand more about the regulatory pathways, the analysis of RIM and RIC upstream circuits would be required. Thereby, an important question would be which natural behavior can induce the simultaneous activation of RIC and RIM with regard to sleep.

6 Abbreviations

ArchT: archaerhodopsin
ATR: all-*trans* retinal
bp: base pair
***C. elegans*:** *Caenorhabditis elegans*
cGMP: cyclic guanosine monophosphate
Clock: circadian locomotor output cycles kaput
COM: completely out of molt
DIC: differential interference contrast
DNA: deoxyribonucleic acid
***E. coli*:** *Escherichia coli*
EEG: electroencephalography
EGF: epidermal growth factor
EMCCD: electron multiplying charge-coupled device
EMS: ethyl methanesulfonate
eVLPO: extended ventrolateral preoptic nucleus
FLP: FMRFamide-related peptides
GABA: γ-aminobutyric acid
GCaMP: genetically-encoded calcium sensor
gf: gain-of-function
GFP: green fluorescent protein
GOI: gene of interest
ICE: interleukin-1β-converting enzyme
INDEL: insertion and/ or deletion of base pairs in DNA
L1-L4 stage: first, second, third and fourth *C. elegans* larval stage
LC: locus coeruleus
LED: light-emitting diode
lf: loss-of-function
mRNA: messenger ribonucleic acid
NGM: nematode growth medium
NLP: non-insulin and non-FMRFamide-related peptides
NMDA: N-methyl-D-aspartic acid

Abbreviations

NREM:	non-rapid eye movement
ORX:	orexinergic neurons
PCR:	polymerase chain reaction
PKG:	cGMP-dependent protein kinase
ReaChR:	red-shifted Channelrhodopsin
REM:	rapid (or random) eye movement
SCN:	suprachiasmatic nucleus
SEM:	standard error of the mean
SNP:	single nucleotide polymorphism
SWS:	slow wave sleep
TGFβ:	transforming growth factor β
TMN:	tuberomammillary nucleus
UMG:	Universitätsmedizin Göttingen
UTR:	untranslated region
VLPO:	ventrolateral preoptic nucleus
WGS:	whole genome sequencing
YA:	young adult

7 List of figures

List of figures

8 List of tables

9 References

1. Hendricks, J. C. *et al.* Rest in Drosophila is a sleep-like state. *Neuron* **25,** 129–138 (2000).
2. Shaw, P. J., Cirelli, C., Greenspan, R. J. & Tononi, G. Correlates of sleep and waking in *Drosophila melanogaster*. *Science* **287,** 1834–1837 (2000).
3. Zhdanova, I. V., Wang, S. Y., Leclair, O. U. & Danilova, N. P. Melatonin promotes sleep-like state in zebrafish. *Brain Res.* **903,** 263–268 (2001).
4. Raizen, D. M. *et al.* Lethargus is a Caenorhabditis elegans sleep-like state. *Nature* **451,** 569–572 (2008).
5. Kayser, M. S. & Biron, D. Sleep and development in genetically tractable model organisms. *Genetics* **203,** 21–33 (2016).
6. Trojanowski, N. F. & Raizen, D. M. Call it Worm Sleep. *Trends Neurosci.* **39,** 54–62 (2016).
7. Artiushin, G. & Sehgal, A. The Drosophila circuitry of sleep – wake regulation. *Curr. Opin. Neurobiol.* **44,** 243–250 (2017).
8. Oikonomou, G. & Prober, D. A. Attacking sleep from a new angle: contributions from zebrafish. *Curr. Opin. Neurobiol.* **44,** 80–88 (2017).
9. Loomis, A. L., Harvey, E. N. & Hobart, G. A. CEREBRAL STATES DURING SLEEP, AS STUDIED BY HUMAN BRAIN POTENTIALS. *J. Exp. Psychol.* **21,** 1–16 (1937).
10. Bringmann, H. Sleep-active neurons: Conserved motors of sleep. *Genetics* **208,** 1279–1289 (2018).
11. Silber, M. H. *et al.* The visual scoring of sleep in adults. *J. Clin. Sleep Med.* **3,** 121–131 (2007).
12. Dijk, D.-J. Regulation and functional correlates of slow wave sleep. *J. Clin. sleep Med.* **5,** S6-15 (2009).
13. Campbell, S. S. & Tobler, I. Animal sleep: A review of sleep duration across phylogeny. *Neurosci. Biobehav. Rev.* **8,** 269–300 (1984).
14. Cirelli, C. & Tononi, G. Is sleep essential? *PLoS Biol.* **6,** 1605–1611 (2008).
15. Allada, R. & Siegel, J. M. Unearthing the Phylogenetic Roots of Sleep. *Curr. Biol.* **18,** 670–679 (2008).
16. Weaver, D. R. The Suprachiasmatic Nucleus: A 25-Year Retrospective. *J. Biol.*

Rhythms **13,** 100–112 (1998).

17. Albrecht, U., Zheng, B., Larkin, D., Sun, Z. S. & Lee, C. C. *mPer1* and *mPer2* Are Essential for Normal Resetting of the Circadian Clock. *J. Biol. Rhythms* **16,** 100–104 (2001).
18. Deurveilher, S. & Semba, K. Indirect projections from the suprachiasmatic nucleus to major arousal-promoting cell groups in rat: Implications for the circadian control of behavioural state. *Neuroscience* **130,** 165–183 (2005).
19. Saper, C. B., Scammell, T. E. & Lu, J. Hypothalamic regulation of sleep and circadian rhythms. *Nature* **437,** 1257–1263 (2005).
20. Sherin, J. E., Shiromani, P. J., McCarley, R. W. & Saper, C. B. Activation of ventrolateral preoptic neurons during sleep. *Science (80-.).* **271,** 216–219 (1996).
21. Gaus, S. E., Strecker, R. E., Tate, B. A., Parker, R. A. & Saper, C. B. Ventrolateral preoptic nucleus contains sleep-active, galaninergic neurons in multiple mammalian species. *Neuroscience* **115,** 285–294 (2002).
22. Porkka-Heiskanen, T. Sleep homeostasis. *Curr. Opin. Neurobiol.* **23,** 799–805 (2013).
23. Borbély, A. A. A two process model of sleep regulation. *Hum. Neurobiol.* **1,** 195–204 (1982).
24. Kattler, H., Dijk, D.-J. & Borbely, A. A. Effect of unilateral somatsensory stimulation prior to sleep on the sleep EEG in humans. *J. Sleep Res.* **3,** 159–164 (1994).
25. Vyazovskiy, V. V., Cirelli, C. & Tononi, G. Electrophysiological correlates of sleep homeostasis in freely behaving rats. *Prog. Brain Res.* **193,** 17–38 (2011).
26. Vyazovskiy, V. V. *et al.* Local sleep in awake rats.pdf. *Nature* **472,** 443–447 (2011).
27. Finelli, L. A., Baumann, H. & Borbe, A. A. Dual Electroencephalogram Markers of Human Sleep Homeostasis : Correlation Between Theta Activity in Waking and Slow-Wave Activity in Sleep. **101,** 523–529 (2000).
28. Schwierin, B. *et al.* Regional differences in the dynamics of the cortical EEG in the rat after sleep deprivation. *Clin. Neurophysiol.* **110,** 869–875 (1999).
29. Hu, J. *et al.* Sleep-deprived mice show altered cytokine production manifest by perturbations in serum IL-1ra, TNFa, and IL-6 levels. *Brain. Behav. Immun.* **17,** 498–504 (2003).

30. Taishi, P. *et al.* TNFα siRNA Reduces Brain TNF and EEG Delta Wave Activity in Rats. *Brain Res.* **1156,** 125–132 (2007).
31. Takahashi, S., Kapa´s, L., Fang, J. & Krueger, J. M. An anti-tumor necrosis factor antibody suppresses sleep in rats and rabbits. *Brain Res.* **690,** 241–244 (1995).
32. Cirelli, C. Functional Genomics of Sleep and Circadian Rhythm Invited Review: How sleep deprivation affects gene expression in the brain: a review of recent findings. *J. Appl. Physiol.* **92,** 394–400 (2002).
33. Colten, H. R., Altevogt, B. M. & Editors. *Sleep Disorders and Sleep Deprivation: An Unmet Public Health Problem*. (2006).
34. Krueger, J. M., Frank, M. G., Wisor, J. P. & Roy, S. Sleep function: Toward elucidating an enigma. *Sleep Med. Rev.* **28,** 42–50 (2016).
35. Rechtschaffen, A. & Bergmann, B. M. Sleep deprivation in the rat by the disk-over-water method. *Behav. Brain Res.* **69,** 55–63 (1995).
36. Braun, A. Regional cerebral blood flow throughout the sleep– wake cycle. *Brain* **120,** 1–25 (1997).
37. Kang, J. *et al.* Amyloid-β Dynamics are Regulated by Orexin and the Sleep-Wake Cycle. *Science (80-.).* **326,** 1005–1007 (2009).
38. Vorster, A. P. & Born, J. Sleep and memory in mammals, birds and invertebrates. *Neurosci. Biobehav. Rev.* **50,** 103–119 (2015).
39. Frank, M. G. & Cantera, R. Sleep, Clocks and Synaptic Plasticity. *Trends Neurosci.* **37,** 491–501 (2014).
40. Wang, G., Grone, B., Colas, D., Appelbaum, L. & Mourrain, P. Synaptic plasticity in sleep: Learning, homeostasis and disease. *Trends Neurosci.* **34,** 452–463 (2011).
41. Tononi, G. & Cirelli, C. Sleep function and synaptic homeostasis. *Sleep Med. Rev.* **10,** 49–62 (2006).
42. Zager, A. & Andersen, M. Effects of acute and chronic sleep loss on immune modulation of rats. *Am. J. Physiol. Regul. Integr. Comp. Physiol.* **293,** R504–R509 (2007).
43. Hakim, F. *et al.* Fragmented sleep accelerates tumor growth and progression through recruitment of tumor-associated macrophages and TLR4 signaling Fahed. *Cancer Res.* **74,** 1329–1337 (2014).
44. Besedovsky, L., Lange, T. & Born, J. Sleep and immune function. *Pflugers*

Arch. Eur. J. Physiol. **463,** 121–137 (2012).

45. Nath, R. D. *et al.* The Jellyfish Cassiopea Exhibits a Sleep-like State. *Curr. Biol.* **27,** 2984–2990.e3 (2017).
46. Joiner, W. J. Unraveling the Evolutionary Determinants of Sleep. *Curr. Biol.* **26,** R1073–R1087 (2016).
47. Sehgal, A. & Mignot, E. Genetics of Sleep and Sleep disorders. *Cell* **146,** 194–204 (2011).
48. Singh, K., Ju, J. Y., Walsh, M. B., DiIorio, M. A. & Hart, A. C. Deep Conservation of Genes Required for Both Drosophila melanogaster and Caenorhabditis elegans Sleep Includes a Role for Dopaminergic Signaling. *Sleep* **37,** 1439–1451 (2014).
49. Zimmerman, J. E., Naidoo, N., Raizen, D. M. & Pack, A. Conservation of Sleep: Insights from Non-Mammalian Model Systems. *Trends Neurosci.* **31,** 371–376 (2008).
50. Van Buskirk, C. & Sternberg, P. W. Epidermal growth factor signaling induces behavioral quiescence in Caenorhabditis elegans. *Nat. Neurosci.* **10,** 1300–1307 (2007).
51. Singh, K. *et al.* C. elegans notch signaling regulates adult chemosensory response and larval molting quiescence. *Curr. Biol.* **21,** 825–834 (2011).
52. Choi, S., Chatzigeorgiou, M., Taylor, K. P., Schafer, W. R. & Kaplan, J. M. Analysis of NPR-1 reveals a circuit mechanism for behavioral quiescence in C. elegans. *Neuron* **78,** 869–880 (2013).
53. Nelson, M. *et al.* The neuropeptide NLP-22 regulates a sleep-like state in Caenorhabditis elegans. *Nat. Commun.* **4,** (2013).
54. Nelson, M. D. *et al.* FMRFamide-like FLP-13 neuropeptides promote quiescence following heat stress in Caenorhabditis elegans. *Curr. Biol.* **24,** 2406–2410 (2014).
55. Turek, M., Besseling, J., Spies, J. P., König, S. & Bringmann, H. Sleep-active neuron specification and sleep induction require FLP-11 neuropeptides to systemically induce sleep. *Elife* **5,** 1–18 (2016).
56. Richter, C., Woods, I. G. & Schier, A. F. Neuropeptidergic Control of Sleep and Wakefulness. *Annu. Rev. Neurosci.* **37,** 503–531 (2014).
57. Turek, M., Lewandrowski, I. & Bringmann, H. An AP2 transcription factor is required for a sleep-active neuron to induce sleep-like quiescence in C. elegans.

Curr. Biol. **23,** 2215–2223 (2013).

58. Kucherenko, M. M., Ilangovan, V., Herzig, B., Shcherbata, H. R. & Bringmann, H. TfAP-2 is required for night sleep in Drosophila. *BMC Neurosci.* **17,** 1–11 (2016).
59. Mani, A. *et al.* Syndromic patent ductus arteriosus: evidence for haploinsufficient TFAP2B mutations and identification of a linked sleep disorder. *Proc. Natl. Acad. Sci. U. S. A.* **102,** 2975–2979 (2005).
60. Félix, M. A. & Braendle, C. The natural history of Caenorhabditis elegans. *Curr. Biol.* **20,** R965–R969 (2010).
61. Sulston, J. & Horvitz, H. Post-embryonic cell lineages of the nematode Caenorhabditis elegans. *Dev.Biol.* **56,** 110 (1977).
62. Sulston, J. E. *et al.* The embryonic cell lineage of the nematode Caenorhabditis elegans. *Dev. Biol.* **100,** 64–119 (1983).
63. Brenner, S. Caenorhabditis elegans. *Methods* **77,** 71–94 (1974).
64. Altun, Z. F. & Hall, D. H. Introduction. *WormAtlas* (2009).
65. Baugh, L. R. To grow or not to grow: Nutritional control of development during Caenorhabditis elegans L1 Arrest. *Genetics* **194,** 539–555 (2013).
66. Cassada, R. C. & Russell, R. L. The Dauerlarva , a Post-Embryonic Nematode Developmental elegans Variant of the Caenorhabditis. *Wild* **342,** 326–342 (1975).
67. Hu, P. J. Dauer. *WormBook* (2007). doi:10.1895/wormbook.1.144.1
68. White, J. G., Southgate, E., Thomsom, J. N. & Brenner, S. THE STRUCTURE OF THE NERVOUS SYSTEM OF THE NEMATODE CAENORHABDITIS ELEGANS. *Philos. Trans. R. Soc. B* **314,** 1–340 (1986).
69. Jarrell, T. A. *et al.* The Connectome of a Decision Making Neural Network. *Science* **337,** 437–444 (2012).
70. Altun, Z. F. & Hall, D. H. Nervous system, general description. *WormAtlas* (2011).
71. Pereira, L. *et al.* A cellular and regulatory map of the cholinergic nervous system of *C. elegans*. *Elife* **4,** 1–46 (2015).
72. Bendena, W. G., Campbell, J., Zara, L., Tobe, S. S. & Chin-Sang, S. S. T. Select neuropeptides and their G-protein coupled receptors in Caenorhabditis elegans and Drosophila melanogaster. *Front. Endocrinol. (Lausanne).* **3,** 1–12 (2012).

73. Pierce, S. B. *et al.* Regulation of DAF-2 receptor signaling by human insulin and. *Genes Dev.* 672–686 (2001). doi:10.1101/gad.867301.4

74. Li, W., Kennedy, S. G. & Ruvkun, G. *daf-28* encodes a *C. elegans* insulin superfamily member that is regulated by environmental cues and acts in the DAF-2 signaling pathway. *Genes Dev.* **17,** 844–858 (2003).

75. Li, C., Kim, K. & Nelson, L. S. FMRFamide-related neuropeptide gene family in Caenorhabditis elegans. *Brain Res.* **848,** 26–34 (1999).

76. Li, C. The ever-expanding neuropeptide gene families in the nematode Caenorhabditis elegans. *Parasitology* **131,** (2005).

77. Nathoo, A. N., Moeller, R. A., Westlund, B. A. & Hart, A. C. Identification of neuropeptide-like protein gene families in Caenorhabditis elegans and other species. *Proc. Natl. Acad. Sci.* **98,** 14000–14005 (2001).

78. Li, C. & Kim, K. Neuropeptides. *WormBook* 1–36 (2009). doi:10.1895/wormbook.1.142.1.Neuropeptides

79. Geffeney, S. L. *et al.* DEG/ENaC but not TRP channels are the major mechanoelectrical transduction channels in a C. elegans nociceptor. *Neuron* **71,** 845–857 (2011).

80. Goodman, M. B., Hall, D. H., Avery, L. & Lockery, S. R. Active Currents Regulate Sensitivity and Dynamic Range in C. elegans Neurons. *Neuron* **20,** 763–772 (1998).

81. Lindsay, T. H., Thiele, T. R. & Lockery, S. R. Optogenetic analysis of synaptic transmission in the central nervous system of the nematode C. elegans. *Nat. Commun.* **2,** (2011).

82. Liu, P., Chen, B., Mailler, R. & Wang, Z. W. Antidromic-rectifying gap junctions amplify chemical transmission at functionally mixed electrical-chemical synapses. *Nat. Commun.* **8,** 1–16 (2017).

83. Liu, P., Chen, B. & Wang, Z.-W. SLO-2 potassium channel is an important regulator of neurotransmitter release in Caenorhabditis elegans. *Nat. Commun.* **5,** (2014).

84. Liu, Q., Hollopeter, G. & Jorgensen, E. M. Graded synaptic transmission at the Caenorhabditis elegans neuromuscular junction. *Proc. Natl. Acad. Sci.* **106,** 10823–10828 (2009).

85. Mellem, J. E., Brockie, P. J., Madsen, D. M. & Maricq, A. V. Action Potentials Contribute to Neuronal Signaling in C. elegans. *Nat. Neurosci.* **11,** 865–867

(2008).

86. O'Hagan, R., Chalfie, M. & Goodman, M. B. The MEC-4 DEG/ENaC channel of Caenorhabditis elegans touch receptor neurons transduces mechanical signals. *Nat. Neurosci.* **8,** 43–50 (2005).
87. Ramot, D., MacInnis, B. L. & Goodman, M. B. Bidirectional temperature-sensing by a single thermosensory neuron in C. elegans. *Nat. Neurosci.* **11,** 908–915 (2008).
88. Liu, Q., Kidd, P. B., Dobosiewicz, M. & Bargmann, C. The C. elegans AWA Olfactory Neuron Fires Calcium-Mediated All-or-None Action Potentials. *bioRxiv* **175,** 359935 (2018).
89. Iwanir, S. *et al.* The microarchitecture of C. elegans behavior during lethargus: homeostatic bout dynamics, a typical body posture, and regulation by a central neuron. *Sleep* **36,** 385–95 (2013).
90. Nagy, S., Raizen, D. M. & Biron, D. Measurements of behavioral quiescence in Caenorhabditis elegans. *Methods* **68,** 500–507 (2014).
91. Trojanowski, N. F., Nelson, M. D., Flavell, S. W., Fang-Yen, C. & Raizen, D. M. Distinct Mechanisms Underlie Quiescence during Two Caenorhabditis elegans Sleep-Like States. *J. Neurosci.* **35,** 14571–14584 (2015).
92. Driver, R. J., Lamb, A. L., Wyner, A. J. & Raizen, D. M. DAF-16/FOXO regulates homeostasis of essential sleep-like behavior during larval transitions in C. elegans. *Curr. Biol.* **23,** 501–506 (2013).
93. Schwarz, J., Lewandrowski, I. & Bringmann, H. Reduced activity of a sensory neuron during a sleep-like state in Caenorhabditis elegans. *Curr. Biol.* **21,** R983–R984 (2011).
94. Schwarz, J., Spies, J.-P. & Bringmann, H. Reduced muscle contraction and a relaxed posture during sleep-like Lethargus. *Worm* **1,** 12–14 (2012).
95. Cho, J. Y. & Sternberg, P. W. Multilevel modulation of a sensory motor circuit during C. elegans sleep and arousal. *Cell* **156,** 249–260 (2014).
96. Nagy, S. *et al.* Homeostasis in C. elegans sleep is characterized by two behaviorally and genetically distinct mechanisms. *Elife* **3,** e04380 (2014).
97. Hendriks, G. J., Gaidatzis, D., Aeschimann, F. & Großhans, H. Extensive Oscillatory Gene Expression during C.elegans Larval Development. *Mol. Cell* **53,** 380–392 (2014).
98. Jeon, M., Gardner, H. F., Miller, E. A., Deshler, J. & Rougvie, A. E. Similarity

of the *C. elegans* developmental timing protein LIN-42 to circadian rhythm proteins. *Science* **286,** 1141–6 (1999).

99. Huang, H., Zhu, C.-T., Skuja, L. L., Hayden, D. J. & Hart, A. C. Genome-Wide Screen for Genes Involved in Caenorhabditis elegans Developmentally Timed Sleep. *G3 Genes, Genomes, Genet.* **7,** 2907–2917 (2017).
100. Huang, H. *et al.* Gap junctions and NCA cation channels are critical for developmentally-timed sleep and arousal in Caenorhabditis elegans. (2018).
101. Wu, Y., Masurat, F., Preis, J. & Bringmann, H. Sleep Counteracts Aging Phenotypes to Survive Starvation-Induced Developmental Arrest in C. elegans. *Curr. Biol.* **28,** 1–14 (2018).
102. Gaglia, M. M. & Kenyon, C. Stimulation of Movement in a Quiescent, Hibernation-like Form of C. elegans by Dopamine Signaling. *J. Neurosci.* **29,** 7302–7314 (2009).
103. You, Y., Kim, J., Raizen, D. M. & Avery, L. Insulin, cGMP, and TGF-β Signals Regulate Food Intake and Quiescence in C. elegans: A Model for Satiety. *Cell Metab.* **7,** 249–257 (2008).
104. Invitrogen. Gateway ® Technology A universal technology to clone DNA sequences for functional analysis and expression in multiple systems - User Manual. (2003).
105. Wilm, T., Demel, P., Koop, H. U., Schnabel, H. & Schnabel, R. Ballistic transformation of Caenorhabditis elegans. *Gene* **229,** 31–35 (1999).
106. Praitis, V., Casey, E., Collar, D. & Austin, J. Creation of low-copy integrated transgenic lines in Caenorhabditis elegans. *Genetics* **157,** 1217–1226 (2001).
107. Turek, M., Besseling, J. & Bringmann, H. Agarose Microchambers for Long-term Calcium Imaging of Caenorhabditis elegans, *J. Vis. Exp.* 1–8 (2015). doi:10.3791/52742
108. Bringmann, H. Agarose hydrogel microcompartments for imaging sleep- and wake-like behavior and nervous system development in Caenorhabditis elegans larvae. *J. Neurosci. Methods* **201,** 78–88 (2011).
109. Singh, K. *et al.* Response and Larval Molting Quiescence. **21,** 825–834 (2012).
110. Nagy, S. *et al.* A longitudinal study of caenorhabditis elegans larvae reveals a novel locomotion switch, regulated by gαs signaling. *Elife* **2013,** 1–15 (2013).
111. Schwarz, J. & Bringmann, H. Reduced Sleep-Like Quiescence in Both Hyperactive and Hypoactive Mutants of the Galphaq Gene egl-30 during

lethargus in Caenorhabditis elegans. *PLoS One* **8,** 1–16 (2013).

112. Lin, J. Y., Knutsen, P. M., Muller, A., Kleinfeld, D. & Tsien, R. Y. ReaChR: A red-shifted variant of channelrhodopsin enables deep transcranial optogenetic excitation. *Nat. Neurosci.* **16,** 1499–1508 (2013).
113. Han, X. *et al.* A High-Light Sensitivity Optical Neural Silencer: Development and Application to Optogenetic Control of Non-Human Primate Cortex. *Front. Syst. Neurosci.* **5,** 1–8 (2011).
114. WormBook. (2006). Available at: www.wormbook.org.
115. Zheng, Y., Brockie, P. J., Mellem, J. E., Madsen, D. M. & Maricq, A. V. Neuronal control of locomotion in C. elegans is modified by a dominant mutation in the GLR-1 ionotropic glutamate receptor. *Neuron* **24,** 347–361 (1999).
116. Brockie, P. J., Madsen, D. M., Zheng, Y., Mellem, J. E. & Maricq, A. V. Differential expression of glutamate receptor subunits in the nervous system of Caenorhabditis elegans and their regulation by the homeodomain protein UNC-42. *J. Neurosci.* **21,** 1510–1522 (2001).
117. Brockie, P. J. & Maricq, A. V. Ionotropic glutamate receptors in caenorhabditis elegans. *NeuroSignals* **12,** 108–125 (2003).
118. Brockie, P. & Maricq, A. V. Ionotropic glutamate receptors: genetics, behavior and electrophysiology. *WormBook* 1–16 (2006). doi:10.1895/wormbook.1.61.1
119. Brockie, Mellem, J., Hills, T., Madsen, D. & Maricq, A. The C. elegans glutamate receptor subunit NMR-1 is required for slow NMDA-activated currents that …. *Neuron* **31,** 617–630 (2001).
120. Bellocchio, E. E., Reimer, R. J., Fremeau, J. & Edwards, R. H. Uptake of glutamate into synaptic vesicles by an inorganic phosphate transporter. *Science (80-.).* **289,** 957–960 (2000).
121. Lee, R. Y., Sawin, E. R., Chalfie, M., Horvitz, H. R. & Avery, L. EAT-4, a homolog of a mammalian sodium-dependent inorganic phosphate cotransporter, is necessary for glutamatergic neurotransmission in caenorhabditis elegans. *J. Neurosci.* **19,** 159–167 (1999).
122. Rankin, C. H. & Wicks, S. R. Mutations of the caenorhabditis elegans brain-specific inorganic phosphate transporter eat-4 affect habituation of the tap-withdrawal response without affecting the response itself. *J. Neurosci.* **20,** 4337–4344 (2000).

123. Alkema, M. J., Hunter-Ensor, M., Ringstad, N. & Horvitz, H. R. Tyramine functions independently of octopamine in the Caenorhabditis elegans nervous system. *Neuron* **46,** 247–260 (2005).
124. Wormatlas. (2012). Available at: http::\\www.wormatlas.org
125. Flibotte, S. *et al.* Whole-Genome profiling of mutagenesis in Caenorhabditis elegans. *Genetics* **185,** 431–441 (2010).
126. Gengyo-Ando, K. & Mitani, S. Characterization of mutations induced by ethyl methanesulfonate, UV, and trimethylpsoralen in the nematode Caenorhabditis elegans. *Biochem. Biophys. Res. Commun.* **269,** 64–69 (2000).
127. Urmersbach, B., Besseling, J., Spies, J. P. & Bringmann, H. Automated analysis of sleep control via a single neuron active at sleep onset in C. elegans. *Genesis* **54,** 212–219 (2016).
128. Zuryn, S. & Jarriault, S. Deep sequencing strategies for mapping and identifying mutations from genetic screens. *Worm* **2,** e25081 (2013).
129. Zuryn, S., Le Gras, S., Jamet, K. & Jarriault, S. A strategy for direct mapping and identification of mutations by whole-genome sequencing. *Genetics* **186,** 427–430 (2010).
130. Gassmann, R. *et al.* A new mechanism controlling kinetochore-microtubule interactions revealed by comparison of two dynein-targeting components: SPDL-1 and the Rod/Zwilch/Zw10 complex. *Genes Dev.* **22,** 2385–2399 (2008).
131. Shaye, D. D. & Greenwald, I. Ortholist: A compendium of C. elegans genes with human orthologs. *PLoS One* **6,** (2011).
132. Cheerambathur, D. K., Gassmann, R., Cook, B., Oegema, K. & Desai, A. Crosstalk Between Microtubule Attachment Complexes Ensures Accurate Chromosome Segregation. *Science (80-.).* **342,** 1239–1242 (2013).
133. WormBase. (2000). Available at: http://www.wormbase.org.
134. S, R. *et al.* C. elegans Codon Adapter. (2011). Available at: https://worm.mpi-cbg.de.
135. Spies, J.-P. Analysis of the sleep homeostat of the nematode Caenorhabditis elegans. (Georg-August-Universität Göttingen, 2014).
136. Rogers, C. *et al.* Inhibition of Caenorhabditis elegans social feeding by FMRFamide-related peptide activation of NPR-1. *Nat. Neurosci.* **6,** 1178–1185 (2003).

137. Serrano-Saiz, E. *et al.* XModular control of glutamatergic neuronal identity in C. elegans by distinct homeodomain proteins. *Cell* **155,** 659–673 (2013).
138. Takamori, S., Rhee, J. S., Rosenmund, C. & Jahn, R. Identifcation of a vesicular glutamate transporter that defnes a glutamatergic phenotype in neurons. *Lett. to Nat.* **407,** 189–194 (2000).
139. Kawano, T. *et al.* An imbalancing act: Gap junctions reduce the backward motor circuit activity to bias C. elegans for forward locomotion. *Neuron* **72,** 572–586 (2011).
140. Chalfie, M. *et al.* The neural circuit for touch sensitivity in Caenorhabditis elegans. *J. Neurosci.* **5,** 956–964 (1985).
141. Rakowski, F. & Karbowski, J. Optimal synaptic signaling connectome for locomotory behavior in Caenorhabditis elegans: Design minimizing energy cost. *PLoS Comput. Biol.* **13,** 1–28 (2017).
142. Nichols, A. L. A., Eichler, T., Latham, R. & Zimmer, M. A global brain state underlies C. Elegans sleep behavior. *Science (80-.).* **356,** 1247–1256 (2017).
143. Ben Arous, J., Tanizawa, Y., Rabinowitch, I., Chatenay, D. & Schafer, W. R. Automated imaging of neuronal activity in freely behaving Caenorhabditis elegans. *J. Neurosci. Methods* **187,** 229–234 (2010).
144. Zheng, M., Cao, P., Yang, J., Xu, X. Z. S. & Feng, Z. Calcium imaging of multiple neurons in freely-behaving C. elegans. *J. Neurosci. Methods* **206,** 78–82 (2012).
145. Faumont, S. *et al.* An Image-Free Opto-Mechanical system for creating virtual environments and imaging neuronal activity in freely moving caenorhabditis elegans. *PLoS One* **6,** (2011).
146. Pirri, J. K. & Alkema, M. J. The Neuroethology of C. elegans Escape. *Curr. Opin. Neurobiol.* **22,** 187–193 (2012).
147. Masurat, F. Control of sleep through sleep-active neurons. (Georg-August-Universität Göttingen, 2018).
148. Guo, Z. V, Hart, A. C. & Ramanathan, S. Optical interrogation of neural circuits in Caenorhabditis elegans. *Nat. Methods* **6,** 891–896 (2009).
149. Conradt, B. & Horvitz, R. The C. elegans Protein EGL-1 Is Required for Programmed Cell Death and Interacts with the Bcl-2–like Protein CED-9. *Cell* **93,** 519–529 (1998).
150. Sawin, E. R., Ranganathan, R. & Horvitz, R. C. elegans locomotory rate is

modulated by the environment through a dopaminergic pathway and by experience through a serotonergic pathway. *Neuron* **26,** 619–631 (2000).

151. Li, W., Kang, L., Piggott, B. J., Feng, Z. & Shawn Xu, X. Z. The neural circuits and sensory channels mediating harsh touch sensation in C. elegans. *Nat Commun* **2,** 1–22 (2011).

10 Appendix

10.1 MATLAB scripts

10.1.1 MATLAB routines to extract neuron intensities

The following MATLAB scripts were used to manually extract neuron intensities. They were written by my former colleague Dr. Jan-Philipp Spies.

```
ipt_localize_manually_mat('*.tif*')
elegans_cut('*.tif','width',12)
roi_files=dir('*roi_*');
mkdir('Cell')
dir_signal_ALM=[pwd,'\Cell'];
for ii=1:length(roi_files)
    movefile(roi_files(ii).name,dir_signal_ALM)
end
% movefile('*average_intensity*',dir_signal_ALM)
% movefile('*manpos*',dir_signal_ALM)
% % ipt_localize_manually_mat('*.tif')
% elegans_cut('*.tif','width',15)
% mkdir('Background')
% dir_background=[pwd,'\Background'];
% clear roi_files
% roi_files=dir('*roi_*');
% for ii=1:length(roi_files)
%     movefile(roi_files(ii).name,dir_background)
% end
% movefile('*average_intensity*',dir_background)
% movefile('*manpos*',dir_background)
```

```
function [ spam ] = ipt_localize_manually(ch1, ch2, varargin)
% Find and mark positions in one of two channels and return them
in a spam struct.
%
% Syntax
%   [ spam ] = ipt_localize_manually(ch1, ch2)
%
% Input parameter
%    ch1       The stack/data array/matrix in which to find the
positions.
%           Alternatively a filename (wildcards allowed, but must
be unique)
%            of an obf/msr file with the image stack (first stack
in file is
%           loaded)
%    ch2      The reference stack which can also shown in the ui
for
%           reference purposes
```

```
%
%  Optional parameter
%   Note: If Optional parameters are given, also ch2 must be
supplied.
%  Use [] for none.
%
%  autoforward: If true, after the first click in each frame, the
next
%                frame is displayed immediately, no need to click
"next"
%
%
% Output parameter
%   spam    A spam struct returned by the function
%            If a filename is given, the data is stored in a file
with
%                the appendix _manpos.spam, and this filename is
returned as a cell.
%
% Help:
% - The gui displays one stack at a time, you can switch between
them with
%   the 'Switch' button. The positions will be associated to the
channel
%   displayed when the left mouse button is clicked.
% - To delete a position from the list, right-click or CTRL-click
it. You
%     can flip through the stack using the 'Prev' and 'Next'
buttons.
% - Scrolling the mouse wheel is a fast shortcut for prev/next
buttons.
% - Use the Hide-button to hide the crosses, if you want to see
the data
%   unobscured.
% - Use the ChOnly button to hide the marked positions in the
other stack.
%   -   The   marked   positions   are   autosaved   in   the   file
ipt_autosave.mat in your
%      TEMP-folder as determined by getenv('TEMP') every 50
positions.
% - The function returns when the user clicks the 'Done' button.

if nargin < 1
    error('Not enough arguments given!');
elseif nargin > 2 && ~isstr(varargin{1}) % catch if optional
arguments but no ch2 is given
    error('If you supply optional input arguments and you have no
ch2, use [] for ch2!')
end

param.autoforward = true;

param = omex_read_params(param, varargin);

%corret it, if the user did not get the difference between true
and 'true':
if strcmpi(param.autoforward,'true')
    param.autoforward = true;
```

```
end
if strcmpi(param.autoforward,'false')
    param.autoforward = false
end

% first we clear it, because we do not want it from last time, we
called
clear global g_ipt;
global g_ipt;

g_ipt.autoforward = param.autoforward;%save parameter in global
variable

% create spam struct
g_ipt.spam = spam_create('Manual Locations');

name_supplied = false;%assume that we get data
if isstr(ch1) % we have a string, i.e. a filename pattern
    files = dir(ch1);
    switch length(files)
        case 0
            error('No matching file found')
        otherwise
            hh = imread(files(1).name);
            hhs = size(hh);
            ch1  =  zeros(hhs(1),hhs(2),length(files));  %allocate
memory
            clear hh hhs
            for kf = 1:length(files)
                ch1(:,:,kf)  =  imread(files(kf).name,  1);  %  read
first data stack, wildcard in filename allowed
            end
            g_ipt.spam.imdata.stackinfo = [];
            g_ipt.spam.imdata.file      = files(1).name;
            name_supplied = true;
    end
end

g_ipt.radius   = 12;
g_ipt.dist     = 3; % both in cm
g_ipt.slice    = 1;
g_ipt.channel  = 1;
g_ipt.hide     = 0;
g_ipt.chonly   = 0;
g_ipt.globmax  = 0;
g_ipt.bak      = 0;
g_ipt.saved    = 1;
g_ipt.pix_size = NaN;
g_ipt.figure   = NaN;
g_ipt.nslices  = size(ch1, 3);

if nargin > 1
    if  name_supplied  &&  ~isempty(ch2)  %  check  if  we  got  a
filename instead of data
        error('With files only one stack is supported so far')
    end
    g_ipt.stack    = cat(4, ch1, ch2);
else
```

```
    g_ipt.stack    = ch1;
end
g_ipt.scaling  = ones(size(g_ipt.stack, 4));

% The columns in the obf stack
g_ipt.spam.columns  =  {'dim4',  'frame',  'x1',  'y1',  'ch1',
'channel'};
g_ipt.spam.fov    = [ 0 0 size(g_ipt.stack, 1) size(g_ipt.stack,
2) ];

more off;
g_ipt.figure = figure;
% adjust height of figure
subplot(15,1,1:14)
slice = g_ipt.stack (:, :, g_ipt.slice, g_ipt.channel);
colormap(hot(255));
h = image(slice);

pos = [5 40 90 14];
g_ipt.edFrame = uicontrol(...
    'style',        'text',...
    'string',       'Frame 0',...
    'position',     pos, ...
    'tooltipstring', 'Display frame number.');

width = 70;
pos = [5 5 width 25];

uicontrol(...
    'tag',           'fff',...
    'string',        'Prev',...
    'style',         'pushbutton',...
    'callback',      @ui_prev_Callback,...
    'position',      pos,...
    'tooltipstring',  'Goto  next  slice  (mouse  wheel  scrolls
also).');

pos(1) = pos(1) + width + 5;
uicontrol(...
    'tag',           'fff',...
    'string',        'Next',...
    'style',         'pushbutton',...
    'callback',      @ui_next_Callback,...
    'position',      pos,...
    'tooltipstring',  'Goto  previous  slice  (mouse  wheel  scrolls
also).');

pos(1) = pos(1) + width + 5;
uicontrol(...
    'tag',           'fff',...
    'string',        'Switch',...
    'style',         'pushbutton',...
    'callback',      @ui_switch_Callback,...
    'position',      pos,...
    'tooltipstring', 'Switch between channels.');

pos(1) = pos(1) + width + 5;
uicontrol(...
```

```
    'tag',           'fff',...
    'string',        'Hide',...
    'style',         'togglebutton',...
    'callback',      @ui_hide_Callback,...
    'position',      pos,...
    'tooltipstring', 'Hide marks');

pos(1) = pos(1) + width + 5;
uicontrol(...
    'tag',           'fff',...
    'string',        'ChOnly',...
    'style',         'togglebutton',...
    'callback',      @ui_chonly_Callback,...
    'position',      pos,...
    'tooltipstring', 'Show marks of this channel only');

pos(1) = pos(1) + width + 5;
uicontrol(...
    'tag',           'fff',...
    'string',        'Done',...
    'style',         'pushbutton',...
    'callback',      @ui_done_Callback,...
    'position',      pos,...
    'tooltipstring', 'Terminate the session');

pos(1) = pos(1) + width + 5;
uicontrol(...
    'tag',           'fff',...
    'string',        'GlobMax',...
    'style',         'togglebutton',...
    'callback',      @ui_globmax_Callback,...
    'position',      pos,...
    'tooltipstring', 'Sets colormap scaling to global max in
stack.');

pos = [pos(1), 35, width * 1.5, 15];
g_ipt.slider = uicontrol(...
    'tag',           'fff',...
    'style',         'slider',...
    'callback',      @ui_slider_Callback,...
    'position',      pos,...
    'tooltipstring', 'Colormap scaling relative to actual
slice',...
    'Max',           1,...
    'Min',           0,...
    'value',         1,...
    'SliderStep',    [0.02, 0.1]);

ipt_refresh;
set(gcf,'windowbuttondownfcn',@ui_btndown);

set(gcf,'WindowScrollWheelFcn',@ui_mousewheel);

waitfor(gcf);

if name_supplied % we had a filename and store the data as file
    namelength = length(files(1).name);
```

```
    namestem    = files(1).name(1:namelength - 4); % name without
extension
    newspamname= [namestem, '_manpos.mat'];
    centers = g_ipt.spam;
    save(newspamname, 'centers'); % save as mat-file
    spam{1} = newspamname; % we return the name of the file we
stored the data in
else
    spam = g_ipt.spam;
end

end

% functions ----------------------------------------------------
----------

function ui_mousewheel(src,evnt)
global g_ipt;
if (evnt.VerticalScrollCount>0),
    % scroll down
    g_ipt.slice = g_ipt.slice - 1;
    if g_ipt.slice < 1
        g_ipt.slice = size(g_ipt.stack, 3);
    end
else
    % scroll up
    g_ipt.slice = g_ipt.slice + 1;
    if g_ipt.slice > size(g_ipt.stack, 3)
        g_ipt.slice = 1;
    end
end;
ipt_refresh
end

function ui_slider_Callback(hObject, eventdata)
% The colormap slider was moved
global g_ipt;
g_ipt.scaling(g_ipt.channel) = get(hObject,'Value');
ipt_refresh;
end

function ui_switch_Callback(hObject, eventdata)
% The switch button was pressed
global g_ipt;

g_ipt.channel = g_ipt.channel + 1;
if g_ipt.channel > size(g_ipt.stack, 4)
    g_ipt.channel = 1;
end
ipt_refresh
end

function ui_prev_Callback(hObject, eventdata)
% The previous frame button was pressed
global g_ipt;
g_ipt.slice = g_ipt.slice - 1;
if g_ipt.slice < 1
    g_ipt.slice = size(g_ipt.stack, 3);
```

```
end
ipt_refresh
end

function ui_hide_Callback(hObject, eventdata, handles)
% The hide (toggle) button was pressed
global g_ipt;
g_ipt.hide = get(hObject,'Value');
ipt_refresh
end

function ui_chonly_Callback(hObject, eventdata, handles)
% The channel only button was pressed
global g_ipt;
g_ipt.chonly = get(hObject,'Value');
ipt_refresh
end

function ui_globmax_Callback(hObject, eventdata, handles)
% The channel only button was pressed
global g_ipt;
g_ipt.globmax = get(hObject,'Value');
g_ipt.globmaxval = median(g_ipt.stack(0.9 * max(g_ipt.stack(:)) <
g_ipt.stack));
% median of the values which are at least 90% of the brightes
pixel
ipt_refresh
end

function ui_next_Callback(hObject, eventdata)
% The next frame button was pressed
global g_ipt;
g_ipt.slice = g_ipt.slice + 1;
if g_ipt.slice > size(g_ipt.stack, 3)
    g_ipt.slice = 1;
end
ipt_refresh
end

function ui_done_Callback(hObject, eventdata)
% The done button was pressed
global g_ipt;
close(g_ipt.figure);
end

function ui_btndown(hObject, eventdata)
global g_ipt;

if g_ipt.channel == 1
    color ='g';
else
    color ='r';
end

st = get(gcf, 'SelectionType'); % which mouse button was blicked

l  = get(gca, 'CurrentPoint');
```

```
% This seems to give the position starting at (1,1) in the upper
left corner
% and ending at (maxx, maxy) in the lower right

v = g_ipt.stack(round(l(1, 2)), round(l(1, 1)), g_ipt.slice,
g_ipt.channel);
x = l(1, 2) - 0.5; % internal coordinate system starts at (0.5,
0.5)
y = l(1, 1) - 0.5;

% test if still in field of view (inside the image)
fov = g_ipt.spam.fov;
if x < fov(1) || x > fov(3) || y < fov(2) || y > fov(4)
    return;
end

% right mouse button? -> delete cross if available
if strcmp(st, 'alt')
    % all necessary columns
    idx = spam_get_columns(g_ipt.spam, 'frame', 'x1', 'y1',
'channel');
    % select current frame and channel
    src = find(g_ipt.spam.events(:,idx(1)) == g_ipt.slice);
    % get x1, y1 values for this frame
    evt = g_ipt.spam.events(src, [idx(2), idx(3)]);
    % estimate nearest position
    dst = (evt(:,1)-x).^2 + (evt(:,2)-y).^2;
    [c, i] = min(dst);
    % if it is less than 10 pixels (and in the right channel),
remove the corresponding cross
    if (c < 10) && (g_ipt.spam.events(src(i), idx(4)) ==
g_ipt.channel)
        g_ipt.spam.events(src(i), :) = [];
        ipt_refresh
    end
else
    % left mouse button

    g_ipt.spam.events = [g_ipt.spam.events; [0, g_ipt.slice, x,
y, v, g_ipt.channel]];
    % draw the cross
    ipt_draw_cross(x, y, color);

    %for autoforward (added by Marcel):
    if g_ipt.autoforward%if the user asked for automatic
switching to the next
        %frame, do so now (call the routine that would be
        %elicted by the "next" button)
        if g_ipt.slice < size(g_ipt.stack, 3)
            ui_next_Callback
        end
    end

end

counter = num2str(size(g_ipt.spam.events, 1));
text(-60, 46, counter, 'FontSize', 10, 'EdgeColor',
color,'color', color, ...
```

```
    'BackgroundColor', 'black', 'Units', 'pixels');

% sava a backup every 50 particles:
g_ipt.bak = size(g_ipt.spam.events, 1);
if g_ipt.bak >= g_ipt.saved * 50
    backupfile = fullfile(getenv('TEMP'),'ipt_autosave.mat');
    autosave = g_ipt.spam;
    save(backupfile, 'autosave')
    g_ipt.saved = g_ipt.saved + 1;
end


drawnow;
end
```

The following MATLAB scripts were used to extract neuron intensities in an automated manner. These scripts were written by my former colleague Dr. Florentin Masurat.

```
%%%%%%%%%%%%%%%%%%%%%%%%%%%INFO%%%%%%%%%%%%%%%%%%%%%%%%%%%%%%%%%%%%%%%%%%%%
%%%%%%%%%
%read_folders works wit

% find_particle_RIS_single_picture
%and find_particle_RIS_max_peak_single_picture
%%%%%%%%%%%%%%%%%%%%%%%%%%%%%%%%%%%%%%%%%%%%%%%%%%%%%%%%%%%%%%%%%%%%%%%%%%%%%%
%%%%%%%%%


dirInfo=dir('*ExtractedGFPFiles*');
isDir = [dirInfo.isdir];
folder = {dirInfo(isDir).name};
num_folder= size(folder,2);
input_lst=[];
for folder_number=1:num_folder
    foldername = folder{folder_number};
    cd(foldername);

    init=0;
%first frame
    intervall=3;
%time between framesdead_
    step=1;
%for debuging set steps=1 or sleepingphase=[] else dim mismatch
    time=0;
%time 0
    sleepingphase=[];
%no sleeping phase or unknown sleeping phase input: []

%sleeping phase between frame number a and b and d and c input:
[a b;d c]
```

```
%DON'T set sleeping phase that is outisde of intevall [init
final]


    ext=('.tif');
    thresh=(1000);
% 1000 for normal ris 20x
    sarea=5;
%total area: (sarea*2+1)^2, normal:5
    high=30;
%number of pixels that are taken as signal, low automatically set
to high-1 low set to numpixels -high, normal: 30
    images = dir('*.tif');
    imname   = images(1).name;
    filestub = imname(1:length(imname)-8);


    final=length(images)-1;
%only if all frames from 0 to last are in folder if not set
manually
    %final=9999;
%to set last frame manually uncomment and set last frame
%     if final>10000
%         filestub = imname(1:length(imname)-9);
%     end


%addpath('C:\Users\fmasura\Desktop\find_particle_RIS_max_peak_1.1
')    %addpath to used function

find_particle_RIS_max_peak_single_picture_other_cd(final,init,ste
p,filestub,ext,thresh,sarea,high,intervall, time, sleepingphase);

    %cd ..

end



% Define a starting folder.
% topLevelFolder = uigetdir('','Where are your files?');
% if topLevelFolder == 0
%     return;
% end
% cd(topLevelFolder)

% read in GCaMP intensity file

fid=fopen('GCaMPIntensity_HBR2174_181228_MyMicroscope_field1,
worm3.txt');
GCaMPsignal=fscanf(fid,'%f',[2,inf])';
fclose(fid);

% cut the GCaMP signal in same pieces as locomotion for sleep
bouts

i=1;
```

```
k=1;

while i <= size(det_bouts,1);
    cutted_GCaMPsignal_quietbout(:,k)=GCaMPsignal(det_bouts(k,2)-
baseline:det_bouts(k,2)+30,2);
    i=i+1;
    k=k+1;
end



% and for wake bouts

% i=1;
% k=1;
%
% while i <= size(det_activity,1);
%
cutted_GCaMPsignal_wakebout(:,k)=GCaMPsignal(det_activity(k,2)-
baseline:det_activity(k,2)+frames_longest_wake_bout,2);
%     i=i+1;
%     k=k+1;
% end

% normalization GCaMP data; 1. average baseline 2. subtract
baseline from
% all values and 3. divide difference by baseline


baseline_quietbouts=cutted_GCaMPsignal_quietbout(1:baseline,:);
% baseline_wakebouts=cutted_GCaMPsignal_wakebout(1:60,:);

mean_baseline_quietbouts=mean(baseline_quietbouts,1);
% mean_baseline_wakebouts=mean(baseline_wakebouts,1);

norm_GCaMPsignal_quietbouts=(cutted_GCaMPsignal_quietbout-
mean_baseline_quietbouts)./mean_baseline_quietbouts;
%         norm_GCaMPsignal_wakebouts=(cutted_GCaMPsignal_wakebout-
mean_baseline_wakebouts)./mean_baseline_wakebouts;
%
mean_norm_GCaMPsignal_quietbouts=mean(norm_GCaMPsignal_quietbouts
,2);
%
mean_norm_GCaMPsignal_wakebouts=mean(norm_GCaMPsignal_wakebouts,2
);

% save some output data

%
table_cutted_GCaMPsignal_quietbout=array2table(cutted_GCaMPsignal
_quietbout);
%
table_cutted_GCaMPsignal_wakebout=array2table(cutted_GCaMPsignal_
wakebout);
%
%
writetable(table_cutted_GCaMPsignal_quietbout,[strain,'_all_cutte
d_GCaMPsignal_quietbout.txt'],'Delimiter','\t');
```

```
%
writetable(table_cutted_GCaMPsignal_wakebout,[strain,'_all_cutted
_GCaMPsignal_wakebout.txt'],'Delimiter','\t');

%
table_norm_GCaMPsignal_quietbout=array2table(norm_GCaMPsignal_qui
etbouts);
%
table_norm_GCaMPsignal_wakebout=array2table(norm_GCaMPsignal_wake
bouts);

%
writetable(table_norm_GCaMPsignal_quietbout,[strain,'_all_norm_GC
aMPsignal_quietbout.txt'],'Delimiter','\t');
%
writetable(table_norm_GCaMPsignal_wakebout,[strain,'_all_norm_GCa
MPsignal_wakebout.txt'],'Delimiter','\t');

table_mean_norm_GCaMPsignal_quietbout=array2table(mean_norm_GCaMP
signal_quietbouts);
%
table_mean_norm_GCaMPsignal_wakebout=array2table(mean_norm_GCaMPs
ignal_wakebouts);

writetable(table_mean_norm_GCaMPsignal_quietbout,[strain,'_all_me
an_norm_GCaMPsignal_quietbout.txt'],'Delimiter','\t');
%
writetable(table_mean_norm_GCaMPsignal_wakebout,[strain,'_all_mea
n_norm_GCaMPsignal_wakebout.txt'],'Delimiter','\t');
```

10.1.2 MATLAB routines to extract quiescence bouts and RIS activity levels in quiescence bouts

The following MATLAB routines were used to analyze sleep bouts in lethargus and to extract RIS activity levels in sleep bouts. These scripts were provided by my colleague Jan Konietzka and I modified them according to my needs.

```
% Requires intensity_[STRAIN].txt files as input

close all
clc;  % Clear the command window.
workspace;  % Make sure the workspace panel is showing.
clear

% Define a starting folder.
topLevelFolder = uigetdir('','Where are your files?');
if topLevelFolder == 0
      return;
end
cd(topLevelFolder)
```

```
%common name of files to work with
common_name='intensity_*.txt';
list_info=dir(common_name);

% %Dialog Box: Worm strain
% Sub-Part: Get list
for list_num=1:length(list_info);
    list_info2=list_info(list_num).name;

%       While working with lists you need to specify at which
category you
%      want to look(e.g. .name) and with list_info(list_num) you
specify
%     the number of element you want to check)

    list_info3=cellstr(list_info2);
    list_info4=regexprep(list_info3,'intensity_','');
    list_info5=regexprep(list_info4,'.txt','');
%     regexprep hear cuts out what is given in '' and replaces it
with what is
%     given in '' thereafter
    list_info_x(list_num,:)=list_info5;
end

% Sub-Part: Dialog Box

[selection,ok] = listdlg('ListString',list_info_x,...
    'SelectionMode','single',...
    'ListSize',[300 150],...
    'Name','Strains:',...
    'PromptString','Choose Strain to analyse:',...
    'OKString','Go for it!',...
    'CancelString','Nahh, I changed my mind.');

%Dialog Box: Analysing specifications
prompt   =   {'Smoothing   method   (loess/rloess):','Smooth   span
(frames):','Threshold   (0-1):','Minimum   quiescence   bout   length
(seconds)','Minimum   wake   bout   length   (seconds)','time   between
frames','duration baseline (frames)'};
dlg_title = 'Analyse';
num_lines = 1;
defaultans = {'rloess','40','0.1','120','60','20','3'};
answer = inputdlg(prompt,dlg_title,num_lines,defaultans);

strain=list_info_x{selection};
input_file=strcat('intensity_',strain,'.txt');
smooth_fit=answer{1,1};
span=str2num(answer{2,1});
thresh=str2num(answer{3,1});
min_bout_length=str2num(answer{4,1});
min_wake_bout_length=str2num(answer{5,1});
intervall=str2num(answer{6,1});
baseline=str2num(answer{7,1});
%get your data
    A1=readtable(input_file);
    A=table2array(A1);
    B=A(2:end,1:2);
```

```
    %round timestamp to seconds
%     B(:,1)=round(B(:,1)/1000);
    B(:,1)=round(B(:,1));
    B_index(:,1) = B(:,1);
%     B_index(:,1) = A(2:end,:);

% for ind=1:size(C,2); %temporary
for ind=1:size(B,2)-1;
    ind

    %find max/min of worm
    B_smooth(:,ind) = smooth(B(:,ind+1), span, smooth_fit);

    %plot standardized raw data
    max1 = max(B_smooth(:,ind));
    min1 = min(B_smooth(:,ind));
    D=(B(:,ind+1)-min1)/(max1-min1);

%       lets imagine you have values between 50 and 100 and 50
should equals
%      0 and 100 should equals 100 than 75 would equals 0,5; to
get this out
%     need to calculate value-min/max-min (e.g. (75-50)/100-50)

    figure
    plot(B_index, D(:,1), 'x');
    hold on

    %plot smoothed data
    smooth_data =(B_smooth(:,ind)-min1)/(max1-min1);
    plot(B_index, smooth_data);

    %build a table with values are above ('thresh') and below
threshold ('0')
    thresh_data(:,1)=B_index;
    for ind2=1:size(B,1);
        if  smooth_data(ind2) < thresh
            thresh_data(ind2,2) = 0;
        else
            thresh_data(ind2,2) = thresh;
        end
    end

    %plot threshold
    plot(B_index, thresh_data(:,2), 'k-')
    hold off

    %search quite bouts:
    i=1;
    j=0;
    k=1;
        while i < size(thresh_data,1)
            if thresh_data(i,2)==0
                %oh a quiet bout...better count the length
                i = i+1;
                j = j+1;
            elseif and(thresh_data(i,2)==thresh, j>0)
                %that's where the shit is happening
```

```
                i = i+1;
                bout_length    =    thresh_data(i,1)-thresh_data(i-
j,1);

                if bout_length > min_bout_length

                    bouts_quiet(k,ind) = bout_length;

                    det_bouts(k,1)=k;
                    det_bouts(k,2)=i-j;
                    det_bouts(k,3)=i;
                    det_bouts(k,4)=bout_length;
                    det_bouts(k,5)=bout_length/intervall;

% In generated data first column= bout_number, 2nd column=start,
3rd
% column=end, 4th column=bout_length, 5th column tells you number
of frames spend in bout; check for longest bout done later in
% script in line 204
                        k = k+1;
                else
                end
                j = 0;

            elseif and(thresh_data(i,2)==thresh, j==0)
                %continued thresh, no quiet bout...walk along
                i = i+1;
                j = 0;



            end
        end

if and(i==size(thresh_data,1), size(bouts_quiet,2)<ind)
%all quiescence bouts were to short, fill bouts_quiet-list
%with zeros
    bouts_quiet(:,ind) = 0;
end

    %search activity bouts:
%     i=900;
%     j=0;
%     k=1;
%         while i >=900 & i<= size(thresh_data,1)
%             if thresh_data(i,2) == thresh
%                 %oh a wake bout...better count the length
%                 i = i+1;
%                 j = j+1;
%
%             elseif and(thresh_data(i,2)==0, j>0)
%                 %that's where the shit is happening
%                 i = i+1;
%                    bout_length = thresh_data(i,1)-thresh_data(i-
j,1);
%
%                 if bout_length > min_wake_bout_length
%                     bouts_activity(k,ind) = bout_length;
```

```
%
%                       det_activity(k,1)=k;
%                       det_activity(k,2)=i-j;
%                       det_activity(k,3)=i;
%                       det_activity(k,4)=bout_length;
%                       det_activity(k,5)=bout_length/intervall;
%
%
%                       k = k+1;
%                   else
%                   end
%                   j = 0;
%
%               elseif and(thresh_data(i,2)==0, j==0)
%                   %continued quiet, no activity...walk along
%                   i = i+1;
%                   j = 0;
%               end
%           end
%
% if and(i==size(thresh_data,1), size(bouts_activity,2)<ind)
% %all quiescence bouts were to short, fill bouts_quiet-list
% %with zeros
%     bouts_activity(1,ind) = B_index(end,1);
%     end

    % % Calculating the difference/distance between "mean" and
the normalized
    % % "50% value" of smoothed fit
    mean_data_smooth = mean(smooth_data);
    mean_dif = 0.5 - mean_data_smooth ;
    mean_distance = sqrt(mean_dif .* mean_dif);
    % % Calculating the standard deviation of raw data set
    standard_deviation=std(B_smooth(:,ind));

    %tables for 'false positive' check (see below)
      tab_check(1,ind) = mean_distance;
      tab_check(2,ind) = standard_deviation;
      tab_check(3,ind) = min1;

    %check for 'false positive' sleep bouts in non-sleeping worms
and
    %remove (you can adjust min1 to "<63" to include them often)
standard
    %is "min1<59"
    if or(or(mean_distance>0.15 , standard_deviation>6), min1<62)
            bouts_quiet(:,ind)=bouts_quiet(:,ind);
%             bouts_activity(:,ind)=bouts_activity(:,ind);
        else
            bouts_quiet(:,ind)=[0];
%             bouts_activity(1,ind)=max(B_index);
            bouts_quiet(2:end,ind)=[0];
        end

% border_list()

end
```

```
%replace '0' with 'NaN' in  the bouts tables
bouts_quiet(~bouts_quiet)=NaN;
% bouts_activity(~bouts_activity)=NaN;

% find longest bout in det_bouts data; only check column with
bout data
frames_longest_bout=max(det_bouts(:,4))/intervall;

% find longest bout in det_activity data; only check column with
bout data

% frames_longest_wake_bout=max(det_activity(:,4))/intervall;

% cut out bouts; starting -baseline frames from bout start point
until + 30 frames; do it both for wake and sleep bouts

i=1;
k=1;

while i <= size(det_bouts,1);
    cutted_bouts(:,k)=A(det_bouts(k,2)-
baseline:det_bouts(k,2)+30,2);
    i=i+1;
    k=k+1;
end

% i=1;
% k=1;
%
% while i <= size(det_activity,1);
%                         cutted_activity(:,k)=A(det_activity(k,2)-
baseline:det_activity(k,2)+frames_longest_wake_bout,2);
%     i=i+1;
%     k=k+1;
% end

% average bouts

mean_cutted_bouts=mean(cutted_bouts,2);
% mean_cutted_wake_bouts=mean(cutted_activity,2);

%  plot averaged bouts

% plot(time_cutted_bouts,mean_cutted_bouts)

%write files
% quiet_array=array2table(bouts_quiet);
%
writetable(quiet_array,[strain,'_all_quiet_bouts.txt'],'Delimiter
','\t');
%
% move_array=array2table(bouts_activity);
%
writetable(move_array,[strain,'_all_move_bouts.txt'],'Delimiter',
'\t');

% save det_bouts; before concert det_bouts array to table and
label the
```

```
% columns

% colNames={'count','start','endpoint','sec','frames'};
%
table_det_bouts=array2table(det_bouts,'VariableNames',colNames);
%                                                                 %
table_det_activity=array2table(det_activity,'VariableNames',colNa
mes);
%
%
writetable(table_det_bouts,[strain,'_all_det_bouts.txt'],'Delimit
er','\t');
%                                                                 %
writetable(table_det_activity,[strain,'_all_det_activity.txt'],'D
elimiter','\t');

% table_cutted_bouts=array2table(cutted_bouts);
table_mean_cutted_bouts=array2table(mean_cutted_bouts);
table_det_bouts=array2table(det_bouts);

% table_cutted_activity=array2table(cutted_activity);
% table_mean_cutted_activity=array2table(mean_cutted_wake_bouts);

%
writetable(table_cutted_bouts,[strain,'_all_cutted_bouts.txt'],'D
elimiter','\t');
writetable(table_mean_cutted_bouts,[strain,'_all_mean_cutted_bout
s.txt'],'Delimiter','\t');
writetable(table_det_bouts,[strain,'_det_bouts.txt'],'Delimiter',
'\t');


%
writetable(table_cutted_activity,[strain,'_all_cutted_activity.tx
t'],'Delimiter','\t');
%
writetable(table_mean_cutted_activity,[strain,'_all_mean_cutted_a
ctivity.txt'],'Delimiter','\t');




% Define a starting folder.
% topLevelFolder = uigetdir('','Where are your files?');
% if topLevelFolder == 0
%     return;
% end
% cd(topLevelFolder)

% read in GCaMP intensity file

fid=fopen('GCaMPIntensity_HBR2174_181228_MyMicroscope_field1,
worm3.txt');
GCaMPsignal=fscanf(fid,'%f',[2,inf])';
fclose(fid);
```

```
% cut the GCaMP signal in same pieces as locomotion for sleep
bouts

i=1;
k=1;

while i <= size(det_bouts,1);
    cutted_GCaMPsignal_quietbout(:,k)=GCaMPsignal(det_bouts(k,2)-
baseline:det_bouts(k,2)+30,2);
    i=i+1;
    k=k+1;
end



% and for wake bouts

% i=1;
% k=1;
%
% while i <= size(det_activity,1);
%
cutted_GCaMPsignal_wakebout(:,k)=GCaMPsignal(det_activity(k,2)-
baseline:det_activity(k,2)+frames_longest_wake_bout,2);
%     i=i+1;
%     k=k+1;
% end

% normalization GCaMP data; 1. average baseline 2. subtract
baseline from
% all values and 3. divide difference by baseline


baseline_quietbouts=cutted_GCaMPsignal_quietbout(1:baseline,:);
% baseline_wakebouts=cutted_GCaMPsignal_wakebout(1:60,:);

mean_baseline_quietbouts=mean(baseline_quietbouts,1);
% mean_baseline_wakebouts=mean(baseline_wakebouts,1);

norm_GCaMPsignal_quietbouts=(cutted_GCaMPsignal_quietbout-
mean_baseline_quietbouts)./mean_baseline_quietbouts;
%         norm_GCaMPsignal_wakebouts=(cutted_GCaMPsignal_wakebout-
mean_baseline_wakebouts)./mean_baseline_wakebouts;
%
mean_norm_GCaMPsignal_quietbouts=mean(norm_GCaMPsignal_quietbouts
,2);
%
mean_norm_GCaMPsignal_wakebouts=mean(norm_GCaMPsignal_wakebouts,2
);

% save some output data

%
table_cutted_GCaMPsignal_quietbout=array2table(cutted_GCaMPsignal
_quietbout);
%
table_cutted_GCaMPsignal_wakebout=array2table(cutted_GCaMPsignal_
wakebout);
```

```
%
%
writetable(table_cutted_GCaMPsignal_quietbout,[strain,'_all_cutte
d_GCaMPsignal_quietbout.txt'],'Delimiter','\t');
%
writetable(table_cutted_GCaMPsignal_wakebout,[strain,'_all_cutted
_GCaMPsignal_wakebout.txt'],'Delimiter','\t');

%
table_norm_GCaMPsignal_quietbout=array2table(norm_GCaMPsignal_qui
etbouts);
%
table_norm_GCaMPsignal_wakebout=array2table(norm_GCaMPsignal_wake
bouts);

%
writetable(table_norm_GCaMPsignal_quietbout,[strain,'_all_norm_GC
aMPsignal_quietbout.txt'],'Delimiter','\t');
%
writetable(table_norm_GCaMPsignal_wakebout,[strain,'_all_norm_GCa
MPsignal_wakebout.txt'],'Delimiter','\t');

table_mean_norm_GCaMPsignal_quietbout=array2table(mean_norm_GCaMP
signal_quietbouts);
%
table_mean_norm_GCaMPsignal_wakebout=array2table(mean_norm_GCaMPs
ignal_wakebouts);

writetable(table_mean_norm_GCaMPsignal_quietbout,[strain,'_all_me
an_norm_GCaMPsignal_quietbout.txt'],'Delimiter','\t');
%
writetable(table_mean_norm_GCaMPsignal_wakebout,[strain,'_all_mea
n_norm_GCaMPsignal_wakebout.txt'],'Delimiter','\t');
```

10.2 Extraction of genomic DNA

The genomic DNA of 4x back crossed mutagenesis candidate worms was extracted using the following protocol. I received this protocol from my former colleague Dr. Judith Besseling and she downloaded the protocol from the website of Oliver Hoberts lab.
(http://hobertlab.org/wpcontent/uploads/2013/02/Worm_Genomic_DNA_Prep.pdf).

Genomic Prep Protocol

DNA Prep using Gentra Puregene Kit (Qiagen)
(Protocol: DNA Purification from Tissue Using the Gentra Puregene Tissue Kit (cat# 158622, 158667, 158689)
Page 39)

IMPORTANT: DO NOT perform phenol extraction at any point because this will interfere with library preparation and cluster formation, which will result in lower coverage!!!

1) Unfreeze tube and add 3ml of Cell Lysis Solution

2) Sonicate – **OPTIONAL!!!** a. Aplitude – 20%

Pulse: ON for 01 sec.

OFF for 01 sec.

Total time: 30 sec.

b. If you choose not to Sonicate, make sure worms lyse well during next step

3) Add 15µl ProteinaseK (20mg/ml) and incubate at 55 degrees for 3 hours or until worms entirely lysed

a. invert worms periodically

4) Let the lysate cool down at room temperature

5) **Add 15µl RNase A Solution and incubate at 37 degrees on a NUTATOR mixer for a minimum of 1 hour!**

6) Cool for 3 min. on ice

7) Add 1ml Protein Precipitation Solution

a. cool for 5 min. on ice

8) Vortex vigorously for 20 sec. at high speed

a. cool for 5 min. on ice 9) Centrifuge for 10 min. at 2000xg

a. transfer supernatant

10) Add 3ml isopropanol and mix by inverting 50 times

a. **OPTIONAL** - Add 3µl of glycogen or Pellet Paint (Novagen, cat# 70748) if you don't see DNA precipitating

b. **OPTIONAL** – Incubate at -20 for 1 hour 11) Centrifuge for 3 min. at 2000xg

a. Remove supernatant

12) Add 3ml 70% ethanol and invert several times to wash DNA pellet

13) Centrifuge for 3 min. at 2000xg

a. Remove supernatant

b. Air dry pellet

14) Add 150µl of DNA Hydration Solution, pipette up/down, transfer to a clean eppendorf tube

15) Incubate at 65 degrees for a minimum of 30 min. or until DNA is dissolved

16) Measure DNA concentration

17) Load 10µl on a gel; should see one band at range >10kb. There should be no RNA

10.3 Sequence of the *rod-1* CRISP allele *syb414*

The sequence of the *rod-1* CRISPR allele *syb414* is given in the following. The CRISPR allele was generated by the company SunyBiotech and the original sequence was downloaded from the wormbase website [133].

>F55G1.4.1(*rod-1*), unspliced + UTR + 2000 upstream + 2000 downstream

- Upstream sequence/ downstream sequence of *rod-1* gene
- UTR of *rod-1* gene
- exon of *rod-1* gene
- exon of *rod-1* gene
- additional DNA sequence SunyBiotech detected while sequencing, which is not in the wormbase sequence
- insertion of 76 bp in the *rod-1* locus in the mutagenesis candidate 1

agagcatttatttctttttcaaaaaaagatttttttttaaatatcaacaacaacaagttatgtgtgaaaagcattacaaaatctaac
ttaatcacttggccagagattttgccatttcatcggccttggtcgaggcagctaccacagcttccataacagcgtaacggaat
ccgttcttctcaagtgcccgaacaccttcaatcgttgtaccgccaggggagcaaaccatatctttgagggatccaaagtgct
gagtttcaatatcaaatccagagttcgaattgagcaccatttgagctgctccgagtactgcttgagcagctaatcttttagcctc
tgctcgtccgagcccttgtgcgacggctccatctgccagtgattcgatgtacataaatgtccatgcaggactactccctccaa
tagccattgccgggttaaagcatctttctgggataagttcgacagttccaacacactcggcgaactcgcgtgccaattcgatg
tgagaatcttgattcataatttttttcattctttttcatagcacatcgtcgaggcgccggctccaatagaacttgctacatttggcatc
aaacgaacaatggtagtgtttcccgaaacgaatggcaactggaaaaatgttatgtacagcaaattatgatttctaaaattatttt
ataactgcttatagtaatcaccttcgcgttgagaacttttaatggaactccagccattacagaaataataaattctggtcttgagt
ttacaggccagcttgacacaacttcttcgaaaacttgaggtttcacacaaatcacatagattgccgtcgaatatctttccagcat
ttccagtgtgtttgtgaaaacgtttttatatcctagttgcctccatttctcagccgatttttccgtttgaacgccaattacaatattgc
ttttcggtgtaaagcctaaaaattagaaaacaatttaattcaaatcaacgaggagaacaatttttttaactcacctttattctggcat
ccttttataattgcagcggccatatttccacctccgatgaacacgaatggcacagactctgaggacccgtttgtcaattcagta
tcgatagtcatggttttgactgaaatcaataataattgtttttgacacaacaaaaagcaacatattaaaaaaaaaagaagaaga
catgagcagaggtttgcccgcttaacgagattctgtttctcaactgcgtctctgtgcgtttaacatataactgggttctattttatg
tctcttgttagacgtctagacgtctaagtctccatttatataaaagttacaataagatatattatggtacatgctgggatcattttag
taccgaaattgacatgaaaaactagtattctataaaaatttgtatcttaaaaccgtgaaaggcacagaaagtcacctagatgat
tattttgtcatcattccagaggccgtatagataataaaatatatttgtcatcggttcagttttgtcatcctgctctggaaaataattc
aaaacgttcaaaccacgaacaaaacagtaggaacaggtgaaacacagaaaataaacacttcaaaatttctttaaaaaatgta
aaattattttatttatgataaaaacttgaaacatctgagcagatacggtagacatattaaaggcgcatgctgaatattggagatg
ggttttgggacgaaaaactacggtctttttcgcctgcccgcgcaaattttaggcgcgaatttctctatatttacacgaatcttaa

Appendix

---

ttcttttggatatcattttaattttcagttattttctcgcctcatcctaataaatcgtttcagactatttatttttgataaatatagtgaaat
ttctgaatttaaagaagttttccggtctaaaattacgtttaaaaaagctgtatagttaggaacacgtaatttccacgtttcgatcaa
tttttactgaatgtgttaattgtttttcattatttaatttttgttcaacacagttaaaggtaaggaaatgtatgagatttgaaacgctttt
cgtgtttagttattggtttttgcttcaaaattcaactatttggttcaaaaaagtcttgtttctctcactctaacacttggaaattgcgc
cctgctgacacttatttcggcggcgaaaaacatttttgaaatgaaattgttcactcatttttataatcgttcttctgttaaatttttta
attagagataccagtgtattataatgtcgtatttgcagaATGGGTCGCCTAGGCGAAGCAAAAGCT
GTGGACTTGGAAGCGGAAACGTCGACTGTGGGCCTTTATGATGTGTGCAC
CGTTGGGCGAATCCTTCCCCgtaagaaaataaaactattatctttatgattaatgtaattaaatgtatgtttca
gTGTTAAATGAGATGTCAATCGATAAGAAATCTCCGGCATGGAAGCTCAA
ACCGAAAAGTAACGAGCGATTTCTTGTTCTTGCGTCGTGCTCCGATCTGGC
AGTCTTCAGTCTTGGCGAGAAAAGCGACTACTCGTTCAACACCGGACTTG
GAGgtatgagctatttcagagtctctggaatgatttctcaacattttcagGAGCCATCACTGATTTCGAA
ATCCTTGGAAGTTCTTCCTTCTTTGTTGGAGTCATTGAACATCGTCGTATTG
TAATTCTCTCGCTGGATAAACAAGAAATTTACTTGAACGAGCCAGCTCCTC
ATGAAATTGACTTCGTTGTCTGTCACACTACTTCCAGTGTTTGCCAATTGA
TTTTCGGGAGCCGATCTGATAATTGGCATACTATCACATTGCCAGGAGAC
GTGGCTGCATCTAAGGAGACTAACCGTTTCGAAAATTGGCACAGAGATCA
GATTCAGGAATTTTTCCACCAGgtaacgctcatcacattcatttaaagtttcaaattaattttaatactctctt
ttcagGCAATGGGAAAAACGGTTTCAAAGTCTGTTGACATGTCGAAGGTCGC
AGGTGACATTACTCTGATCTCCAATGGGCCACTTCAGACGTTCGCTTCAAT
TGATCAGCAAAGAGGGATTCACTGGTGTGGTCTCGTCGAATCGGAGTTTG
AGGTGATTGGCATGGAAAAACAATTCTTGCAAGTCCGTGATGGAGGTAGA
TTCTCTCTTCACCTCGACACGGATGGATGGATTCATGTCTTTGATTCATTG
GTATCATCCTTCTGCCACGAATTTGACATGAAGATGTCTCCAGACGACAA
AATTCTTGATTTTGTGATCATTGACAAGAATGAAGTTGAAGTTCCGAAGAT
GTTCGCAATTTTGGTTCTGCCACGTGACGGAGATAGCACAAAGgtatttgaatcgt
atttgttaaattttaataatttctttttagATGATGATATACGATCGATTGAATAAAGACAATTG
TTTCGCTTTGGATTCATCCACGTCTACAACTCTTTTTGCTTATGGAGGAAG
TGATCGTGTCTTGATAGCCGTTGAAGAATTGGAAAATTCTCTGGCAGACG
AACAGGACGGCAGTCAAATTGTTGTCAGACAAGTCTCACAGTCTCGCCCT
GAAATGCGTTTCGAATCTCTTCTGAAGAATAACAGATTTGAAGAAGCTGA
GAAGTTCGCCATGGCATTCATGCTGGATGTACAAAAGGTTTACAAAGGAC
ACGTACATTATCTGATGGACTCTTGTGATGAAAGCGATGAATCTTTTGAGA
CTCTGATGACGAAGATGGGACAAATTCAAGATCATAATATGGTTGCTGAA
ACATACTTCACTCTTGTTGGAATGAGTCGGCGCTGTGATCGTATCCGCACC
TACTTGACTCATGCAAAGAAGCGCAGAATAACGGATCTGGATATTCTGAA
AATGATTGAGGCACTTTGCTACACGTGGGGAACTTATCGAATCATTGCTG
GTCCAGAAGAAAACGAACCAAGTCGTCCACAAGTTAATGAAACGATTTGG
GATTTGTTCGTCGAAGCTTTGCATGATGCGAACCCGTGGATCGAAATCTAT
AATGAATTCATTTCTGACGCCCAGTTCACTgtcagtttcaatcttatgaagtttttgtactcaatca
tacaatttttcagCAAGCCCGTGTTATCTTCAGTCGCCATGGGAAATCTATAACTG
ATTATATGTGTGATGATGAGGAGAACACCATTTCTCGTCTTGAAACACTTT
TCCGAATGTTCATCGATGCGATTTCTTCTGATATCAGCAAATGGAGCAATG
TGATCGAACACGTAACGACAGACATTTTACCAGCATGTGTCATGATTACA
GAAGAGgtgatttttaaattaaaatttaactatgtttaaatctttctttttcagCTAATTCCATGCCTCGAAT
CACTCATCACTTCTCTTATTTCACTTCTTGAATATCGAGATTCTACAAATTG
GCCTGAGAATGCAATCAAAGCAGCAAGCAGTTACGATACCATGACCAAA
ATATTGTCGAACAATGGAAATACTCCAGCTACACAATGTATTCTGGTAAT
GTATGGAAGCAAGTTGGGATCTTCTGCCGGTAACAAGCCTTCGTCAATGT
CACGGATCAAGAAGATATACTATGATTTGATTGAATTGAAACGCCTGAAA

GATGTTTACGAGTGTTCAATCAGTTTCTCAGTATTCCAAAATATGTCATCT
GAACAAATTTGCCACAAGATTCTTCAAAATGCGTTGGCCAACCCAAACAT
GACACATGCCAAAATTGAGAAATTCGTGAAGCCGTTCATGGCTGAACGTC
ATCTTGATCAGGAACAAACAATCGTCAATTATATCCAGATGATGTCAGGA
GCTGCAGTGACAAATGCAAATCTTTTTGGATGGGAGAAACAATGTGTGCA
GTTATGTGCAAGTCTCATGGATGAAACTCGACGTTGTTGCTCCATCATCTC
GATCGCTTCAACTGCTAAGATTCCATGGCCAGCTGAACTGAATGAAGCTG
TGGAGAAGATCCTTGCAAGTCGTACACTCCTGAGATCAGAAATTGAACAA
ATGCATTTGGTTTGTAAACGTACCGAACTCTACAAGATGTTATCGTCGTAT
GGCTTCAGTCGACAGGACATCGAACTGCTGACTACTCCTGACTCAAATAT
GGACATTATCTTGACAATTCGCTGCATGCTTGCTCATCGTGAAAAGGCTTC
TCGATTTGTGGATGTGATCAAGTTGGTGGATTTGCTCAAAGCAATGCAAG
GAAGCTCTCAACCTCGTACATTGAGAATTGAATATGTGCAATCATTTGCA
ATTATTCATATGATGTCTCATCAAGATGTAACCATTTCAATTATCAATTAC
ATTGATAGTCTTGGCGATCGTGAACGAGTAAAGACAATATCTCTTGTATTT
TCATTCATCGAATGCGTTGCCAATGCACCAGCAACTGGAGACAACGTCTT
GGAACGCGAAAAGATCCTCGGGGTTGGTGAAGAGCTGATGTCTCACTATA
CATGTCGTGATAATAATTTCAATGATCCTGAAAGACGTTTAAAGGATGAG
CTTGTCCTTCTTCGCGAAGTCCAGAAAACTGAGACTAAAGCAGTTCTTTTG
TCTGAATTGAAAGATGAAGATTGGCAGCGACGGTTCTTGGAAAGATTGAT
CGAATCAAATTCGTCGATGAGCTTGgtaatttttatttaatatgaacggaatatttttattattaatttcag
AATCTTGGAAGATGTAGCTACATGGGAATTTCACCGGAACATCTCATTGA
AATGATTTTAACGAAAGCTACGGTAGAAAACGACATGGACACAATTGTTG
ATAGTATCACGAATTATGTCGAGTTCATAAATTCATTGACGGATTCTTCTC
GGGAAATGCTTGAACCTATCGTGCAAATTCTGAGCTGGATTACATTCAGA
CTTCCGAAGTTACTACCAAATGAGACTGAGATGGCACGTGCTGACTATgtaa
gtgatggtttctgcaaactataaaaataattgattttcagATTGCTTTCGTTGTCAAACGTATCGGCC
GTGTTGTTCGGGAGACACTCAGACGCTTCTCTTTTGATGTTATTAGCGACG
ATCTTGATTATCTTCTACAATTGGAAGCATTTTATCACTTGGGAGAGCACA
TTATCAAGCAGTCACTACGAGGCCAAGAGAATGAAAATGAAAAGCAAGA
AATGTTCAGATCAGACGATGATACATTCTTACCAACTGATTCTTCGAATCC
ATTTTCCAATCAGTCATCTCTCCGCATTTTTGAGTTCAAACGCCCACTGGG
AACATTTGATTTCTCCAACGATCCAGCTTTATTTGAAGGAGTTCAAGGAGT
TCTTGCTCTTGCGATGGTTGCACCTTCTGTTGCCAGGCCATATGATTCTGA
GATCTCACCAGATGATGCGAATGAATTCAGATCAAGTTGGGAGCAACTAA
ACATGTTCCTTGCAATGCATTCACAAGATCTTCTGGATATTTCAGCTCGTG
TGTTTGCCGGATCTCTCAgtaagatttatttccattttcaatttttattttttcatttcagAATGTTGGGCT
GGTGAATATCTACAAGGAATCGTTGAAATGGAGCAACCCATTCTGTCAGT
CGTCGAAAGAATGCTGCAACAGAAAAAATTCGATTTCTGGCATGCAGTTA
CTCTTCTTGGTGGAATCCCGTTGGAACGATTAGACAGAGCTATAATCGATC
TCCAGAAACGACAAGGTGTGAGAAGTTCGACGAAAGCGACAATCCAGTA
TCTTCAATTAGCTTTTGTGATGAGTTTGTTGGCTAGAAATATGGAAAAAGT
TCCCACAATCGTTTCTGCTTATGAACAAAAGTATTTGGTGAAGAAGCTTGC
TGAAGAAGGCATTCGTGTCTCAATTACTCAAGACTTTGTCGATAAAGTTCT
ACAACAGGCGATAGATCTGCGACAGCCACTCTCTCCATTGCGTCTTCATG
AgtgagtttcataaaataatagaaaaaataattttgaatatttcagTTATGTCAAGAAGTATGTCGAAA
AGTTGATTCGGAACTCGAAGATTTCAGTTGGAGAATACATGGTTCGATAT
GCGACTCTTCTCATTCGAAAAGCGTCTGTTGCTGGACGACACACTGATCG
GGAAATTCGCAAAGAAGAAATAGAGAAGTACATCGAAGCAGCTAGAATC
GCGTTGAGAgtaatagttgttgagtgataatcttttgaaaatctgttttcttttcagATTGCCGAGGAAGA

Appendix

AGATGCTTCTTGCATTTGTAATTATCTCCATTGTTTGCTTTACGTTGTGTGT
CCATATAACTACGAAGTCATCCAATTTATTGTAACTTCGTATGGAAAGTAT
GCCACTGAAACAGTCGAGATTGAATTTAATAAAAACTTGAAATCGgtgagcca
atatttaaaaaataaaattcaattcatcaatgattcagATAATGGCATTCTTATGGGCTTATCAACG
TACAAATCATATCAGTAATGAGGAATCAATTTGGTTTACGAAGCGAGAGA
GTGTTCTAATGAAAGATGAGAAAGAGTTTGAGAAAACTGGAAGAATGCTC
GATCCATTTGGACATTCACTTCGTGTTGTCTATGAAGATGACGGAAGCAAT
ATGTCAGATTCGTATAATTCGGATTTGGCACTTTCAAGTGATGCCATGGTT
TATGAGAGGAACAGTGTGATTATCAGTGATCTGCCAAGCCTTgtatgtcgactggc
aatcatttaattgaaatcaaaatattctttaattttagGCGGAGCAATATCTTCCATTCCATGCATTC
CTTCTTCGCAAAAAAGAGGAAATTGACGAAATTGTGATGGGAATTGTGAA
AGCAGAATTATCGATCTTCAATGTTCCAATCTGGCAAACATTCCTCCGTGA
AGTTTCTTGGCTATCCTCACGGTTTTCGCGTTCGCAACTTTTGTCATCTGCA
ATTTTTGCTCACGCCAACAAATATGCAAAGTTTGGAAAGAGTCTACCAGA
TGGAGAACGAAACGTGATTTATGAACTTCTTAATTCTGCGTCTCAACGTCA
TGTTGTGGTTTCGACGATCGCTCTTCTATTCAAAAGAATCATTCTCAGTGA
TGTTAAAATTGAACTTCTTCAAATGGGAGTCAATATTTCGGAGAGATGGA
CTTCTGATTTAACTGGTGAAGAACAACAGGAAATGGAAGAACAAAGTGCT
CGATTGAAAGACGGAATCGCAAAGTTTTCTACCGAACTTGAACTGAAAAA
GAATGGACTGTACAATGAAAAAACTGCGGATAACATTGAAAATGTATCTG
AACTATGTTCATTAATTTACAATGAAATGGTCCAGTGGGATGATTCTAGA
GATGTTCTCAAAAAGTGTCAAGTGGTGGATAAAATTGCAAAGGCTAATGG
ACTCGATTTGACTGCTTTGCATGAACAGCTTGTCTTCTCGTGGGTTGAGGA
TACGCAGACTATCATTTCAATTAATCATGTTGATATGAACGAGgttagtttgtaca
ggggattttgaattcttatagttttaatttacagTCAATTGGTGGAACTTCTTTCTTGGATCACAA
AGATGAAACAGACGATCAAAATGATTTGAGAATTCCATTATTTGACGGGA
TTCTCGACAAAGTTGTTGTTCTCTGCCAAAGAATTGATAAAAAGCGTCTTC
TGACAAGACTCGGAAGTATTCTGATGAGAGGAGGTCGCAAAGCGACGGG
CGGTTATACTGCTGTAGTTCGTGCTACATGTATAATTCTGCGTTCTTTTACT
GATACTGAAGTCTCTGAATTGCTGTCTGGAGCTGACATGTTTGCATTATGgt
tggtttcttgatttaaaattattgtcctctataaataatacattttcagCAGTACACTTGAAAATCAACTCTA
CGAACGATTGTTTGAGAAGGCTGAAGTTAAGGGAGATTGTAAAACAGAC
AAAATGCAATTAATCAAGTCTCTTCTTCAATGTCCATCACGAACACACCCA
ATGACTGCACTTATTGCATGTCTAATCATTGATCATGAGTTCAAGGATCCG
AAAAGTATCGAACAAGTGATGACACGTCTACAAATTAGCAAACAATGGA
ATACACTTCGTGCTCTACTCAACTATGTTCGTTCGAATCAAATGGATTCCA
TGATCCGCTCGTTCCCGCTTATTTGGTTCCGTGTTTATGAAAATGCCTTGAT
TGAATTGAATGGTGGATCCATGGCGAATCCAGATTGGAATTACGAACAAT
GCGTTATGCTTCGAAAATGGACTTTGTGGGCAATGAGCAGCAATGTCGAA
GGAGGACGTCAACCAAATATTGCTCGATTCCTCCGTGAAATCAATTGTCC
CATCAGTGCCTCGATTATTTCTGTCCTTTCTAACTGGAGATCCGAACTATT
GATGTAAGTTCAATTTAAACAATATTTATAATCATTTAATTTACCAATATC
ATTTCAGAAAATGGACGACGTTGACTCTTCCAAGTTGGATCCGAAATCCA
TCGAGCAAGTTATGACCCGCCTTCAGATCTCTAAGCAATGGAACACTCTC
CGTGCCCTTCTCAACTACGTCCGTGACATTTCACTTGGATGGGATGTAGGA
TGCGTTCCTGTTAGCGCAAACTCTTCCAACTCTTAAataaattcgttggtttttatttgttttat
cctgtaaactagcatagatctcaataaaggggactattattttctcagtattttaatttaatttttacgctctattacatctttctacc
aaattatggtaaatcatcgagaaagtttttattcaattgtaaattcaaacgattaaataaattatattcatcttaagaaagagaag
cattcatttttaacatacgacctgaagtttgaaagaaaagttgataaaatcgaaatatttcctcaacactgctttccaggtgaac
agaaaacgaaataaatgcaaagaaaagtgaatcaaacaggattgaagttgatagcttttcgaattatcacaatttcgttcaaca

ttcactattaacgtgtcttcaagatttataataataaaaaacaatttattcaattgatagttaggatttcagataattgtggccctaa
agagggccgttgggttcggttgggtttttaagaaaaaagttcttattccttgtctccaccagtcttctttggaagaagaacagct
tggatatttggaagaactcctccttgggcgatggtcactccggccaaaagcttgttgagctcctcgtcgtttcggacagcgag
ttgaagatgtcttggggcgatacgggtcttcttgttgtcacgggcagcattaccggccaattcgagaacctcagcagcgagg
tattcaagaacagcggccaagtaaactggagctccggctccaacacgttgagcatagtttcctttgcgaagaatacgatgaa
gacgaccgactgggaattgaagtccagctcttgatgagcgtgacttggcctttcccccggtcttggctttgcctccctttccac
gtccagacatgatgagcggttggtgttcgtaagacgaatctgaagaatgaaccgaaactgtctgtttatattcatttcttcggtg
gcggggcggagcttactgcggggacacctctcggttctctgtccctcaccctcccctgttatctctagcctcattgtttgtctg
cgacacagagtctctgtgtctcaaatttacatgcatcggtgcattcggagtgttgtgtgcactctgaaatgtgtccctgcagga
agctccgcccatccaccgcagtttttacttaaatatctgccgctccgaccatttcctcatacttgattcaagtccattctcatcatg
ccaccaaagccatccgccaagggagccaagaaggccgctaagaccgtcgttgccaagccaaaggacggaaagaagag
acgccatgcccgcaaggaatcgtactccgtctacatctaccgtgttctcaagcaagttcacccagacaccggagtctcctca
aaggccatgtctatcatgaactccttcgtcaatgatgtcttcgaacgcatcgcctcggaagcttctcgtctcgctcactacaac
aagcgttctaccatctcttctcgcgaaattcaaaccgctgttcgtttgattcttccaggagagcttgccaagcacgccgtgtct
gagggaaccaaggccgtcaccaagtacacctccagcaagtaagccattggctgaaaactaaccaaccgaacccaacgg
ccctctttagggccacaaatattgaaatccttacaaaactacatgttcgttaataaattatatgcactcttatatattcacgtctttta
tattaggtcttttcttgaaatcttaatctagtattacgttttcctagccttcgaaggaattcaagagttcgaacttatcattcataaaa
atgcgttcaatctaatcaatctaaataaaataaatctcgtctgtttaatgaggaaactcaaatttaattaaggtggaatttcacattt
caaatgtcgcagaggaaatcgatcggtgaccgaagaagcttagagaaggtaacatgaaaatgtctatattcacggaaattta
aagtttgtgtcacaaaaataataaaggcaacaaactaattaaacaacaaatttttagaccatgtaccaagaaatttagtttcaata
atcttcagaacacggtgactgctctggtgaatttccaagcgataatttgttcaggcaaaggaacacattaaacgtcggaataa
tgatggtgattgtcagcttcatgtgcaaaattaattaaatttttatcgaacctga

11 Acknowledgements

First, I want to thank my supervisor Henrik Bringmann for giving me the great opportunity to do a PhD in his lab. He introduced me to the great world of *C. elegans* and the almost unlimited ways to experiment with this model organism. He always had an open ear for my questions and always took his time to discuss results.

Second, I want to thank my committee members, who guided me through my PhD. I am thankful for all discussion we had during the committee meetings and I am thankful for the extra time they took to discuss topics in additional meetings.

I am thankful to my former colleagues Judith Besseling, Michal Turek and Florentin Masurat. Their support was essential at the beginning of my PhD. They were the ones turning me from a plant person to a worm person. Furthermore, I want to thank them for their great work, on which I could later on base my PhD project.

Furthermore, I want to thank the whole Bringmann group for the great working atmosphere. I thank Anastasios Koutsoumparis for the numerous discussions about my project, for all the food groups and for all the effort he took to proofread my thesis, literally to discuss every single sentence. I thank Jan Konietzka for all the MATLAB help and for all the confetti rains and soap bubble fights we had. I thank Inka Busack for the great cooperation's on the rebound project and for each single song she was singing in the lab to increase the mood during difficult times. I also thank Marina Sinner for that and for being the one person to discuss with about the most important think in the world despite science: horses. Finally, I thank Yin Wu for always being positive and asking the right questions.

I also want to mention here Maximilian Fritz. He was a great person and a greater scientist and there are no ways to fill the gap his dead left in our lab.

Acknowledgements

Next people to thank are my student assistants Maurice Hädrich and Tora Fougner-Okland. You made my life so much easier with all your help in the lab and all the extra hours you were willing to spend during evenings or weekends.

I also want to thank Sabine König and Sylvia Gremmler for their work in the lab. Sabine König for her assistants with crossings and injections and Sylvia for always providing as with all plates and buffers we needed.

I also want to thank my family for all their support during my PhD and also during my studies. You were the ones telling me to always be curious and always question what other people tell me, which is the basis for being a good scientist.